MAMMARY EPITHELIAL CELL DIFFERENTIATION IS REGULATED BY PROGRAMMED AUTOPHAGY AND SIM2S

A Dissertation

by

JESSICA LEE ELSWOOD

Submitted to the Office of Graduate and Professional Studies of
Texas A&M University
in partial fulfillment of the requirements for the degree of

DOCTOR OF PHILOSOPHY

Chair of Committee,	Weston W. Porter
Committee Members,	Scott V. Dindot
	Michael C. Golding
	Ivan Ivanov
Intercollegiate Faculty Chair,	David W. Threadgill

May 2020

Major Subject: Genetics

ABSTRACT

Normal physiological or developmental processes, including invasion, proliferation, metabolic reprogramming, and apoptotic escape, are often hijacked in malignant states to drive disease occurrence or progression. As malignant states often involve a complicated combination of initiating factors, these processes are best studied in their native environment during tissue development. Metabolic reprogramming is a hallmark of tumor cells; however, the underlying cause remains unknown. Therefore, we investigated metabolic reprogramming in the mammary gland between gestation and lactation when a dramatic metabolic transition occurs under the influence of local and hormonal signals. To do so, we utilized an *in vitro* model of mouse mammary epithelial cell differentiation in combination with mouse models to interrogate changes in mitochondrial homeostasis, including fission, fusion, biogenesis, and mitophagy (targeted macroautophagy of mitochondria). Through transmission electron microscopy and real-time fluorescent time course studies, we found that mitochondria underwent mitophagy in response to differentiation cues *in vitro*. Importantly, full differentiation was impaired if autophagy was inhibited pharmacologically or genetically, via knockdown of *Atg5* or *Atg7*. Furthermore, differentiation was completely abrogated with knockdown of the mitophagy factor, parkin (*Prkn*). To address the upstream mechanism, we evaluated mitophagy and mitochondrial function in two in-house mouse models that have development phenotypes: MMTV-*Sim2s* mice, which demonstrate precocious differentiation, and $Sim2^{fl/fl}$ conditional knockout mice, which we demonstrate here to

have reduced lactation function. *Sim2s* is the short splice variant of single-minded 2s, a master regulator of central midline development in drosophila as well as a tumor suppressor in breast cancer. Interestingly, we found that over-expression of *Sim2s* enhanced mitophagy and prolonged lactation capability, whereas loss of *Sim2s* impaired lactation performance. To address the mechanism of these effects, we evaluated the localization of SIM2s. Surprisingly, SIM2s localized to mitochondria and interacted with LC3B, which associates with the phagophore membrane. Mutation of two putative LC3B interacting region motifs in *Sim2s* abrogated the differentiation enhancement of *Sim2s* overexpression. Together, these data suggest that SIM2s is an integral link in the programmed mitophagy that occurs during mammary epithelial cell differentiation. Future studies will contribute to our understanding of the tumor suppressive role of SIM2s in breast cancer as well as to how the regulatory biology of mitochondria contributes to development. We expect continuation of this work to advance therapeutic approaches to combatting mitochondrial dysfunction and resulting disease states.

ACKNOWLEDGEMENTS

I would like to thank my committee chair, Dr. Porter, Dr. Rijnkels, and my committee members, Dr. Dindot, Dr. Golding, and Dr. Ivanov for their guidance and support throughout the course of this research. In addition, I thank the members of Dr. Porter's lab, Dr. Gile's lab, Dr. Guo's lab, and Dr. Safe's lab for their support and assistance throughout this process. Dr. Barhoumi, Dr. Payne, and Dr. Burghardt at the Texas A&M University College of Veterinary Medicine & Biomedical Sciences Image Analysis Laboratory, supported by NIH-NCRR (1S10RR22532-01) grant, were of tremendous assistance in the acquisition of the transmission electron microscopy and confocal images presented in this work. I am grateful to Dr. Benjamin Morpurgo, Dr. Andrei Golovko, Ms. Amy Gonzalez, and the Texas A&M Institute for Genomic Medicine for their contributions to the mouse projects. I would also like to acknowledge the Histology Core Facility at Texas A&M University College of Veterinary Medicine & Biomedical Sciences for tissue preparation and H&E staining. Finally, thanks go to my family and friends for their continued support and encouragement throughout this process.

CONTRIBUTORS AND FUNDING SOURCES

Contributors

This work was supervised by a dissertation committee consisting of Professors Weston Porter, Scott Dindot of Veterinary Pathobiology, Michael Golding of Veterinary Physiology and Pharmacology, and Ivan Ivanov of Veterinary Physiology and Pharmacology.

The conditional *Sim2* knockout mouse was designed by previous members of the Porter laboratory, including Rick Metz, and was generated at the Texas Institute for Genomic Medicine under the supervision of Drs. Benjamin Morpurgo and Andrei Golovko. The MMTV-*Sim2s* mice were previously developed in the Porter laboratory, and the cytochrome C oxidase subunit 4 immunostaining in MMTV-*Sim2s* and wild type mammary tissue sections presented in Chapter IV was performed by Dr. Kelly Scribner. All other work conducted for the thesis (or) dissertation was completed by the student independently.

Funding Sources

This work and graduate study was made possible in part by the National Cancer Institute through R21CA190941, R01HD083952, and R21CA185460. Fellowship funding was provided by the Texas A&M University College of Veterinary Medicine. The contents of this work are solely the responsibility of the authors and do not necessary represent the official views of the funding agencies.

NOMENCLATURE

Acetyl-CoA	Acetyl coenzyme A
ACLY	ATP citrate lyase
ACTB	Actin beta
AHR	Aryl-hydrocarbon receptor
AHRR	Aryl-hydrocarbon receptor repressor
AIP	AHR interacting protein
AKT1	AKT serine/threonine kinase 1
ARNT1/2	Aryl hydrocarbon receptor nuclear translocator 1/2
ARNTL1/2	Aryl hydrocarbon receptor nuclear translocator like 1/2, BMAL1/2
ATG3/5/7/12	Autophagy related 3/5/7/12
ATM	Ataxia telangiectasia mutated
ATP	Adenosine triphosphate
bHLH	Basic-helix-loop-helix
BNIP3	BCL2 interacting protein 3
BNIP3L	BCL2 interacting protein 3 like, NIX
BRCA	BRCA DNA repair associated
cAMP	Cyclic adenosine monophosphate
CASP3	Caspase 3
CEBPB	CCAAT enhancer binding protein beta
CLOCK	Clock circadian regulator

CME	Central midline element
CMV	Cytomegalovirus
CNS	Central nervous system
COX4/8	Cytochrome C oxidase subunit 4/8
CRY1/2	Cryptochrome ½
CSN2	Casein beta
DDR	DNA-damage repair
DNA	Deoxyribose nucleic acid
DNM1L	Dynamin 1 like, DRP1
DRE	Dioxin response element
DSCR	Down's syndrome critical region
ECAR	Extracellular acidification rate
ELF5	E74 like ETS transcription factor 5
EPAS1	Endothelial PAS domain protein 1, HIF2A
ERBB2	Erb-b2 receptor tyrosine kinase, HER2
ESR1/2	Estrogen receptor 1/2
FCCP	Carbonyl cyanide-4-(trifluoromethoxy)phenylhydrazone
FOXA1	Forkhead box A1
FUNDC1	FUN14 domain containing 1
FYN	FYN proto-oncogene, Src family tyrosine kinase
GAS	Gamma-interferon activated sequence
GATA3	GATA binding protein 3

GLUT1	Solute carrier family 2 member 1, SLC2A1
H&E	Hematoxylin and eosin
HIF	Hypoxia-inducible factor
HIF1A	Hypoxia-inducible factor 1 subunit alpha
HRE	Hypoxia response element
IF	Immunofluorescence
IHC	Immunohistochemistry
IMM	Inner mitochondrial membrane
IMS	Inner mitochondrial membrane space
IP	Immunoprecipitation
JAK2	Janus kinase 2
K14	Keratin 14
LALBA	Lactalbumin alpha
LC3B	Microtubule associated protein 1 light chain 3 beta
LIF	LIF interleukin 6 family cytokine
MEC	Mammary epithelial cell
MFN1/2	Mitofusin 1/2
MMP	Matrix metalloprotease
MMTV	Mouse mammary tumor virus
mtDNA	Mitochondrial DNA
MYOD1	Myogenic differentiation 1
MYOM2	Myomesin 2

NAD	Nicotinamide adenine dinucleotide
NADP	Nicotinamide adenine dinucleotide phosphate
NF-κB	Nuclear factor κ-light-chain-enhancer of activated B cells
NOTCH	Notch receptor
NPAS	Neuronal PAS domain protein
OCR	Oxygen consumption rate
OMM	Outer mitochondrial membrane
OPA1	Optic atrophy 1
OPTN	Optineurin
OSM	Oncostatin M
pADPr	Poly (ADP-ribose)
PARP	Poly (ADP-ribose) polymerase
PAS	PER-ARNT-SIM
PCR	Polymerase chain reaction
PER1/2/3	Period 1/2/3
PGR	Progesterone receptor
PINK1	PTEN induced kinase 1
PPARG	Peroxisome proliferator activated gamma
PPARGC1A	PPARG coactivator 1 alpha
PRKN	Parkin RBR E3 ubiquitin protein ligase
PRLR	Prolactin receptor
RANK	TNF receptor superfamily member 11a, TNFRSF11A

RANKL	TNF superfamily member 11, TNFSF11
ROS	Reactive oxygen species
SIM1/2	Single-minded 1/2
SNAI2	Snail family transcriptional repressor 2
SQSTM1	Sequestosome 1
SREBF1	Sterol regulatory element binding transcription factor 1, SREBP1
STAT3/5	Signal transducer and activator of transcription 3/5
TCA	Tricarboxylic citric acid
TEM	Transmission electron microscopy
TOMM70	Translocase of outer mitochondrial membrane 70
TUBA	Tubulin alpha
VDAC1	Voltage dependent anion channel 1
VHL	von-Hippel Lindau tumor suppressor
WT	Wild type

TABLE OF CONTENTS

Page

LIST OF FIGURES

Page

LIST OF TABLES

Page

CHAPTER I

INTRODUCTION

Breast cancer is a substantial clinical challenge due to the immense intra- and inter-tumoral heterogeneity of the disease. Six major breast cancer subtypes have been identified based on histological and molecular profiling and clinical prognoses: normal-like, luminal A, luminal B, HER2 (ERBB2, erb-b2 receptor tyrosine kinase 2) enriched, claudin low, and basal-like [1-3]. Although these classifications inform treatment decisions, patient responses are still diverse within subtypes, suggesting that additional heterogeneity contributes to therapeutic outcomes [3-5]. The source of this heterogeneity has been pursued in the breast cancer field and has uncovered unique roles for the mammary gland stem cell hierarchy, hormone receptors, genetic factors, and the tumor microenvironment, to name a few. As the complex contribution of these factors to the normal development of the mammary gland is not fully understood, it is not surprising that treating the heterogeneous disease remains challenging.

Normal physiological or developmental processes are often hijacked in malignant states to drive disease occurrence or progression. In fact, many developmental events in the mammary gland also occur in breast cancer, including stromal invasion, proliferation, and apoptotic escape [6, 7]. Developing a more complete understanding of the hormonal, transcriptional, and metabolic mechanisms that direct normal development will provide insight into the dysfunction that occurs in disease states. A large body of work has addressed the requirement of ovarian, pituitary, and adrenal hormones to the development of the mammary gland, and the signaling and transcriptional networks that

arise directly or indirectly from these hormones are under active investigation by our lab and others. Much less is known about the contribution of metabolism and mitochondria to the development of the mammary gland; therefore, a primary goal of this work was to investigate metabolic contributions to mammary gland development.

Mammary gland development

The majority of mammary gland development occurs after birth, which allows for detailed analysis of the sequential events that ultimately enable lactation. Lactation is achieved through the coordination of sequential hormonal signals that regulate pubertal ductal elongation, ductal side branching, alveologenesis, and lactogenesis (Figure 1) [8, 9]. The morphology of these stages of mammary gland development is well defined in mice, and begins with a rudimentary ductal tree that originates from the nipple [10]. At approximately three weeks of age, terminal end buds appear and invade through the stroma, initiating ductal elongation [10]. Terminal end buds eventually reach the boundaries of the gland, and ductal side branching is initiated, which also coincides with the onset of cyclical estrous cycles [10]. Alveologenesis is initiated in the adult virgin gland with the cyclical production of ovarian hormones during estrous, and alveolar cells continue to expand and differentiate during pregnancy [8, 10]. Pregnancy also marks the initiation of lactogenesis, which is divided into two phases [8]. The first phase, sometimes termed lactogenesis I or secretory differentiation, begins alveolar differentiation and involves the expression of some differentiation-dependent genes, such as caseins [8, 11]. The second phase, termed lactogenesis II or secretory activation, is marked by milk secretion and also involves the closure of tight junctions and the

mobilization of lipid droplets [8]. Together, these processes refer to the differentiation of mammary epithelial cells (MECs) and are guided in large part by the endocrine system and surrounding stroma. MECs are subdivided into basal, or myoepithelial, and luminal compartments, and luminal MECs can be further subdivided into ductal and alveolar luminal cells. The mammary gland stem cell hierarchy is thought to inform the identity of each subtype, and many different hierarchical schemes have been suggested [12-14]. Thus, the considerable heterogeneity observed in breast cancer is not surprising given the diverse array of cell types present in the normal developing mammary gland. For the purposes of this work, discussions will center around the terminal lactogenic differentiation of luminal MECs.

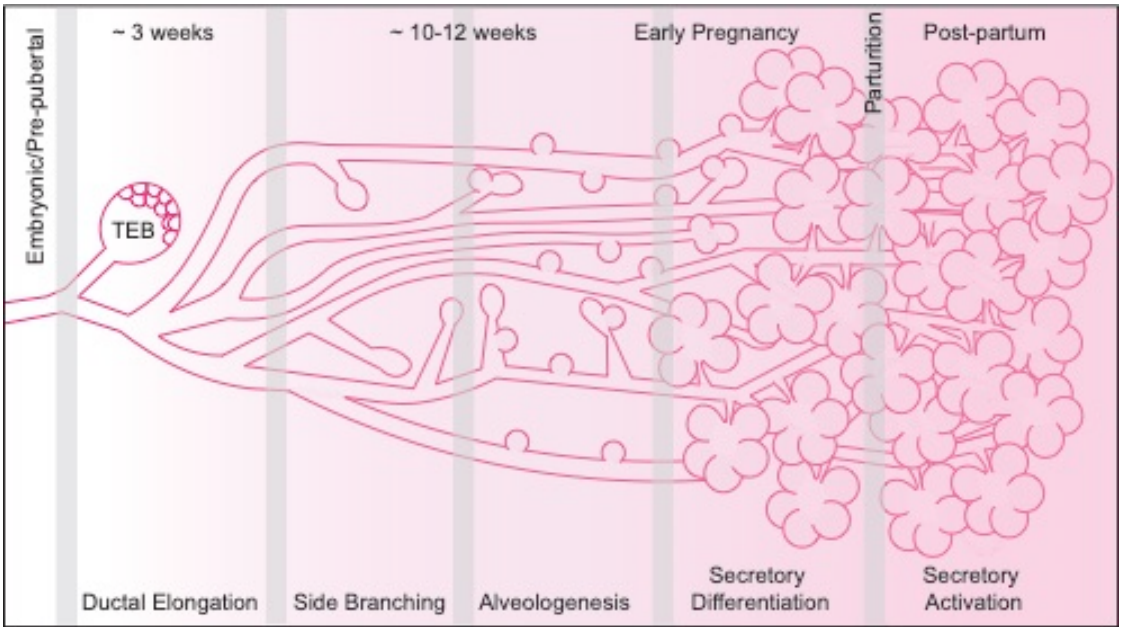

Figure 1 Model of mammary gland development.

Hormonal regulation

As an endocrine organ, the post-natal development of the mammary gland is largely guided by external ovarian, pituitary, and adrenal hormones as well as by placental hormones and hormones produced locally within the mammary gland [9]. The requirement of each hormone during mammary gland development was initially determined by providing the hormone in question to non-lactating animals lacking the source of the hormone, i.e. ovariectomized, hypophysectomized, or adrenalectomized animals [15, 16]. Development of transgenic models refined this approach by abrogating the expression of hormone receptors. The resulting developmental defects in the mammary gland implied the earliest requirement of each hormone, and transplantation studies determined the epithelial or stromal origin of the signal [17]. More specifically, these studies identified the ordered epithelial requirement of estrogen, progesterone, and prolactin for mammary gland development beginning at puberty (Figure 2) [8]. First, estrogen is required for pubertal ductal elongation of the rudimentary ductal tree [18, 19]. Progesterone is required next for side branching during puberty and gestation [20, 21], and, finally, prolactin is required for alveologenesis and lactogenesis during gestation and lactation [22]. Growth hormone and cortisol are also required during mammary development, and several other hormones contribute to various development stages, including thyroid hormones, leptin, vitamin D, and sex hormone precursors [8, 9, 14, 15]. Of note, the requirement of estrogen, progesterone, and prolactin has been determined by eliminating their receptor expression, and although these studies inform

what we know about the earliest role of each, additional specific roles at later stages of development have not been as clearly established.

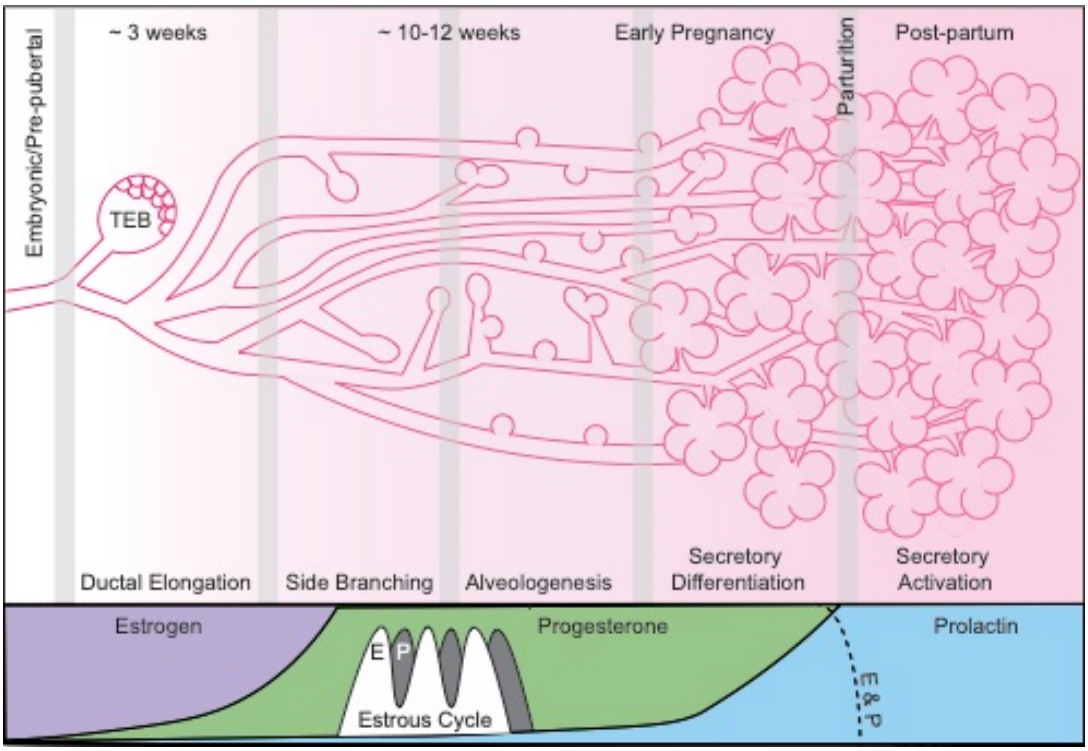

Figure 2 Hormonal control of mammary gland development.

Transcriptional regulation

Hormone activation of cellular receptors results in intracellular signaling cascades, which regulate transcription factors and their target genes. A considerable amount of work has gone into dissecting the signaling networks that originate from each hormone; however, complexities are readily apparent. First, some hormones are capable of activating multiple receptors, and, likewise, most receptors can recognize multiple hormonal signals. Further, there is considerable overlap in the phenotypes of several loss of function models for hormone receptors and transcription factors, indicating that

signaling pathways likely overlap or coordinate during mammary gland development. Nevertheless, advances in our understanding of these signaling pathways have led to the definition of the major molecular subtypes of breast cancers and have translated into the development of important therapies for breast cancer patients. Therefore, a discussion of the complex contribution of some of the major transcription factors that regulate mammary gland development is warranted. We anticipate that the diverse milieu of hormonal and transcriptional signaling during important transitions in mammary gland development will inform the metabolic changes that occur as well as provide insight into therapeutic windows of opportunity.

Estrogen and progesterone steroid hormone receptors (ESR1, ESR2, and PGR) function as intracellular transcription factors in the mammary gland. Notably, estrogen and progesterone receptors can influence transcription directly by binding DNA or indirectly by interacting with other transcription factors or coactivators in response to ligand binding [23]. These receptors are also capable of influencing signaling through nongenomic mechanisms, including the generation of cAMP (cyclic adenosine monophosphate) [23, 24]. In contrast, prolactin receptor (PRLR) is a transmembrane protein that canonically signals through the JAK-STAT (Janus kinase – signal transducer and activator of transcription) or MAPK (mitogen activated protein kinase) transcriptional pathways [25]. Genetic ablation of the steroid and peptide hormone receptors and other transcription factors has helped to uncover their contribution to the development of the mammary gland. Although there is still some concern regarding compensation from other pathways, these studies have established the ground work for

the transcriptional regulation of mammary gland development. Below is a brief discussion of major transcription factors involved in the establishment and/or differentiation of luminal MECs: ESR1, GATA3 (GATA binding protein 3), FOXA1 (forkhead box A1), PGR, RANKL (TNFSF11, TNF superfamily member 11), STAT5 (signal transducer and activator of transcription 5), ELF5 (E74 like ETS transcription factor 5), and STAT3.

Ductal Elongation

Early in pubertal mammary development, ductal elongation is achieved through proliferation of mammary epithelial cells at the terminal end buds and invasion of the duct into the surrounding stroma [14, 26]. Ductal elongation is severely impaired with loss of estrogen or ESR1, suggesting that ESR1 contributes to the proliferation of MECs and invasion into the stroma (Figure 3) [16, 19, 27]. Paradoxically, the highly proliferative cap cells in the terminal end bud are predominantly ESR1 negative and hormone receptor positive cells are less proliferative than hormone receptor negative cells, implying that the mitogenic effect of estrogen is indirect [23]. Eventually, it was determined that estrogen-mediated proliferation occurs in a paracrine manner from ESR1 positive epithelial cells to ESR1 negative epithelial cells [19]. Consequently, investigation of the paracrine mediators of estrogen function has contributed greatly to the current understanding of hormone responsiveness in breast cancer. The original search for these mediators involved factors whose loss resulted in similar defects in ductal elongation and terminal end bud function, such as those observed in conditional GATA3 deletion mice and FOXA1 null mammary transplants and grafts.

In the developing mammary gland, GATA3 is expressed during embryonic development, during pubertal development in the terminal end buds and mature ducts of 5-week-old virgin mice (Figure 3) [28], and during pregnancy-induced development and lactation [29]. Complete loss of GATA3 results in embryonic lethality; therefore, multiple *LoxP* conditional models have been used to reduce GATA3 expression in the mammary epithelium during embryonic (*keratin 14* [*K14*]-*cre*), pubertal (mouse mammary tumor virus [*MMTV*]-*cre*), and pregnancy-induced (whey acidic protein [*Wap*]-*cre*) mammary development. Although the majority of *K14-cre;Gata3* mice die shortly after birth, all neonates lack nipples, and rare survivors also predominantly lack mammary epithelium by six weeks of age [29]. Two independent groups generated *MMTV-cre* and *Wap-cre Gata3* conditional knock out lines. In these mice, both groups concluded that prepubertal (non-hormonal) mammary gland development was normal [28, 29]. The groups further agreed that loss of *Gata3* resulted in impaired ductal elongation and alveolar differentiation as well as expansion of an undifferentiated luminal progenitor population of MECs [28, 29]. Importantly, Asselin-Labat and colleagues demonstrated that overexpression of *Gata3* enhanced expression of differentiation-dependent factors in luminal progenitor cells both with and without lactogenic stimulus [29]. Together, these studies suggest that GATA3 is required for cell fate determination during embryonic development and for ductal elongation and luminal differentiation during post-natal development of the mammary gland.

FOXA1 is required for ductal elongation in a similar manner as estrogen, ESR1, and GATA3. In fact, ESR1 and FOXA1 colocalize in roughly 30% of virgin ductal

epithelial cells, and cells expressing ESR1 alone are sparse (<5%) [7]. During normal mammary gland development, FOXA1 is expressed in the terminal end buds and ducts of the virgin gland but not in terminal end bud cap cells [7]. As pregnancy-induced development progresses, FOXA1 expression is largely absent, which is similar to patterns of ESR1 expression but differs from the elevated expression of GATA3 observed during early lactation (Figure 3) [29]. FOXA1 null mice are perinatal lethal [30]; therefore, alternative deletion strategies have been used to interrogate the post-natal mammary gland development with loss of FOXA1. Strikingly, FOXA1 null transplants completely fail to form ductal outgrowths, even in the presence of hormonal stimuli, suggesting that FOXA1 is required for ductal elongation [7]. Due to the severity of the ductal outgrowth phenotype, FOXA1 function was further interrogated using renal capsule grafts from FOXA1 null mice. Renal capsule grafts allow for the investigation of developmental phenotypes of embryonic or perinatal lethal mutant mice [31]. In FOXA1 null renal capsule grafts, ductal elongation is severely stunted, but alveolar development and lactogenesis proceed normally [7]. Notably, the ductal elongation impairment was attributed to a block in luminal cell expansion and invasion but not to a defect in lineage specification. In sum, this work highlights the requirement of FOXA1 in ductal elongation during pubertal mammary gland development and demonstrates important parallels to ESR1 and GATA models.

Several important parallels can be drawn between ESR1, GATA3, and FOXA1. First and foremost, GATA3 and FOXA1 are positively correlated with good prognosis in luminal A and luminal B (ESR1 positive) breast cancer subtypes and have similar

development defects when lost, as discussed above [7, 23, 32-36] Moreover, loss of both GATA3 and FOXA1 also reduces ESR1 expression, suggesting that these factors are transcriptionally interdependent [7, 28]. This interrelation is supported by observations that overexpression of GATA3 results in elevation of FOXA1 expression [37] and GATA3 recognizes and binds a regulatory region of FOXA1 [28]. However, loss of FOXA1 does not impact GATA3 expression, and FOXA1 expression is not lost in GATA3 deficient mammary glands [7]. Further, FOXA1 is required for ESR1 action in several studies [7, 38, 39], ESR1 binding sites are present on both FOXA1 and GATA3 [40], and GATA3 and ESR1 appear to positively regulate each other [23, 41]. Collectively these findings led Bernardo and colleagues to propose a model in which FOXA1 and ESR1 expression predominates in ductal cells, whereas GATA3 functions in ESR1- and FOXA1-negative lobulo-alveolar cells [7]. Together, these studies suggest that the ESR1/GATA3/FOXA1 transcriptional network is complex and may depend on and vary with the developmental state of the cell (Figure 3).

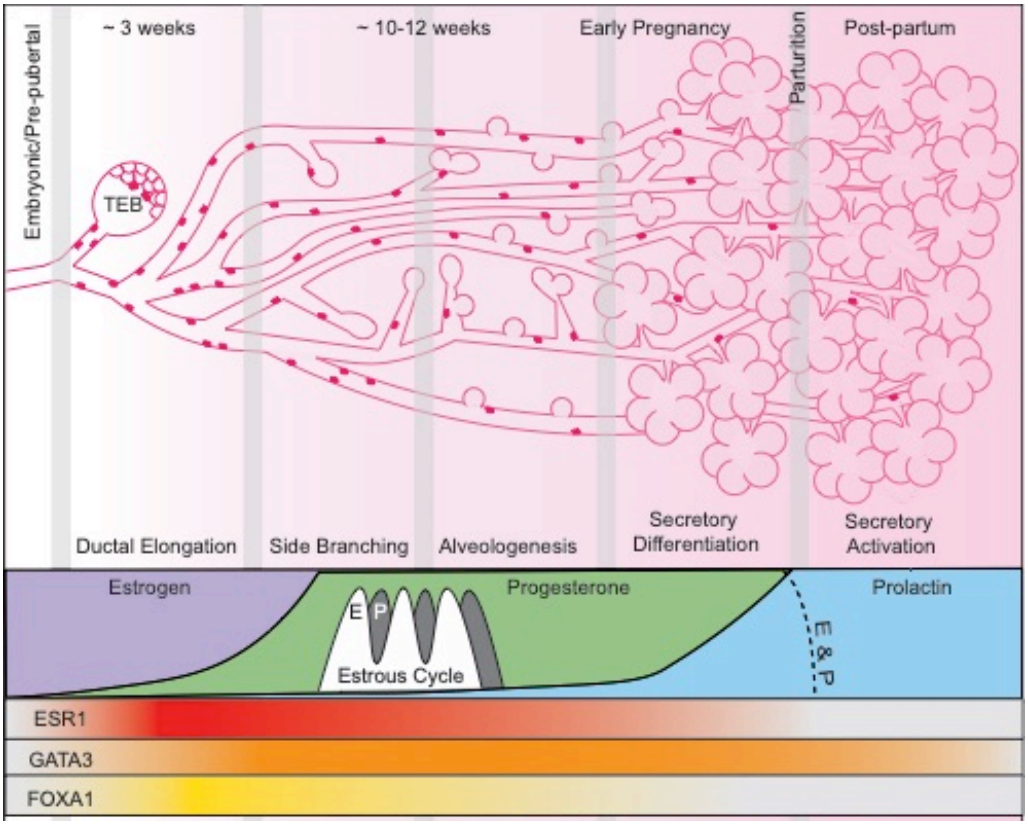

Figure 3 Transcription factor control of early ductal elongation.

Ductal side branching and alveologenesis

Estrogen and progesterone are synergistic in inducing the early phases of side branching and alveologenesis in the mammary gland [23]. In the post-natal murine mammary gland, PGR expression is not present until seven weeks of age [42, 43], whereas ESR1 expression has been observed as early as 3 weeks (Figure 4) [44]. Loss of ESR1 results in completely stunted ductal elongation as well as an absence of side branching and alveologenesis [27], whereas loss of PGR results in reduced side branching and failed alveologenesis, placing the requirement for PGR subsequent to ESR1 [20]. Interestingly, most mammary epithelial cells that express ESR1 also express

PGR, and both hormone receptors operate in a paracrine manner, as demonstrated by transplantation experiments with steroid hormone receptor null and wild-type epithelium [19, 21]. More specifically, in the presence of PGR wild-type cells, PGR null epithelial cells were capable of contributing to proliferation and alveologenesis, similar to ESR1 [21]. Despite the considerable similarities between ESR1 and PGR, ESR1 is dispensable for side branching and alveologenesis and PGR is not, demonstrating the precise hormonal and temporal control that guides mammary development.

Several mediators of PGR paracrine signaling have been suggested, and, interestingly, the osteoclast differentiation factor ligand RANKL is an attractive candidate. Mammary gland recombination studies again suggest that epithelial RANKL is required for side branching before and during pregnancy, which is consistent with the presence of progesterone in the endocrine system during adult and pregnancy-induced development (Figure 4) [45, 46]. Loss of RANKL did not impact apoptosis, PGR expression, or milk protein expression, suggesting that RANKL mediates side branching proliferation specifically, potentially in response to paracrine signaling through PGR [46]. Consistent with this hypothesis, ectopic expression of RANKL rescues the PGR null mammary development phenotype [46]. Further, progesterone induces RANKL expression, which is primarily observed in PGR positive luminal cells, again suggesting that RANKL may be involved in paracrine signal to neighboring cells [45, 47]. RANKL is recognized by the transmembrane protein RANK and signals through NF-κB (nuclear factor kappa B) to initiate transcription of target genes [45]. Clinically, RANKL is

associated with proliferation in PGR-dependent breast cancers, and RANKL inhibitors may prove useful in treating these patients [14, 46, 48, 49].

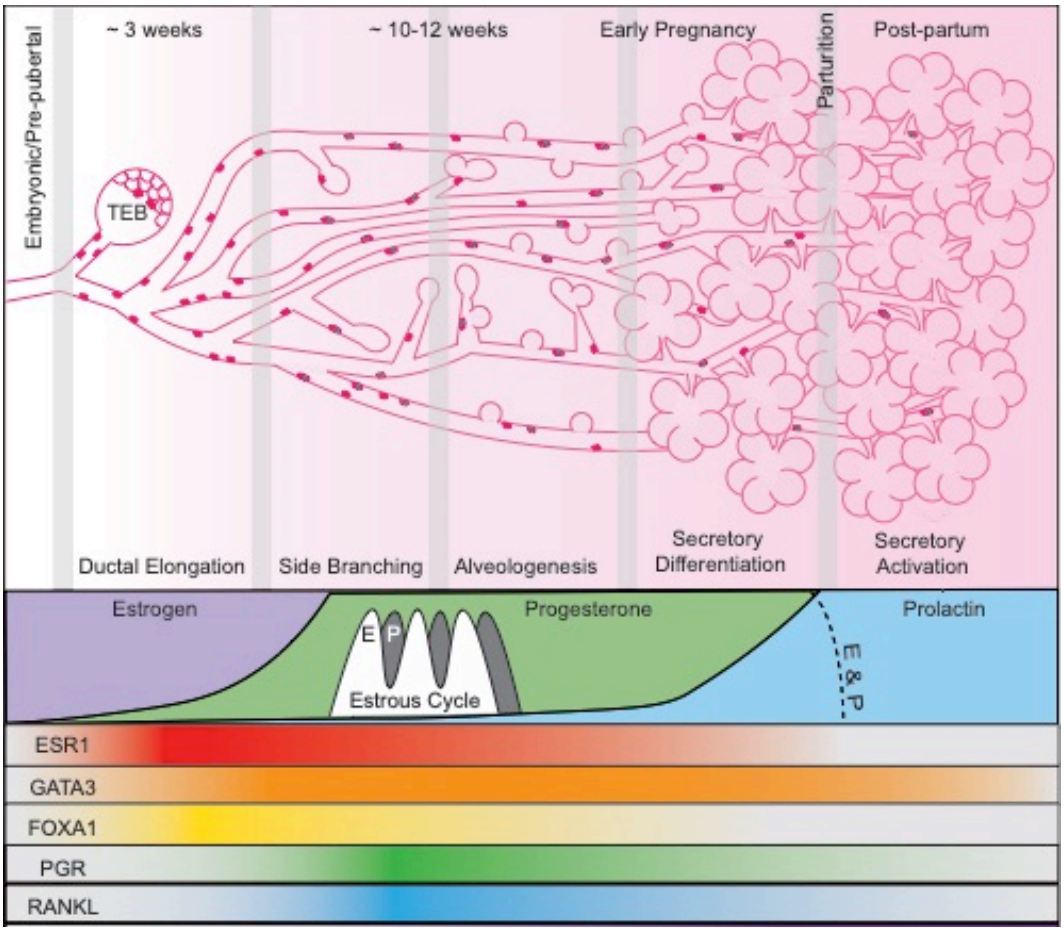

Figure 4 Transcription factor control of ductal side branching.

Alveologenesis and lactogenesis

The final stage of mammary gland development involves the terminal differentiation of luminal MECs into lobulo-alveolar cells that secrete milk proteins, lipids, and other metabolites. In a series of landmark studies, a compound purified from the anterior pituitary gland was found to induce lactation in virgin rabbits [25, 50, 51]. Based on this finding, the compound was named prolactin. Subsequent studies

demonstrated that the dopamine analog bromocryptine inhibits prolactin secretion from the anterior pituitary gland, completely abrogating lactogenesis until withdrawn [8, 52, 53]. Although PRLR (prolactin receptor) is predominantly expressed at late pregnancy, prolactin null models demonstrated sterility and reduced gland complexity, side branching, serum progesterone, and serum estrogen [8, 22, 54, 55], suggesting that prolactin has a systemic effect on ovarian hormones. Indeed, prolactin stimulates the release of ovarian hormones, notably progesterone, and restoration of progesterone rescues the absence of ductal side branching and sterility seen in ovariectomized prolactin null models [14, 54, 56]. The mammary epithelium intrinsic role of prolactin was determined by transplantation of PRLR null mammary epithelium into wild-type mice, which demonstrated that ductal elongation and branching proceed normally, but alveologenesis and lactogenesis fail [54, 55]. Together, these studies demonstrate that prolactin coordinates hormonal signaling to the developing mammary gland, and PRLR is required for alveologenesis (Figure 5).

PRLR is a transmembrane cytokine receptor that dimerizes upon ligand binding and mediates the cross-phosphorylation of JAK2 (Janus kinase 2), FYN (FYN proton-oncogene), and MAPK. Both JAK2 and its downstream target gene, STAT5, are necessary for alveologenesis and lactogenesis, as targeted deletion in the mammary epithelium results in phenotypes similar to PRLR null mice [14, 57, 58]. STAT5 is a member of a family of seven genes that encode latent transcription factors. STAT proteins are activated by tyrosine phosphorylation, dimerize, and translocate to the nucleus where they bind GAS (gamma interferon activated sequence) elements in

regulatory regions to control transcription [59]. STAT5 is present in the mammary gland in two isoforms (STAT5A and STA5B), which are both essential to the proliferation, differentiation, and survival of MECs [58, 60, 61]. Simultaneous loss of both STAT5A and STAT5B driven by *MMTV-cre* expression abrogates alveologenesis and reduces the generation of alveolar progenitors [60]. These alveolar defects are rescued by expression of STAT5A even after ductal elongation, suggesting that STAT5A is necessary and sufficient for the establishment of luminal progenitor cells (Figure 5) [60]. Beyond just STAT5, a balance of STAT protein activation exists in the developing mammary gland with high STAT5 activation beginning at day 14 of gestation and persisting through lactation and high STAT3 activation beginning with involution [62, 63]. The developmental expression pattern of STAT5 and the lactation failure observed with loss of STAT5 suggest that STAT5 activation is critical to the terminal differentiation of MECs [25]. Indeed, expression of the differentiation-dependent genes *Csn2*, *Wap*, and β-lactoglobulin, which contain GAS elements (TTCNNNGAA) in their promoter regions, is lost in the absence of STAT5 [25]. These differentiation-dependent genes are often used as indicators of terminal MEC differentiation and represent terminal function of the mammary gland.

Similar to STAT5, the Ets transcription factor ELF5 is required for alveolar differentiation [64]. Moreover, GAS elements have been identified in regulatory regions of ELF5, and ELF5 expression is lost in STAT5A/B deficient glands [60]. Conversely, ELF5 binding sites are present in the STAT5 promoter, suggesting a complex regulatory network [65, 66]. An important difference between the two factors is their effect on the

luminal progenitor lineage of MECs. Loss of STAT5 results in a reduced population of luminal progenitors, whereas loss of ELF5 initiates an expansion of luminal progenitors [67, 68]. These results indicate that STAT5 is likely upstream of ELF5 and enables the generation of luminal progenitors, whereas ELF5 enables the differentiation of progenitors [60]. ELF5 expression in differentiated progenitors may then control the expression of STAT5 [66]. Because ELF5 expression is associated with terminally differentiated lobulo-alveolar cells, and lobulo-alveolar cells are typically ESR1 negative, it has been postulated that ELF5 expression could be a marker of estrogen insensitivity and resistance to antiestrogen therapies [69, 70].

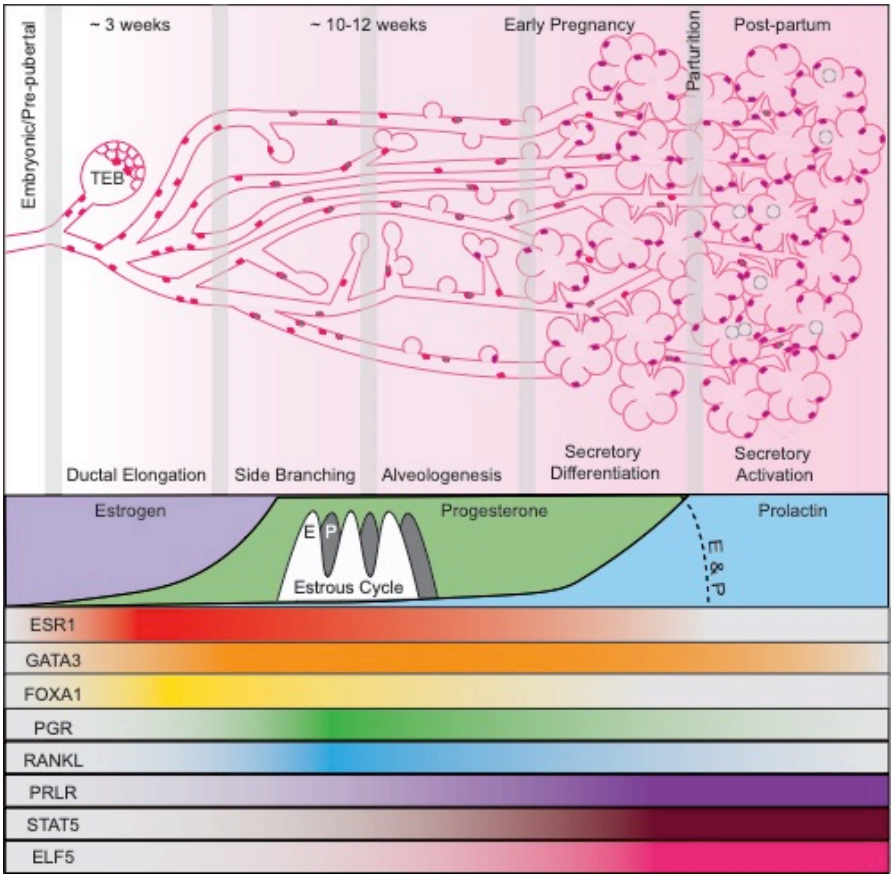

Figure 5 Transcription factor control of alveologenesis and lactogenesis.

Involution

Although lactation is typically considered the terminal differentiation of MECs, involution also represents an additional stage of MEC function, owing to the phagocytotic behavior that MECs demonstrate [71]. During involution the mammary gland regresses, resetting the gland for future reproductive events. Involution occurs in two stages: a reversible initial phase and an irreversible secondary phase [14]. Unlike the other stages of post-natal mammary gland development, the first phase of involution occurs in response to local cues rather than hormonal cues and evokes a wave of cell death [72, 73]. The second phase of involution responds to a fall in systemic hormones, which can be abrogated by glucocorticoid treatment [72, 73]. The second phase of involution is also accompanied by a rise in circulating factors that balance protease activity as well as alveolar collapse, basement membrane remodeling, and adipocyte differentiation [14]. The transcriptional signaling that coordinates the termination of lactation and the initiation of involution is of interest due to the dramatic transition in function that occurs. During this transition, STAT5 phosphorylation declines and STAT3 is rapidly phosphorylated (Figure 6). The PRLR-STAT5-AKT axis promotes the survival and lactogenic function of MECs [74, 75], whereas STAT3 antagonizes this signaling to promote apoptotic pathways [14]. Leukemia inhibitory factor (LIF) has been implicated in the upstream activation of STAT3 [76], which signals through STAT3 to upregulate the expression of IGFBP5 [77], cathepsin B, and cathepsin L [78]. Importantly, overexpression of STAT5A or AKT1 or loss of STAT3 or LIF delays

involution [74-76, 79], suggesting that activation of STAT3 or STAT5 can independently promote or delay apoptosis, respectively [14, 80].

Although the long-term benefit of pregnancy at an early age is a reduced risk of breast cancer [81], the involution period poses an increased risk for women [82]. This risk is thought to come from the generation of a tumor permissive or even promoting microenvironment. In summary, the developmental stage of the mammary gland holds key insight into the initiation and progression of breast cancer.

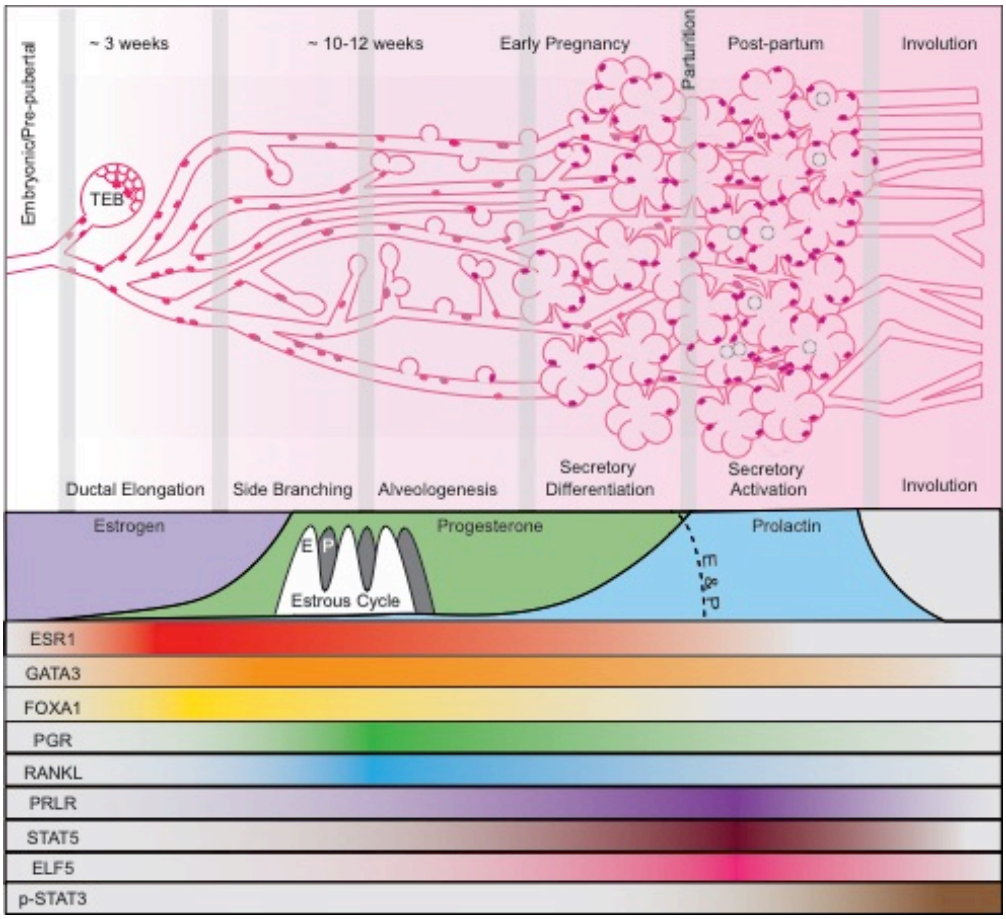

Figure 6 Transcription factor control of involution.

Metabolic regulation

Thus far we have established that a complex array of hormones and transcription factors regulate the development of the mammary gland. The ultimate function of mammary gland development is to synthesize and secrete milk to support neonatal life. Milk is composed of macronutrients (proteins, lipids, and carbohydrates), micronutrients (vitamins and minerals), and bioactive factors [83]. Thus, it is not surprising that milk production is energetically demanding and requires the systemic cooperation of the female body. Recent studies have indicated that metabolic adaptations can both respond to and direct functional tissue changes. Although metabolic adaptations are clear in the developing mammary gland, the causes and/or consequences of these adaptations are not.

The majority of major metabolic adaptations in the mammary gland occur leading up to and during the transition to lactation. The mammary gland begins preparing for lactation during early pregnancy and completes the process in two phases: secretory differentiation (lactogenesis I) and secretory activation (lactogenesis II) [8, 84]. During secretory differentiation, alveolar cells continue to proliferate and cluster into lobuloalveolar units, completely filling the gland. Cytoplasmic lipid droplets also become readily apparent and increase dramatically in size until secretory activation [84]. Secretory activation is initiated by a sharp fall in serum progesterone and is associated with milk secretion [84-86].

Transcriptional regulation of mammary gland metabolism

The transcriptional changes that occur in secretory differentiation and activation coordinate the massive production of proteins, lipids, and lactose – the primary carbohydrate found in milk and synthesized solely in mammary epithelial cells. Transcriptional changes between pregnancy day 12 and lactation day 9 have been quantitatively clustered into trajectories based on whether expression of a set of factors increased, decreased, or remained constant between two consecutive developmental time points [87, 88]. Using this trajectory clustering, the Neville group demonstrated that milk protein expression rises from the earliest time point studied, pregnancy day 12, until lactation day 2 when expression levels off [87]. This supports the observation that milk protein genes are expressed as early as five days after conception in rats [11]. Early elevation of milk protein genes is concomitant with decreased expression of adipocyte and collagen factors, likely due to regression of the mammary fat pad [84, 87]. As discussed above, the majority of milk protein transcription is controlled through PRLR and subsequent STAT5 activation.

In contrast, lipid biosynthesis is more tightly controlled around parturition, when fatty acid and cholesterol synthesis gene expression rises (Figure 7) [84, 87]. Expression of factors involved in degradation of fatty acids (beta-oxidation) decrease at this time, supporting the idea that MECs shuttle free fatty acids into triglyceride synthesis [87]. Further, alpha-lactalbumin (LALBA), the rate limiting cofactor for lactose synthesis, is strongly upregulated upon secretory activation [84]. Notably, the synthesis of both fatty acids and lactose requires an elevated concentration of glucose. Correspondingly,

GLUT1 is strongly upregulated at parturition to transport glucose from plasma to MECs [89]. Glucose is utilized for lactose synthesis at the Golgi, which is supported by increased localization of GLUT1 to the Golgi itself [90]. Moreover, increased expression of hexokinase 2 (HK2) and reduced expression of HK1 is thought to allow more free glucose to enter the Golgi and to activate the pentose phosphate shunt [84, 91]. Activation of the pentose phosphate shunt, which generates NADPH for lipid synthesis, is further aided by reduced expression of glucose-6-phosphate isomerase after parturition [84, 92]. Lipid synthesis is supported by upregulation of aldolase C to facilitate glycerol formation [93], mitochondrial production of citrate, and upregulation of ATP citrate lyase (ACLY) [92], which converts citrate to acetyl-CoA for the subsequent synthesis of malonyl-CoA. With the exception of GLUT1, many of these factors are thought to be controlled at the transcriptional level by SREBF1 (sterol regulatory element binding transcription factor 1, or SREBP1c) [94, 95], potentially through AKT1 [96-98].

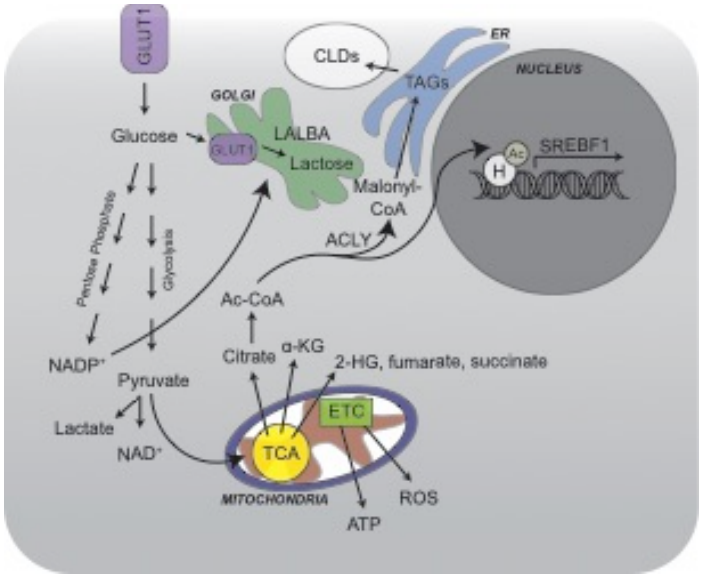

Figure 7 Model of mitochondrial metabolites during differentiation.

Based on the current body of knowledge, expression of milk protein and metabolic enzyme genes during secretory differentiation is thought to occur through PRLR mediated activation of STAT5, whereas the expression of genes involved in fatty acid, lactose, and cholesterol synthesis during secretory activation is thought to occur through AKT1 mediated activation of SREBF1 after the release of progesterone antagonization [84]. Of note, AKT1 activation can occur through PRLR dependent or independent mechanisms. Together, these observations create the basis for our understanding of metabolic adaptation in the mammary gland (Figure 8). However, many studies have shown that post-translational modifications to proteins and enzymes as well as the output of organelles, such as mitochondria, can have dramatic and dynamic effects on cell state and function [99, 100]. Future studies will need to consider the broader picture of metabolic events that enable lactation. In this study, we identify a novel process, mitophagy, and a novel function for a known factor, SIM2s, in the regulation of MEC metabolic reprogramming during differentiation.

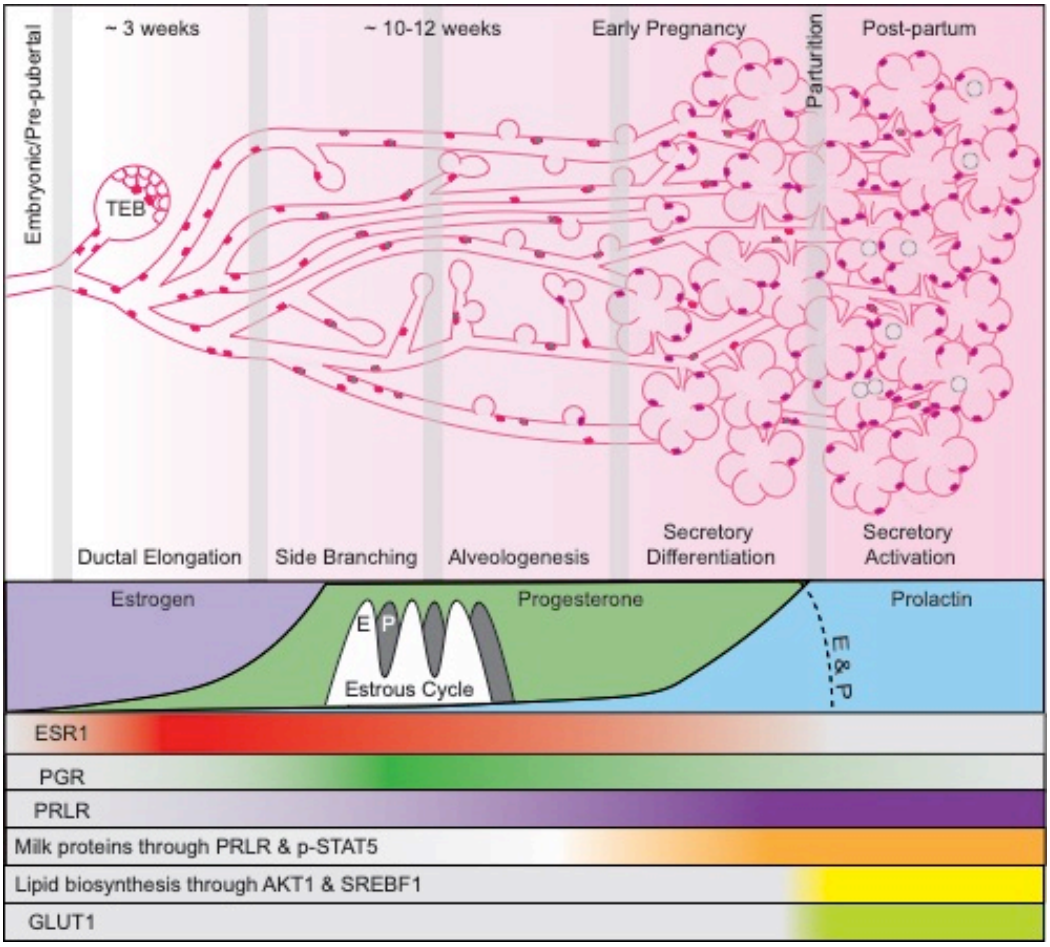

Figure 8 Factors related to metabolic differentiation of MECs are expressed in two waves.

Metabolism and mitochondrial homeostasis

Metabolism can be broadly defined as the biochemical reactions in a cell that break down (catabolize) or build (anabolize) molecules. Importantly, cellular metabolism responds both to intrinsic signaling pathways and extrinsic environmental factors. Homeostatic fluctuations in metabolism allow a cell to respond to signaling or environmental stimuli. In contrast, metabolic reprogramming has distinct effects on the function of a cell. The observation that tumor cells undergo a metabolic transition

toward aerobic glycolysis, termed the Warburg effect, generated substantial interest in understanding the regulation of metabolic reprogramming [101]. Fortunately, metabolic reprogramming and the Warburg effect both occur in normal cells and offer insight into development and malignancy [99]. For example, myoblast differentiation relies on a metabolic transition from a glycolytic state to an oxidative state [102], whereas neuroblast differentiation into retinal ganglion cells relies on the reverse transition from an oxidative state towards a glycolytic state [103]. As noted in these examples as well as others listed in Table 1, many of the metabolic reprogramming events that have been documented coincide with development or differentiation. Although metabolic reprogramming has dramatic consequences for cell function, it is not yet clear how cells acquire a particular metabolic state or whether intrinsic or extrinsic factors are involved.

The developing post-natal mammary gland is a unique model in which MECs transition from a catabolic state of rapid proliferation to an anabolic state of milk production. The metabolic reprogramming between these two states is dramatic, and the regulation of the transition has been largely attributed to hormone-induced transcriptional changes [8, 84, 87, 92]. Other changes occur during this transition as well, including elongation of mitochondria [104, 105]. In fact, dramatic changes in mitochondrial organization and structure are observed during development of the mammary gland as well as in the differentiation of other cell types. Thus, hormonal, transcriptional, metabolic, and mitochondrial adaptations occur during MEC differentiation and collectively support the lactogenic function of the gland. In comparison to the hormonal, transcriptional, and metabolic adaptations, we know very

little about how mitochondria contribute to mammary gland development. Based on the connection between mitochondrial form and function [106], as well as the connection between mitochondria and metabolic processes, our lab is interested in understanding the initiation and functional outcome of mitochondrial adaptations during mammary gland development.

Table 1. Metabolic transitions in development and differentiation are regulated by mitochondrial fission (pink), fusion (purple), biogenesis (green), and mitophagy (blue).

Tissue	Model	Beginning Energy State	Ending Energy State	Transition	Factor involved	Ref.
Adipose	Mouse	Thermogenic beige fat	Quiescent white fat	Beige adipocyte to white adipocyte transition	ATG5 ATG12	[107]
Adipose	Mouse	Basal metabolism	Quiescent	Adipocyte differentiation	PARL through cleavage of PINK1	[108]
Adipose	Mouse	Fatty acid oxidation	Quiescent	Embryonic adipogenesis	ATG7	[109, 110]
Blood	Mouse Human	Basal metabolism	Quiescent	Erythrocytes differentiation to mature erythroid cells	NIX/ BNIP3L	[111]
Blood	Mouse Human	Glycolytic	Fatty acid oxidation	Hematopoietic stem cell expansion	PINK1, PRKN	[112]
Eye	Mouse	Oxidative	Glycolytic	Embryonic retinal ganglion cell differentiation	NIX/ BNIP3L	[103]
Heart	Mouse	Glycolytic (Glucose metabolism)	Fatty acid oxidation	Embryonic cardiomyocyte differentiation	PRKN by way of MFN2 mutation	[113]
Heart	Mouse	Embryonic stem cell (ESC)	Cardio-myocyte	ESC to cardiomyocyte differentiation	MFN1/2 & OPA1, NOTCH and calcineurin	[114]
Immune cells	Human	Aerobic glycolysis	Fatty acid oxidation, Oxidative	Effector T cell to memory T cell transition	OPA1	[115]
iPSC	Human	Oxidative	Glycolytic	Somatic cell reprogramming to iPSC	DNM1L	[116]
iPSC	Human	Oxidative	Glycolytic	Somatic cell reprogramming to iPSC	ATG3	[117]

Table 1 Continued.

Tissue	Model	Beginning Energy State	Ending Energy State	Transition	Factor involved	Ref.
Mammary	Mouse	Unknown	Unknown	Transition from reversible to irreversible stage of involution	ATG7	[118]
Mammary	Mouse	Quiescent	Energetic	Differentiation of mammary epithelial cells	ATG5, ATG7, PRKN	[119]
Muscle	Mouse	Glycolytic	Oxidative	Myoblast differentiation to myotubules	ATG5, SQSTM1	[102]
Muscle	Mouse	Glycolytic	Oxidative	Myoblast differentiation to myotubules	ATG7, BNIP3	[120]
Muscle	Mouse	Glycolytic	Oxidative	Fiber type IIX, IIB versus type I, IIA	MFN1/2 dependent	[121]
Neuronal	Human	Glycolytic	Oxidative	Undifferentiated glioblastoma to differentiated induced astroglia	cAMP-CREB-PGC1A	[122]
Tumor	Human	Oxidative	Glycolytic	RAS-induced transformation of cancer cells	DNM1L	[123]

The powerhouse of the cell

Mitochondria are double membrane organelles that operate as a central hub for many metabolic processes by sensing and responding to the cellular environment to maintain homeostasis [106, 124]. Mitochondria are famous for their role in ATP generation and are the site of the tricarboxylic acid (TCA) cycle and electron transport chain, which is responsible for mitochondrial respiration. Additionally, mitochondria maintain their own DNA (mtDNA), and elevated mtDNA mutations lead to early aging in mice [125, 126], supporting the observation that mitochondrial function declines with age and is critical for longevity [127]. Many notable metabolites are generated in mitochondria, including citrate, acetyl-CoA, alpha-ketoglutarate, reactive oxygen species

(ROS), NADH, and ATP. Importantly, these metabolites contribute to cell state and differentiation. For example, mitochondrial production of alpha-ketoglutarate is a rate limiting factor for alpha-ketoglutarate-dependent dioxygenases, which demethylate DNA, ultimately influencing the epigenetic state of embryonic stem cells [128]. Further, ROS have been implicated as signaling molecules, and ROS generated from complex III of the electron transport chain direct adipocyte differentiation through induction of PPARG (peroxisome proliferator activated receptor gamma) transcriptional activity [129, 130]. Thus, the functionality of mitochondria is important to cell state and has been suggested to direct to cell fate (Table 1, Figure 9).

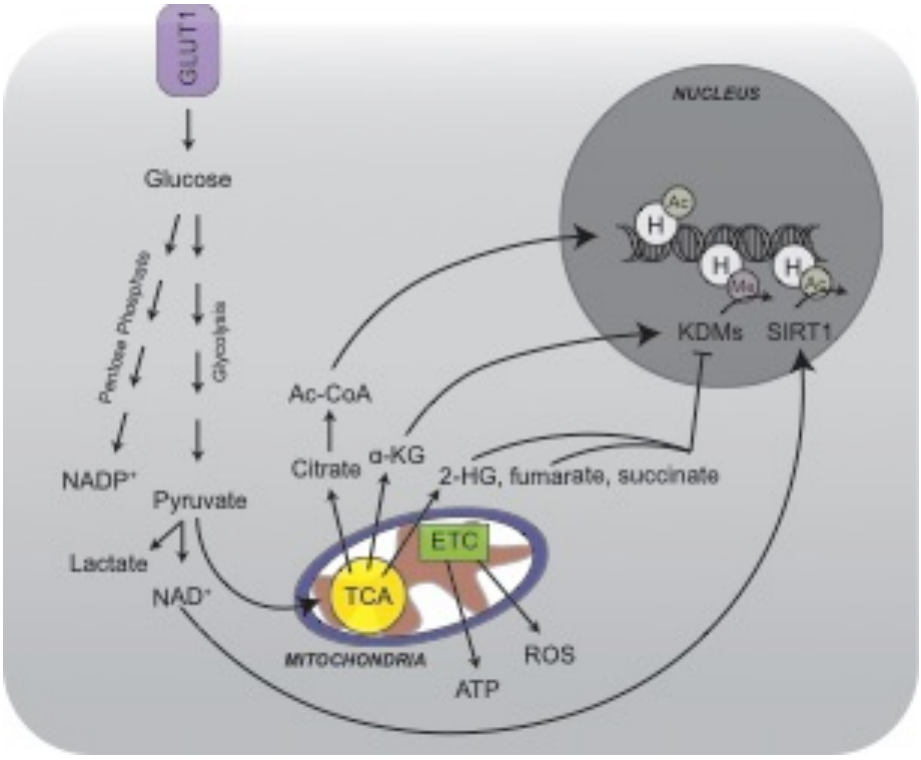

Figure 9 Model of contribution of mitochondrial metabolites to cell signaling.

The generation of mitochondrial metabolites is influenced by mitochondrial homeostasis, which is maintained through the coordination of fission, fusion, mitochondrial specific autophagy (mitophagy), and biogenesis (Figure 10) [131]. These processes can be governed by both intrinsic signaling pathways and extrinsic environmental cues, allowing cells to finely tune metabolic responses. Many studies have now shown that factors involved in these processes also enable mitochondria to instruct function by contributing to epigenetic status, cell fate decisions, and differentiation [102, 107, 115, 132], largely through the generation of metabolites or lack thereof. A working understanding of the crosstalk between fission, fusion, mitophagy, and biogenesis is required to understand mitochondrial homeostasis and how its disruption contributes to disease.

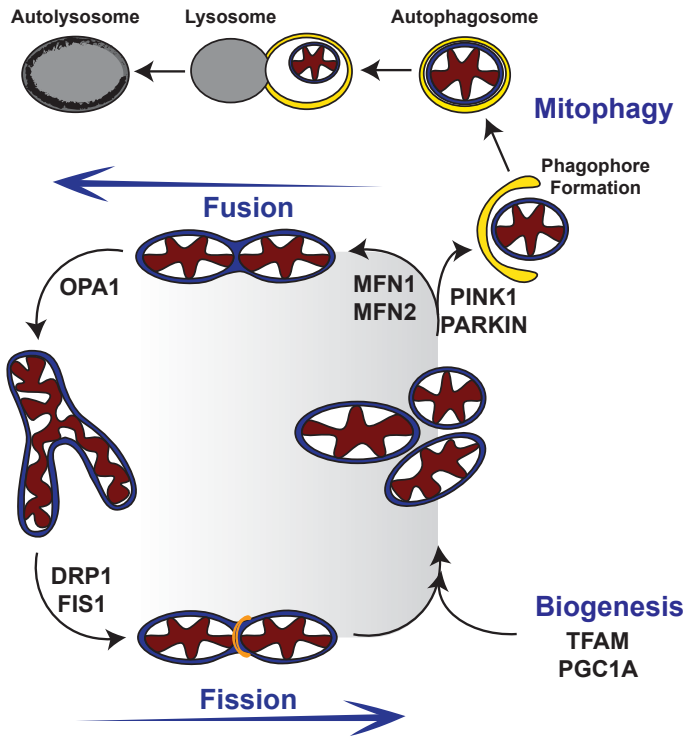

Figure 10 Model of mitochondrial homeostasis.

The long and short of mitochondria

Fission and fusion, termed mitochondrial dynamics, are responsible for homeostatic alterations in mitochondrial number, mass, and morphology that allow mitochondria to maintain dynamic networks within the cell [131]. Fission divides mitochondria into smaller organelles, and plays important roles in biogenesis, motility, and stress response. In contrast, fusion joins mitochondria together, forming larger networks and contributing to the dispersion of mtDNA, proteins, and metabolites. In brief, mammalian mitochondrial dynamics are primarily mediated by the dynamin-related guanosine triphosphatases: dynamin 1 like (DNM1L [also known as DRP1]), mitofusin 1 and 2 (MFN1/MFN2), and optic atrophy 1 (OPA1) [131]. During mitochondrial fission, FIS1 (fission, mitochondrial 1) interacts with DNM1L and anchors it to the outer mitochondrial membrane (OMM). DNM1L oligomerizes around mitochondria, forming a collar that eventually contracts and divides mitochondria into separate organelles. On the other hand, mitochondrial fusion is initiated by docking of two mitochondria through the interaction of mitofusins between mitochondrion, which enables the fusion of the OMMs. Subsequently, OPA1, located on the inner mitochondrial membrane (IMM), mediates the fusion of IMMs, completing the fusion process. These processes are highly integrated as decreased fission gives rise to an elongated mitochondrial network, and decreased fusion results in mitochondrial fragmentation [133]. This integration allows cells to respond to both intrinsic and extrinsic stimuli to adjust metabolic output. In general, mitochondrial fission is associated with cellular proliferation and reduced respiration [116, 134], whereas

mitochondrial fusion has been linked to enhanced cellular respiration, ROS production, mitophagy escape, and differentiation [114, 135-137].

The importance of mitochondrial dynamics is underscored by the serious human diseases that result from disruption of the factors involved [138]. For example, mutations in OPA1 and MFN2 that disrupt mitochondrial fusion result in autosomal dominant optic atrophy and Charcot-Marie-Tooth disease type 2a, respectively [139, 140]. Although mitochondrial dynamics factors are widely expressed, their mutation primarily affects neurons, which tightly regulate mitochondrial function and distribution [138]. Severe defects also occur with dysregulation of mitochondrial dynamics in other highly metabolic tissues, including the heart and muscle, suggesting that mitochondrial dynamics may play a role in the mammary gland during lactation.

Consistent with this hypothesis, mitochondrial dynamics have recently been shown to impact cell fate and differentiation. For example, MFN2-mediated mitochondrial fusion is required for cardiomyocyte differentiation through NOTCH signaling [114], and DNM1L-mediated mitochondrial fission is required for somatic cell reprogramming to induced pluripotent stem cells and involves MAPK1 (mitogen-activated protein kinase 1 [also known as ERK]) signaling [116]. Although the investigation of mitochondrial dynamics in development and differentiation is in its infancy, it is clear that mitochondrial form instructs mitochondrial function and is well worth investigating in cell types with specialized functional states, such as the lactating mammary gland.

Taking out the trash, or maybe just recycling

Mitochondrial dynamics is tightly coupled to mitophagy and mitochondrial biogenesis [141]. Inhibition of mitophagy results in the accumulation of fragmented mitochondria, whereas inhibition of fission results in mitophagy escape [142]. In turn, each of these alterations has an effect on the respiratory machinery, causing reduced membrane potential and reserve respiration capacity, respectively [143, 144]. Further, as mitochondria cannot be generated *de novo*, they necessarily rely on mitochondrial fission for proliferation [138, 141]. Recent studies have highlighted the importance of fission, fusion, mitophagy, and biogenesis in cell and tissue differentiation and maintenance of cellular homeostasis. In fact, mitophagy-dependent differentiation programs, termed programmed mitophagy, have recently been established in a number of models and tissues [102, 107, 113]. Programmed mitophagy occurs in response to a differentiation-dependent cue and independent of cellular stresses, such as nutrient deprivation [103]. The recent recognition of a role for mitophagy in differentiation has generated a number of unanswered questions, and leaders in the autophagy field have emphasized several.

> *"...the mechanism of mitophagy under physiological (as opposed to experimental) conditions, the post-translational and structural modifications that occur to temporally control receptor-ligand interactions, and the regulatory pathways that integrate stress and developmental signals to coordinate the mode of selective autophagy with precise cellular needs." [145]*

Mammary gland development and mammary epithelial cell differentiation provide excellent tandem *in vivo* and *in vitro* models to address these unanswered questions. More specifically, our lab is interested in pursuing the unknown regulatory pathways that engage mitophagy during specific developmental time frames. We have recently shown that differentiated HC11 MECs attain a highly energetic state that relies on oxidative phosphorylation, glycolysis, and autophagy [119]. We hypothesize that MEC differentiation relies heavily on this metabolic reprogramming, which may occur through mitophagy.

In general, mitophagy is initiated when mitochondria are flagged for degradation by mitophagy receptors and proceeds when mitophagy receptors are recognized by autophagy receptors on the autophagore membrane [146]. After cargo recognition, mitophagy proceeds in the same manner as macroautophagy with the engulfment of cytoplasmic material into an autophagosome, lysosome fusion, and enzymatic degradation of vesicle contents [147]. The best characterized mitophagy pathway is the PINK1 (phosphatase and tensin homolog [PTEN] induced putative kinase)/PRKN (parkin) pathway (Figure 11). PINK1 is imported into the inner membrane space (IMS) of healthy mitochondria and rapidly cleaved. Mitochondrial damage or stress often triggers mitochondrial depolarization, which prevents protein import into the IMS. Thus, PINK1/PRKN-dependent mitophagy is initiated by accumulation of PINK1 on the OMM of depolarized mitochondria [113, 148]. PRKN then recognizes proteins phosphorylated by PINK1 and translocates to mitochondria to ubiquitinate OMM proteins. These ubiquitin chains are recognized by specific autophagy receptors, such as

SQSTM1 (sequestosome 1), and initiate phagophore recruitment through interaction with LC3 (microtubule associated protein 1 light chain 3), setting autophagic flux in motion. The PINK1/PRKN mitophagy pathway has also been implicated in the inhibition of fusion and promotion of fission, again highlighting the complex interplay between mitochondrial dynamics and mitophagy [142, 149].

Figure 11 Model of PINK1/PRKN mediated mitophagy.

In addition to the PINK1/PRKN pathway, a number of novel mitophagy and autophagy receptors have been recently identified, including BNIP3 (BCL2 interacting protein 3) [111], NIX/BNIP3L [111, 150], FUNDC1 (FUN14 domain containing 1) [151, 152], and OPTN (optineurin) [153]. These factors may contribute to the cell type specificity of mitophagy, which is of particular interest in differentiating cells. Interestingly, single-minded 2 (SIM2), a transcription factor first identified in drosophila, has been shown to be bound and subsequently ubiquitinated by PRKN [154], suggesting that SIM2 may be involved in PRKN-mediated mitophagy. Here, we present data to suggest that SIM2s regulates mammary epithelial cell differentiation, not as a classical transcription factor, but by interacting directly with mitochondria and modulating both mitophagy and dynamics. The precise mechanism by which SIM2s regulates mitophagy and dynamics, and the general interplay of these factors during development are topics for future investigation. On a broad level, we are interested in

understanding how the regulatory biology of mitochondria contributes to development, which we expect will provide insight into therapeutic approaches for combatting mitochondrial dysfunction and resulting disease states.

Single-minded 2s

The bHLH-PAS family of transcription factors

Members of the bHLH-PAS (basic helix-loop-helix PER-ARNT-SIM) family function in signaling modules that respond to the environment, physiology, and development [155]. As the name implies, bHLH-PAS proteins contain a DNA binding basic region, a dimerization HLH region, and two protein interacting PAS domains. Although numerous bHLH-PAS proteins have been identified in a wide range of organisms, the most notable mammalian variants include the aryl hydrocarbon receptors (AHR and AHRR), hypoxia inducible factors (HIF1A, HIF2A/EPAS1, and HIF3A), circadian regulators (ARNTL/BMAL1, ARNTL2/BMAL2, and CLOCK), aryl hydrocarbon receptor nuclear translocators (ARNT and ARNT2), and single-minded proteins (SIM1 and SIM2) [156]. These proteins share a basic domain structure, with a bHLH domain at the N-terminus followed by two PAS domains. Despite low sequence homology, the three-dimensional PAS domain structure is surprisingly well conserved between bHLH-PAS proteins and forms a PAS-fold, which is thought to be the site of small molecule interactions and protein binding [156, 157]. Indeed, human single nucleotide variants in the PAS domains of SIM1 and SIM2 show reduced dimerization ability, suggesting that the PAS domain is vital to protein-protein interactions [158]. Interestingly, the C-terminus of bHLH-PAS proteins contains a large degree of

variability [159], and several studies have identified transcriptional activation or repression domains in this region [160-164]. Altogether, the conserved structure of the bHLH and PAS domains as well as the intrinsic disorder of the C-termini contribute to the diverse nature of bHLH-PAS protein signal transduction [159, 165]. Due to their significant role in signal transduction, the responses of bHLH-PAS proteins to physiological and environmental stimuli have been studied in detail; however, the developmental signaling pathways of bHLH-PAS proteins remain elusive (Table 2).

The difficulty in assessing the developmental role of bHLH-PAS factors lies in their essentiality to development itself. For example, HIF1A and HIF2A knockout mice die *in utero* [166-168], SIM1 and SIM2 knockout mice die perinatally [169-172], and ARNT knockout mice die *in utero* [173, 174]. Due to these severe phenotypes, tissue-specific or inducible models have been used to study the function of these proteins and have contributed to our current understanding of the signal transduction pathways, which are described in more described below. In contrast, ARNTL/BMAL1 and CLOCK are not essential to embryonic development [175]. ARNTL/BMAL1 knockout mice have disrupted circadian rhythmicity, altered sleep patterns, reduced activity, and shortened life spans [175-179]. CLOCK knockout mice do not demonstrate completely dysregulated circadian rhythmicity but do have shortened oscillations and altered responses to light [180-182]. These phenotypes do not rule out the role of the circadian bHLH-PAS factors in development but also do not suggest that they are heavily involved in development. Although AHR is also dispensable for embryonic development, several developmental phenotypes are present in AHR knockout mice, including reduced body

weight and liver size [183-185]. It has been posited that endogenous developmental ligands or physiological activation mechanisms are responsible for AHR signal transduction during development; however, the identity of these ligands remains elusive [156]. Similarly, little is known about developmentally-engaged bHLH-PAS signaling in general.

Outside of development, bHLH-PAS proteins have been demonstrated to sense light, oxygen, toxins, cAMP, and NADH [157]. Upon ligand sensing, bHLH-PAS proteins initiate a transcriptional signaling response. This signaling response is often regulated by cytoplasmic to nuclear translocation of the bHLH-PAS protein and dimerization with a bHLH-PAS partner [186]. Interestingly, it remains unclear whether dimerization precedes or is followed by nuclear translocation. Dimerization ability of bHLH-PAS proteins is generally guided by class: class I (HIF1A, HIF2A, HIF3A, AHR, AHRR, NPAS1, NPAS2, NPAS3, NPAS4, SIM1, SIM2, and CLOCK) and class II (ARNT, ARNT2, ARNTL/BMAL1, ARNTL2/BMAL2) [165]. Class II members are general binding partners of class I members, are generally capable of forming homodimers, and are ubiquitously expressed, whereas class I members are thought to be expressed in a spatiotemporal or signal dependent manner. Importantly, the identity of the bHLH-PAS heterodimer specifies the transcriptional response, with each bHLH-PAS pair recognizing a specific sequence in the regulatory regions of target genes [187]. Thus, the cytoplasmic to nuclear translocation and dimerization of bHLH-PAS proteins provide important regulatory steps in the signal transduction pathway.

For example, cytosolic AHR is constitutively bound to HSP90 (heat shock protein 90), p23, and AIP (AHR interacting protein). Upon binding to its ligand (dioxin), AHR dissociates, translocates to the nucleus, and binds to ARNT. The AHR:ARNT heterodimer then binds to xenobiotic or dioxin response elements (XRE/DRE, TNGCGTG) in the upstream region of target genes to initiate their transcription [156].

HIF1A also initiates transcription of its target genes after binding to ARNT; however, nuclear translocation of HIF1A is dependent on protein stabilization rather than dissociation from a protein complex, and HIF1A:ARNT heterodimers recognize the hypoxia response element (HRE, RACGTG) [186]. HIF1A is rapidly degraded in the cytosol under normoxic conditions by hydroxylation of proline and asparagine residues, which are then recognized by von Hippel Lindau (VHL), targeting HIF1A for proteasomal degradation [156]. In response to low oxygen conditions, hydroxylation of HIF1A residues is inhibited, allowing for HIF1A accumulation, ARNT binding, nuclear translocation, and subsequent target gene transcription.

The last well-characterized bHLH-PAS signaling pathway is the circadian timing system, which is mediated by the bHLH-PAS proteins ARNTL/BMAL1 and CLOCK as well as by the PAS-containing periods (PER1, PER2, and PER3) and non-PAS-containing cryptochromes (CRY1 and CRY2). Nuclear ARNTL:CLOCK dimers recognize E-box signatures (CACGTG) and initiate transcription of the negative circadian transcriptional regulators PER1, PER2, PER3, CRY1, and CRY2 [186]. Phosphorylation of the PERs and CRYs results in nuclear translocation and interference in the ARNTL:CLOCK complex, halting transcription of ARNTL:CLOCK target genes

with a rhythmicity of approximately 24 hours [156]. In summary, the cytosolic to nuclear translocation of bHLH-PAS dimers is regulated by direct interaction with the ligand, as in AHR binding of dioxin, and by indirect ligand sensing through post-translational modifications, as in oxygen-sensitive hydroxylation of HIF1A and phosphorylation of PER and CRY proteins, which then influence ARNTL:CLOCK transcriptional activity.

In contrast, SIM1 and SIM2 signaling networks are relatively poorly understood. Studies in Drosophila have provided the most insight into the transcriptional network of *sim*. Drosophila *sim* is known to form heterodimers with *tango*, the drosophila ortholog of mammalian ARNT, and bind to CNS midline elements (CMEs, ACGTG) to activate transcription [163, 188]. In this context, nuclear translocation of *sim* is dependent on dimerization with *tango* [163]. Similar to mammalian AHR, *sim* also interacts with *hsp90*, and this interaction is disrupted by *sim* dimerization with *tango* or *per* [189]. Mammalian SIM1 [190] and SIM2 also interact with HSP90 [191] and form heterodimers with ARNT [160, 190, 192, 193]. Interestingly, the SIM1:ARNT heterodimer activates transcription of target genes [160, 194], whereas the SIM2:ARNT heterodimer was initially reported to lack transcriptional activity [161, 164]. These reports identified mammalian SIM2 as the first bHLH-PAS transrepressor. The repressor activity of SIM2 is thought to occur through competition with SIM1 [160], AHR [193], and HIF1A [161] for ARNT binding; through competition with SIM1:ARNT and HIF1A:ARNT complexes for binding at regulatory regions [194]; and through two transcriptional repression domains in the C-terminus of SIM2 [161]. Several

transcriptional targets of SIM2 have been described, including MYOM2, MYOD1, and BNIP3 [195-197], and a recent study identified over 1,000 DNA binding sites for SIM2 in mouse embryonic stem cells via ChIPseq analysis [198]. Although these studies have provided insight into the dimerization and transcriptional activities of SIM, the signal transduction pathways that regulate the activation or cytoplasmic to nuclear translocation of SIM2 are unknown. Based on the clear developmental role of SIM2 and the lack of knowledge regarding its regulation, our lab has sought to understand the underlying molecular biology of this bHLH-PAS protein.

Table 2. bHLH-PAS protein regulation.

bHLH-PAS	Binding Partner	Binding Element	Lethality of loss	Development Stimulus	General Stimulus
AHR	ARNT, ARNT2	XRE: TNG**CGTG**	None	**Unknown**	Xenobiotics, dioxin
HIF1A	ARNT, ARNT2	HRE: RA**CGTG**	*In utero*	Hypoxia	Hypoxia
HIF2A	ARNT, ARNT2	HRE: RA**CGTG**	*In utero*	Hypoxia	Hypoxia
CLOCK	ARNTL/ BMAL1, ARNTL2/ BMAL2	E-box: CA**CGTG**	None	Ubiquitous	Ubiquitous
SIM1	ARNT, ARNT2	CME: A**CGTG**	Peri-natal	**Unknown**	**Unknown**
SIM2	ARNT, ARNT2	CME: A**CGTG**	Peri-natal	**Unknown**	Ethanol, DNA damage

Discovery of single-minded

L(3)S8 was first identified by complementation group analysis of the *rosy* locus in Drosophila [199] and was later renamed *single-minded* based on its expression along the midline of the neuroepithelium [200]. Homozygous mutation of *sim* results in late embryonic lethality and failure of midline cell emergence [200]. Further analysis of *sim*

mutant embryos revealed that loss of midline cells during neurogenesis is due to failed midline cell differentiation. In contrast, ectopic expression of *sim* can force a midline cell differentiation program in non-midline cells of the lateral CNS and is the reason that *sim* is often referred to as a master regulator of CNS midline development [201]. *Sim* is also expressed in a subset of ventral muscle precursor cells, and localization of the ventral oblique muscles is aberrant in *sim* null flies, which is attributed to dysfunctional *sim* signaling from the CNS [202]. Of note, *sim* expression in the CNS appears to be broadly conserved across species, ranging from *Xenopus* and *Gallus* to a variety of arthropods [203-208]. Together, these early studies demonstrate that *sim* is essential for midline development, which is driven by the CNS.

Initially, *sim* expression was observed to be limited to the nucleus of cells along the midline of the neuroepithelium in Drosophila [209], and early analysis of the sequence of *sim* revealed strong similarity to *period*, which regulates circadian rhythms in Drosophila [209]. Eventually, *sim* was defined as a bHLH transcription factor, and characterization of the transcriptional network suggested that *sim* is required for the expression of *slit*, *toll*, *rhomboid*, *engralled*, and *91F* but is repressed by *snail* during midline cell differentiation [210, 211]. Additional targets of *sim* include *47F*, *cdi*, and *sim* itself [211]. The transcriptional activity of *sim* relies on its three C-terminal activation domains, the bHLH domain, and the PAS dimerization domain [162]. Analysis of the full-length *sim* gene revealed that *sim* has two promoters, which are temporally activated and denoted as early (upstream of exon 2) and late (upstream of exon 1) based on the timing of their activity during embryonic development [211].

Although the majority of studies in Drosophila indicate that *sim* is a transcriptional activator, some reports demonstrate that *sim* can function as a transcriptional repressor. For example, sim represses *wingless*, *hedgehog*, and *ventral nervous system defective* to hinder ventral ectodermal cell fate [212]. These studies establish the basis of the downstream transcriptional signaling network of *sim* in Drosophila, but our understanding of the upstream signaling pathways that activate *sim* remains limited.

Post-embryonic and functional analyses of *sim* are limited by its recessive embryonic lethal phenotype. To study the post-embryonic function of *sim*, a temperature-sensitive mutant allele was identified, isolated, and analyzed under permissive and restrictive temperatures [213]. The authors found that, in addition to the previously observed CNS midline cell effects, *sim* mutant flies were sterile and displayed marked behavioral abnormalities, indicating defects in the brain central complex [213]. The involvement of *sim* in Drosophila CNS development and function lends support to the idea that the mammalian ortholog, SIM2, contributes to the etiology Down Syndrome, which is discussed below.

Chromosomal location of single-minded 2

Down Syndrome is the most common chromosomal disorder in the United States, affecting roughly 1 in 700 births [214]. The prevalence of Down Syndrome has increased from 1999 to 2014 and is characterized by distinctive facial features and mental aberrations [214]. Down Syndrome typically results from the presence of an extra copy of chromosome 21, but analysis of rare patients with partial trisomy 21 narrowed this definition down to a 1.6-megabase region in chromosome 21q22.2 known as the

Down Syndrome critical region (DSCR) [215-217]. The genes encoded in this region are of interest for a number of reasons. First, it has been postulated that an extra copy of a gene (or genes) in the DSCR contributes to the Down Syndrome phenotype [218]. Second, individuals with Down Syndrome are at increased risk for childhood leukemias and decreased risk for solid tumors, particularly breast tumors [219]. This malignancy profile suggests that leukemia and tumor suppressor genes may be present in the DSCR [219]. Finally, variations in the DSCR are thought to alter the function of DSCR genes, contributing to the variability observed in Down Syndrome phenotypes [220].

Human SIM2 was originally associated with the DSCR by exon trapping [221-223] and was later found to have two transcripts: SIM2-long (SIM2l) and SIM2-short (SIM2s), a shorter alternative splicing variant [223]. At the same time, murine *Sim1* and *Sim2* were identified in a low stringency screen for the Drosophila *sim* bHLH domain [224]. *Sim1* maps to murine chromosome 10, and *Sim2* maps to murine chromosome 16, which is syntenic to human chromosome 21 and supports the identification of human SIM2 in the DSCR [224]. In further support of a connection between SIM2 and Down Syndrome, SIM2 is expressed in the diencephalon during embryonic development in mice [164, 225-227] and humans [228] and is found in regions of the brain that are implicated in Down Syndrome phenotypes, including the fetal neocortex, hippocampus, dentate gyrus, and cerebellum [228]. This overlap led to the development of numerous mouse models both overexpressing and silencing expression of SIM2.

Trisomy 16 mice were the first mouse model of Down Syndrome and demonstrated some of the morphological and molecular features of trisomy 21 with two

notable discrepancies. First, mouse chromosome 16 and human chromosome 21 are not entirely conserved; thus, trisomy 16 mice lack some genes located on human chromosome 21 and express an extra copy of genes not located on human chromosome 21 [229]. Second, trisomy 16 mice do not survive to birth [230]. These discrepancies were largely resolved with the development of the Ts65Dn mice [231, 232], which are a partial trisomy 16 model, and the Ts1Cje mice, which are trisomic for genes in the DSCR specifically [233]. Yeast and bacterial artificial chromosomes have been used to introduce additional copies of single genes in the DSCR to evaluate the gene dosage effect. Comparison of phenotypes of these transgenic strains with the Ts65Dn and Ts1Cje mouse models has helped to associate specific Down Syndrome features with single genes [229]. Two mouse models that systemically overexpress *Sim2* have been developed with this goal in mind. Overexpression of *Sim2* driven by the chicken beta-actin promoter [234] or by bacterial artificial chromosome incorporation [235] did not result in any obvious developmental or reproductive abnormalities; however, both models did demonstrate mild behavioral deficits, including reduced learning, increased pain tolerance, anxiety-related behavior, and reduced exploratory behavior [234, 235]. These phenotypes mirror some of the observations made in the Ts1Cje mice but do not fully or consistently reproduce distinct features, suggesting that multiple genes contribute to Down Syndrome phenotypes and that precise gene dosage studies are necessary to establish a truly translational model [235]. Furthermore, injection of pcDNA3-*mSim2* directly into the hippocampus of rats impairs the spatial learning and expression of synapsin 1, supporting the observations made in mice [236]. Although

these studies suggest that SIM2 contributes the phenotypes observed in Down Syndrome, they do not fully address the molecular function of SIM2.

To further investigate the molecular function of SIM2, various knockout models have been generated. Consistent with a role in development, SIM2 null mice die shortly after birth [170-172]. Although this lethality was confirmed by three independent groups, each group reported differing causes of perinatal death. One group reported breathing failure and lung collapse, which they attributed to structural defects of the ribs, intercostal muscle attachments, and diaphragm [170], and another group reported craniofacial abnormalities, including cleft palate and malformations of the tongue and sphenoid bone, which resulted in aerophagia and accumulation of gas in the gastrointestinal tract [171]. More recently, a third group generated a SIM2 knockout mouse strain by targeting the first exon of *Sim2* [237]. In this model, homozygous knockout was lethal in approximately half of the mice. Perinatal death was accompanied by severe gas distension in the gastrointestinal tract, which had been observed previously [171], and intestinal epithelium-specific loss of *Sim2* demonstrated the same phenotype [237]. The variability observed between the different SIM2 knockout lines could be due to the underlying genetic design of each model or to the influence of another unidentified factor. Surprisingly, the embryonic development of SIM2 null mice is largely normal [172]. Due to the lethality of SIM2 loss, additional inducible or tissue-specific knockout models will provide valuable insight into the function of SIM2.

Single-minded 2 in the mammary gland

Our lab uses the mammary gland as a model to study SIM2 based on the distinctive tumor profile of Down Syndrome patients, the contribution of SIM2 to the Down Syndrome phenotype, and the established role of SIM2 in development. Interestingly, results from these studies have also allowed us to use SIM2 as a model to study mammary gland development as well as breast cancer initiation, progression, and metastasis. The mammary gland provides an ideal model to study SIM2, because functional differentiation of the gland occurs postnatally, and Down Syndrome patients are at reduced risk of breast tumors. Based on these observations, we hypothesized that SIM2 may contribute to the differentiation of the mammary gland and may operate as a tumor suppressor in breast cancer.

Although SIM2 has been evaluated in a number of tissues and is highly expressed in the mouse embryo, kidney, and skeletal muscle [193, 238], the expression of SIM2s has not been fully characterized. Interestingly, SIM2s is the predominant variant expressed in the mammary gland and its expression peaks at mid-lactation when mammary epithelial cells are functionally differentiated [239-241]. This observation contrasts the early expression pattern of SIM2 in rat primary neuron differentiation [242], suggesting that SIM2 and SIM2s may play tissue-specific roles in cell differentiation.

Because loss of *Sim2* results in perinatal lethality, the mammary-specific effect of *Sim2* loss was evaluated by transplanting mammary epithelium from one-day-old *Sim2*$^{-/-}$ pups into the cleared fat pad of nude mice [241]. Outgrowths from these

transplants showed aberrant ductal elongation, with dense ducts and markers of an epithelial to mesenchymal transition [241]. Although aberrant ductal elongation with loss of *Sim2* suggests that *Sim2* is required for mammary gland development, terminal mammary epithelial cell differentiation during lactation could not be evaluated in the transplant model. To study the contribution of *Sim2* to terminal mammary epithelial cell differentiation, our lab developed mice that overexpress *Sim2s* via the mouse mammary tumor virus (MMTV). MMTV-*Sim2s* mice demonstrate precocious alveolar differentiation [240] that is maintained to such an extent that it delays involution and prolongs the existence of milk-producing alveoli up to a year after cessation of lactation [243]. Together, these studies suggest that *Sim2s* contributes to the establishment and maintenance of mammary epithelial cell differentiation and mammary gland development in the mouse. Of note, *SIM2* is the most significant differentially expressed sequence tag during the early transition from gestation to lactation in the tammar wallaby [244], supporting a role for *SIM2* in mammary gland development and differentiation.

Tumor suppressive and oncogenic roles of single-minded 2s

Consistent with the idea that SIM2s plays a role in the maintenance of mammary epithelial cell differentiation, the loss of SIM2s has been implicated in the progression of breast cancer [239, 241, 245]. SIM2s is expressed at relatively high levels in the normal breast and in ductal carcinoma *in situ*, but is lost during the progression to invasive ductal carcinoma [239, 245]. The role of *SIM2s* as a tumor suppressor in breast cancer is supported by observations in cultured cells, which demonstrate that loss of *SIM2s* in

estrogen receptor positive MCF7 breast cancer cells results in an epithelial to mesenchymal transition [241], and oncogenic transformation of the mammary epithelial cell line MCF10A results in the repression of *SIM2s* [246]. Moreover, a genetic linkage analysis in non-BRCA associated familial breast cancer patients uncovered a significant locus in the DSCR, which contains *SIM2* [247]. Functional single nucleotide variants in SIM2 have also been associated with Down Syndrome related malignancies [218, 220]. These associations suggest that single nucleotide variants could alter the function of SIM2 and contribute to a risk for breast cancer. How SIM2s functions as a tumor suppressor in the breast remains unclear. It is known that SIM2s is a transcriptional repressor of MMP2, MMP3, and SNAI2 (snail family transcriptional repressor 2) [239, 241]. SIM2s also represses NF-κB (nuclear factor kappa B) and PTGS2 (prostaglandin-endoperoxide synthase 2) through AKT (AKT serine/threonine kinase 1) [248], but it is unclear whether regulation of AKT relies on the transcriptional activity of SIM2s. On the other hand, SIM2 is repressed by NOTCH and NF-κB through direct transcriptional regulation and by CEBPB (CCAAT enhancer binding protein beta) in an undetermined manner [246, 248]. Further, another report identified MAGED1 as a novel non-transcriptional activator of SIM2, although the mechanism of action was unclear [249]. These studies begin to define the manner in which SIM2s senses the cellular environment and initiates a signaling response, but we still do not understand the molecular mechanism or order of these events.

Paradoxically, SIM2 functions as an oncogene in other malignancies, including colon cancer [250-253], prostate cancer [254-256], pancreatic cancer [257], glioblastoma

[258, 259], and esophageal squamous cell carcinoma [260]. SIM2s is highly expressed in colon cancer, pancreatic cancer, and glioblastoma, whereas SIM2l is also highly expressed in prostate cancer, and SIM2 is generally implicated in esophageal squamous cell carcinoma. In these tissues, SIM2 expression is low or non-existent in normal tissue and is overexpressed in tumor cells or tissues. Of note, this expression pattern differs from tissues that express higher levels of SIM2 in a normal state, which include breast, lung, and ovarian tissue [254]. These findings again highlight the tissue- and cell-state specific function of SIM2. Therefore, it is critical to expand our understanding of the upstream signaling pathways that activate SIM2 to perform these disparate functions.

Until recently, a ligand for SIM2 had not been identified, and SIM2 is considered to be constitutively expressed. Although SIM2s may be ubiquitously expressed, it is also rapidly degraded, with a half-life of approximately 2 hours [194]. We recently demonstrated that SIM2s is stabilized by ATM-mediated phosphorylation in response to DNA damage, which can be induced through treatment with ionizing radiation or genotoxic agents [261, 262]. This is the first report of a "ligand" for SIM2s and suggests that SIM2s indirectly senses DNA damage through post-translational modification-induced stabilization and nuclear translocation, similar to HIF1A. However, the role of SIM2s after nuclear translocation differs from its canonical transcriptional response. Instead of activating gene transcription, SIM2s localizes to the site of DNA damage and associates with the DNA damage repair (DDR) machinery [261]. In this complex, SIM2s enhances the loading of RAD51 onto DNA double stranded breaks during homologous recombination [262]. As a result, loss of *SIM2* results in unresolved DNA damage repair

foci, replication stress caused by stalled replication forks at sites of double-stranded DNA repair, and induction of genomic instability [262]. This genomic instability presents a therapeutic window, as loss of homologous recombination-associated factors sensitizes cells to synthetic lethality treatments, such as PARP inhibitors [263-267]. Thus, if a patient presents with low SIM2s expression, concurrent treatment with platinum salts and a PARP inhibitor could induce synthetic lethality in tumor cells, as has been observed in BRCA1 or BRCA2 mutation carriers [266]. This line of thinking is supported by *in vitro* studies that show synthetic lethality in two breast cancer cell lines (MCF7 and DCIS.COM) with synthetic loss of *SIM2* by inclusion of *shSIM2* and PARP inhibitor treatment [261]. Additional studies are necessary to validate the utility of SIM2s as a therapeutic marker and to further assess the role of SIM2s in breast cancer and other malignancies.

A single-minded future

As important cellular sensors, it is not surprising that bHLH-PAS proteins play roles beyond transcriptional activation or repression. Recently, an increasing number of non-canonical roles for bHLH-PAS proteins have been identified. One of the most surprising discoveries was the localization of bHLH-PAS transcription factors to the mitochondria. Both AHR and HIF1A localize to mitochondrial fractions and influence the respiratory status of the cell [268-270]. AHR localizes to the mitochondria with the assistance of its cytosolic binding partners, AIP and HSP90, and is imported to the mitochondrial inner membrane space by TOMM20 (translocase of outer mitochondrial membrane 20) [270]. In contrast, HIF1A is restricted to the outer mitochondrial

membrane and helps to attenuate oxidative stress-induced apoptosis [271]. The presence of AHR and HIF1A at the mitochondria seems to contribute to the homeostatic response of the cell to environmental stimuli. Of note, the ligands for AHR and HIF1A have opposing effects on their mitochondrial localization. More specifically, dioxin exposure results in the degradation of mitochondrial AHR [270], and oxidative stress triggers the accumulation of HIF1A at mitochondria [271]. Thus, it is still important to understand the upstream signaling events that activate or differentially localize bHLH-PAS factors. Here, we report for the first time that SIM2s is increasingly localized to mitochondria during mammary epithelial cell differentiation. The targeting stimulus and the direct impact of SIM2s at the mitochondria remain unknown but offer exciting new avenues of investigation.

Future studies of bHLH-PAS factors will help to uncover the signaling pathways responsible for bHLH-PAS protein localization and the outcomes of this localization. A number of other transcription factors have been found at the mitochondria and provide insight into the potential roles of bHLH-PAS proteins. Some transcription factors, including NF-κB, AP1, and CREB, bind to regions of the mitochondrial DNA [272-274], whereas others directly influence the mitochondrial electron transport chain, such as STAT3 [275, 276]. Additional outcomes that are of interest for future studies include altered epigenetic states due to modulation of mitochondrial outputs [277], mitochondrial retrograde signaling back to the nucleus [278], and respiratory complex composition, which may influence the use and efficiency of oxidative phosphorylation [279]. The studies presented here expand our understanding of the role of SIM2s during

terminal differentiation of mammary epithelial cells and provide insight into the non-canonical function of SIM2s. We anticipate that future studies will build on these results with particular emphasis on establishing and maintaining a differentiated cell state and prolonging differentiated cell survival, which are of key interest in both developmental and cancer settings.

CHAPTER II

METHODS

Cell culture

HC11 cells were purchased from the American Type Culture Collection (ATCC, CRL-3062). Cells were maintained and differentiated, as previously described [240]. Briefly, lactogenic differentiation was achieved by incubating confluent cells in priming media (RPMI 1640, HEPES [Thermo Fisher Scientific, 42401018] containing 10% charcoal-stripped horse serum [Atlanta Biologicals, S12150] and supplemented with 50 µg/ml gentamicin [Thermo Fisher Scientific, 15750078], 5 µg/ml bovine insulin [Sigma-Aldrich, I5500], 1 µg/ml hydrocortisone [Sigma-Aldrich, H0888]). After 24-h incubation in priming media, media was replaced with priming media containing 1 µg/ml ovine prolactin (National Hormone and Peptide Program, oPRL-21). Addition of prolactin was considered the initiation of differentiation and was timed from this point on (Figure 12). Bafilomycin A_1 (6.25, 12.5, 25, and 100 nM; Cayman Chemical Company, 11038-500), chloroquine (10 and 20 nM; Sigma-Aldrich, C6628), and mitoquinol (1 µM; Cayman Chemical Company, 845959-55-9) were applied in the priming media and maintained for differentiation time points or for 24 h for primed or undifferentiated time points. Live-cell videos were collected on a Zeiss Cell Discoverer 7 (Oberkochen, Germany) at 15-min intervals. Videos are presented at a playback speed of five frames per second, and the time codes represent the duration of maintenance or priming, as appropriate.

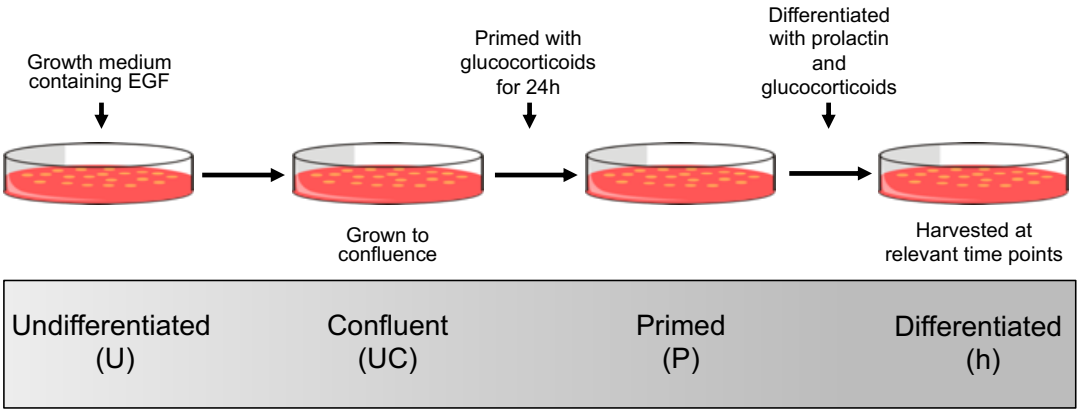

Figure 12 Model of *in vitro* mammary epithelial cell differentiation.

Short hairpin RNA (shRNA) constructs were stably introduced into cells, as previously described [241]. Two constructs targeting different regions of the target transcript were used as follows: *shAtg7_1* (TRCN0000092163), *shAtg7_2* (TRCN0000092166), *shAtg5_1* (TRCN0000099431), *shAtg5_2* (TRCN0000099432), *shPrkn_1* (TRCN0000041144), and *shPrkn_2* (TRCN0000041145). All constructs were purchased from Sigma-Aldrich and compared to the pLKO.1-puro non-targeting control construct (*shNT*). Following viral transduction, puromycin selection (2 μg/ml; Sigma-Aldrich, P8833) was maintained for one week, and cells were used for experiments between 14 and 28 d post-transduction [280].

Generation of cell lines

Long cDNA synthesis was used to generate point mutations in the *Sim2* gene (Invitrogen, custom). Subcloning Efficiency™ DH5α™ competent cells (Life Technologies, 18265017) were used to amplify plasmids containing the *Sim2* and *Sim2* mutant constructs. After amplification, plasmid DNA was isolated with the HiPure

Plasmid Maxiprep kit (Life Technologies, K210026). Plasmid DNA (10 μg) and GeneJuice (EMD Millipore, 70967-3) were combined in 1 mL of Opti-MEM (Life Technologies, 31985-062) and incubated for 15 minutes at room temperature. The Opti-MEM mixture was added to the media of Phoenix-AMPHO lentiviral packaging cells (ATCC, CRL-3213), and cells were incubated for 24 hours at 32°C and 5% CO_2. After incubation, the media was collected and syringe filtered (0.45 μm). Polybrene (1.2 μL/12mL; Sigma, TR-1003-G) was added to the filtered media, which was then used to culture the indicated target cells in 6-well plates. To increase transduction efficiency, plates were spun at 200 × g for 60 minutes and incubated overnight at 32°C and 5% CO_2. Collection, filtration, and treatment of the viral media to target cells was repeated a second time on the following day. Puromycin selection (2 μg/ml; Sigma-Aldrich, P8833) was begun the following day and maintained for at least a week.

MitoTimer

HC11 cells were transiently transfected with 2.5 μg of *pMitoTimer* (Addgene, 52659, deposited by the Zhen Yan Lab) in 500 μl of Opti-MEM (Thermo Fisher Scientific, 31985-062) and 10 μl of GeneJuice (EMD Millipore, 70967-3) for 24 h. Following transfection, cells were washed, and appropriate media was replaced. Live cell imaging was performed in Nunc Lab-Tek 2-well chamber slides (Thermo Fisher Scientific, 155380) on a Zeiss LSM 780 NLO Multiphoton Microscope with a 63× plan-apochromat objective. Subsequent image analysis was performed with ImageJ (NIH) and a custom python script. The methodology was based on existing studies [281]. Briefly, saturated pixels (gray level=255) were excluded, and single-channel means intensities

were measured. For each image, the mean RFP signal intensity was divided by the mean GFP signal intensity. Finally, the mean ratios were compared between time points. To evaluate red-only punctate mitochondria, saturated pixels (gray level=255) were removed, and the low red signal was excluded at a threshold of >175. Positive regions were watershed, and red dots of greater than 20 pixels and with signal intensity 2.5× greater than green intensity were considered positive mitochondria. Accuracy of automated counting was confirmed, and the average number of positive mitochondria per cell was calculated and compared between time points.

RNA isolation and real-time qPCR (RT-qPCR)

High Pure RNA Isolation Kits (Roche, 11828665001) were used to extract total RNA from cells and tissues per the manufacturer's protocols. Reverse transcription was performed with 1 µg total RNA using the iScript cDNA Synthesis Kit (Bio-Rad, 1708891BUN). Subsequent qPCR was performed with 1 µl of cDNA, 1 µM forward and reverse primer mix, and 5× GoTaq qPCR Master Mix (Promega, A6002) on a CFX384 qPCR (Bio-Rad, Hercules, CA, USA). Primers were synthesized by Integrative DNA Technologies, and the primer sequences are listed in Table 3. The $2^{-\Delta\Delta Ct}$ method was used to analyze qPCR data, and normalization was performed relative to *Actb*. The standard deviation of the target gene and reference gene Ct values were used to calculate the sum of squares of the standard deviation of each group. This value was used to find the positive and negative errors. The ΔΔCt, positive error, and negative error values were then log-transformed and presented as the fold $\pm$ 1 standard deviation. Statistical analyses were performed on the ΔCt values.

Table 3. Primer list.

Target	Forward	Reverse
Actb	GCAACGAGCGGTTCC	CCCAAGAAGGAAGGCTGGA
Atg5	TGAAGGCACACCCCTGAAAT	TGATGTTCCAAGGAAGAGCTGA
Atg7	GCAGTTCGCCCCCTTTAATAG	CGTTCAACTTCTTCTGGGTCAGT
mt-Co1 **(mtDNA)**	TGCTAGCCGCAGGCATTAC	GGGTGCCCAAAGAATCAGAAC
Csn2	TGTGCTCCAGGCTAAAGTTCACT	GGTTTGAGCCTGAGCATATGG
Dnm1l	CACCCGGAGACCTCTCATTC	CCCCATTCTTCTGCTTCAAC
Ndufv1 **(nDNA)**	CTTCCCCACTGGCCTCAAG	CCAAAACCCAGTGATCCAGC
Opa1	TCTTCCTGCAGGTCCCAAAT	CTGACACCTTCCTGTAATGCTTG
Prkn	GGCTGCGGGTTTGTTTTCT	CGCAATCCCCTTCATGGTAT
Sim2s	AACCAGCTCCCGTGTTTGAC	ACTCTGAGGAACGGCGAAAA
Tfam	AAGGGAATGGGAAAGGTAGA	AACAGGACATGGAAAGCAGAT

Immunoblotting

Protein was isolated from cells, as previously described [261]. Tissues were powdered under liquid nitrogen, washed with cold PBS (137 mM NaCl, 2.7 mM KCl, 10mM Na_2HPO_4O, 2 mM KH_2PO_4O, pH 7.4), and lysed in high salt lysis buffer containing 50 mM HEPES (Sigma-Aldrich, H3375), 500 mM NaCl (Sigma-Aldrich, S7653), 1.5 mM EDTA (Sigma-Aldrich, E5134), 10% glycerol (Sigma-Aldrich, G5516), 1% Triton X-100 (Sigma-Aldrich, T8787), 1 mM Na_3VO_4 (Sigma-Aldrich, S6508), and 1 mM complete ULTRA tablets mini EDTA-free Easy Pack (Roche, 5892791001) at pH 7.5. Cell and tissue protein concentrations were assessed by DC protein assay (Bio-Rad, 5000112). Equivalent amounts of protein were combined with 6× Laemmli buffer (250

mM Tris-HCl [Sigma-Aldrich, T5941], 8% SDS [Sigma-Aldrich, L3771], 40% glycerol [Sigma-Aldrich, G5516], 0.4 M dithiothreitol [Fisher Scientific, BP172-5], pH 6.8) and heated at 95˚C for 5 min prior to loading on 10% or 15% SDS-PAGE gels. Western blotting was performed as previously described [261], and the antibodies used are listed in Table 4. Bands were visualized with enhanced chemiluminescence reagent (Genesee Scientific, 20-300S) and digitized on a ChemiDoc MP Imaging System (Bio-Rad). Band intensities were measured using Fiji (version 2.0.0, NIH) and normalized first to the loading control. These normalized values were normalized again to the control sample for each experiment, resulting in a value of 1.00 for control samples. Western blots are representative of a minimum of three independent experiments.

Table 4. Antibody list.

Target	Manufacturer	Product Number	Dilution
ACTB	Cell Signaling Technology	37005	WB: 1:5,000
ATG5	Proteintech	10181-2-AP	WB: 1:1,000 IHC: 1:250
ATG7	Proteintech	10088-2-AP	WB: 1:1,000 IHC: 1:250
COX4	Thermo Scientific	PA5-19471	WB: 1:1,000 IHC: 1:500
CSN2	Santa Cruz Biotechnology	sc-166530	WB: 1:250 IHC: 1:100
DNM1L	EMD Millipore	ABT 155	WB: 1:1,000 IHC: 1:100
FLAG	Cell Signaling Technology	8146S	WB: 1:1,000
LC3B	Novus Biologicals	NB100-2220	WB: 1:1,000
OPA1	BD Biosciences	612607	WB: 1:1,000 IF: 1:100
PARP1	Cell Signaling Technology	9542	WB: 1:1,000
PINK1	Proteintech	232741-1-AP	WB: 1:1,000 IHC: 1:250
PRKN	Abcam	ab77924	WB: 1:500 IHC: 1:200
p-STAT3 (Tyr705)	Cell Signaling Technology	9131	WB: 1:1,000 IHC: 1:250
p-STAT5 (Tyr694)	Cell Signaling Technology	9359S	WB: 1:1,000

Table 4 Continued.

Target	Manufacturer	Product Number	Dilution
SIM2	Aviva	AB81292	WB: 1:500
SIM2	Millipore	AB4145	WB: 1:1,000
STAT3	Proteintech	10253-2-AP	WB: 1:1,000
STAT5	Santa Cruz Biotechnology	sc-1081	WB: 1:500
SQSTM1	MBL	PM045	IHC: 1:500
TOMM70	Proteintech	14528-1-AP	WB: 1:1,000 IHC: 1:100
TUBA	Santa Cruz Biotechnology	sc-8035	WB: 1:1,000
VDAC1	Abcam	ab14734	WB: 1:1,000
Anti-mouse HRP	Cell Signaling Technology	7076	WB: 1:5,000
Anti-rabbit HRP	Cell Signaling Technology	7074	WB: 1:5,000
Anti-mouse biotinylated	Vector Laboratories	BMK-2202	IHC: 1:250
Anti-rabbit biotinylated	Vector Laboratories	BA-1000	IHC: 1:250

Co-Immunoprecipitation

For co-immunoprecipitation (co-IP) of FLAG, cells were lysed in high salt buffer. Equivalent amounts of protein lysate (typically 100 μg) were mixed with 200 μl of anti-FLAG M2 beads (Sigma, M8823) or IgG control beads (Cell Signaling, 5873S). After equilibrating the beads, IP was conducted according to the manufacturer's instructions and as previously described [261]. After elution from the beads, β-mercaptoethanol (Sigma, M-7522) was added to protein immunoprecipitants, and samples were boiled for an additional 5 minutes. Immunoblotting was performed as described above.

Cellular respiration and glycolysis

Cellular respiration was analyzed on a Seahorse XFe96 Bioanalyzer (Agilent Technologies, Santa Clara, CA, USA). Briefly, cells were seeded at a density of 10,000 per well, growth media was replaced with priming media once cells reached confluence, and the media was again replaced by priming media containing prolactin after 24 h, as described above. The Seahorse XF Cell Mito Stress Test Kit (Agilent Technologies, 103015-100) was used to measure the oxygen consumption rate (OCR) and the extracellular acidification rate (ECAR), according to the manufacturer's protocol with two exceptions; oligomycin was used at a final concentration of 1.5 μM, and FCCP was used at a final concentration of 1 μM. Cell number was normalized to the protein content of each well, measured by DC protein assay (Bio-Rad, 5000112). Mean OCR and ECAR values from a minimum of nine replicates per group were compared. As there are no current standards for energy phenotype quadrants, ranges were assigned based on the transition of the control cells. Specifically, consecutive time points were compared by student's t-test, and quadrants were assigned where the least significant difference between consecutive time points occurred, which indicates a static or change point during the metabolic transition.

ROS, CASP3 (caspase 3) activity, and JC-1 assays

Mitochondrial derived ROS was measured using mitoSOX (Thermo Fisher Scientific, M36008) according to the manufacturer's instruction. Fluorescent analysis was performed using a FACSCalibur flow cytometer (BD Biosciences, San Jose, CA, USA) with biological triplicates at a minimum (time course data) or with a BioTek

Synergy microplate reader (Winooski, VT, USA) with six biological replicates at a minimum (cell line comparisons). Fluorescent intensity was compared between groups. CASP3 activity was assessed using the EnzChek Caspase 3 Assay Kit #2 (Thermo Fisher Scientific, E-13184) according to the manufacturer's protocol. Activity was measured by fluorescent intensity on a BioTek Synergy microplate reader, and mean values were compared between groups. For JC-1 analyses, cells were grown to the indicated state (undifferentiated, confluent, or primed for 24 h) on Nunc Lab-Tek 2-well chamber slides (Thermo Fisher Scientific, 155380). FCCP (1 μM, Sigma-Aldrich, C2920) was used as a positive control to induce membrane depolarization. Cells were incubated with 10 μM JC-1 (Thermo Fisher Scientific, T3168) for 30 min, washed twice with PBS, and imaged in phenol red-free media on a Zeiss LSM 780 NLO Multiphoton Microscope with a 63× plan-apochromat objective. A minimum of 10 images were taken at each time point, and the experiment was repeated three times. Subsequent image analysis was performed with ImageJ (NIH). For each image, the mean RFP signal intensity was divided by the mean GFP signal intensity, and the mean ratios were compared between time points.

Transmission electron microscopy

Monolayer cells and tissues pieces measuring 1 mm × 1 mm were fixed in 2% glutaraldehyde (Electron Microscopy Sciences, 16020) and 2.5% formaldehyde (Electron Microscopy Sciences, 15686) in 0.1 M sodium cacodylate buffer (Electron Microscopy Sciences, 12300) for 1 h at room temperature followed by overnight fixation at 4˚C. The next morning, samples were washed and stored in 0.1 M sodium cacodylate

buffer until processing by Dr. H. Ross Payne in the Image Analysis Lab of the College of Veterinary Medicine at Texas A&M University. Briefly, samples were post-fixed in 1% OsO_4 and 1% $K_4(Fe[CN]_6)$ in 0.1 M sodium cacodylate buffer for 1 h at room temperature and then washed twice in 0.1 M sodium cacodylate buffer. Dehydration was performed in graded ethanol (30%, 50%, 70%, 80%, 90%, 95%, and 100%), and samples were rinsed twice in propylene oxide and embedded in epoxy resin. Ultrathin sections were cut on a Leica EM UC6 Ultramicrotome (Wetzlar, Germany) and post-stained with uranyl acetate and lead citrate. Images were collected on a Morgagni 268 transmission electron microscope (FEI, Eindhoven, The Netherlands), and additional image analysis was performed with ImageJ. All images were auto-corrected for contrast using identical parameters.

Immunofluorescent staining of cells

For immunofluorescent (IF) assays, cells were grown on glass coverslips in 6-well plates. Cells were then fixed with 2% paraformaldehyde (Santa Cruz Biotechnology, sc-281692) for 15 min, permeated with 0.2% Triton X-100 (Sigma-Aldrich, T8787) for 15 min, and blocked in 5% bovine serum albumin (BSA; Fisher Bioreagents, BP1600) in TBST overnight at 4 °C. The next day, cells were incubated with the indicated primary antibodies (Table 4) for 3 hours. After three, 5-minute washes with TBST, cells were incubated with the indicated secondary antibodies for 1 hour at room temperature. Nuclei were stained with Hoechst 33342 (Life Technologies, 62249) for 10 minutes, and slides were washed in water prior to coverslip mounting with

ProLong Gold Antifade Mountant (Life Technologies, P36934). All images were taken using a using a Zeiss 780 confocal microscope.

Immunostaining tissue sections

Collected tissues were fixed in 4% paraformaldehyde (Santa Cruz Biotechnology, sc-281692) overnight, washed in cold PBS, and stored in 70% ethanol until processing by the Texas A&M University Veterinary Medicine & Biomedical Science Histology Laboratory. Immunostaining was performed on unstained sections, as previously described [282]. The antibodies and dilutions used are listed in Table 4. Images were collected on a Zeiss Axio Imager.Z1 with a 40× or 63× plan-apochromat objective.

Animals

All mice were housed under a standard 12-h photoperiod and provided access to food and water *ad libitum*. Three to five female FVB mice were analyzed for each developmental time point. Mice were sacrificed by CO_2 asphyxiation followed immediately by cervical dislocation. The fourth inguinal mammary glands were harvested at pregnancy days 6, 16, and 18, lactation days 1, 7, and 10, and 72 h after forced involution [243]. Glands were used for histological sectioning, RNA isolation, and TEM. All procedures were approved by and followed the guidelines of the Texas A&M University Animal Use and Care Committee.

Extended lactation was performed similarly to a previously published study [283]. The first litters of FVB and MMTV-*Sim2s* were cross-fostered using ICR litters. On day one of lactation, the litters of each FVB and MMTV-*Sim2s* female were replaced

by 10, one-day old ICR pups, normalized by weight. Litter weights were recorded every day for the first two weeks. At 14 days, the litters were removed and replaced by 10, seven-day old ICR pups. These litters were weighed on the day of cross-fostering and again a week later. Removal of aged pups and addition of younger pups was repeated at 21, 28, and 35 days. On day 42, the final litter weights were recorded, and the dams were sacrificed for tissue collection.

Primary mammary epithelial cell isolation and culture

Primary MECs were isolated from the inguinal and thoracic mammary glands. Tissues were placed in wash buffer (1 × DMEM/F12 [Life Technologies, 11320082], 5% FBS [Atlanta Biologicals, S11550], and 50 µg/mL gentamicin [Life Technologies, 15750078]) after dissection until mechanical homogenization with scalpels (VWR, 82029-860). Homogenates were then incubated with shaking in 2 mg/mL Collagenase A (Roche, 11088793001) in wash buffer for ~1.5 hours at 37°C. Organoids were pelleted at 600 × g for 10 minutes in a cooled centrifuge, and supernatants were aspirated. Organoids were treated with DNAseI (100 µg/mL DNAseI [Sigma-Aldrich, D4263] in DMEM/F12) if necessary and were enriched by pulse spinning at 450 × g. Organoids were utilized at this point or were subsequently processed to single cell suspensions. For single cell isolations, organoids were digested in 1 mg/mL trypsin (Life Technologies, 15400-054) at 37°C for ~20 minutes. Trypsin digestion was halted by the addition of 10mL of growth media (DMEM/F12, 10% FBS, 100 units/mL penicillin/streptomycin [Life Technologies, 15140-122], 5 µg/mL insulin [Sigma-Aldrich, I5500], and 50 µg/mL gentamicin, 1 µg/mL hydrocortisone [Sigma-Aldrich, H0888], 10 ng/mL mouse

epidermal growth factor [EGF; Life Technologies, PMG8041]). Single cells were washed with growth media and pelleted at 450 × g for 3 minutes three times. Finally, primary MECs were plated on fetuin-coated (Sigma-Aldrich, F-3385) 10 cm plates and cultured at 37°C and 5% CO_2.

Statistical analysis

All experiments were done biological triplicates with technical duplicates at a minimum, and each comparison was performed in a minimum of two independent assays. Box and whisker plots are presented from the 25th to 75th percentile, with the line at the median and the whiskers extending to the minimum and maximum values. Energy phenotypes, mitoSOX, CASP3 activity, and *pMitoTimer* analyses are presented as the mean ± the standard deviation (SD). Statistical analyses were performed with JMP Pro (version 14.1.0, SAS Institute Inc.) or Prism (version 7.0c, GraphPad Software). Prior to conducting two-tailed Student's t-tests, normal distribution was confirmed, and $p < 0.05$ was considered statistically significant.

Study approval

Animal studies were approved by the Texas A&M University Laboratory Animal Care Committee.

CHAPTER III

AUTOPHAGY REGULATES FUNCTIONAL DIFFERENTIATION OF MAMMARY EPITHELIAL CELLS*

Introduction

The transformation of the mammary gland into a milk-producing nutrient supply for the neonate requires profound and systemic metabolic adaptation. Metabolic adaptation occurs in the mammary gland during the transition from gestation to lactation through hormonal, transcriptional, and bioenergetic control. The coordination of hormonal and transcriptional signals during mammary gland development has been well studied [25, 92]; however, the contribution of cellular metabolism or bioenergetic control to differentiation remains poorly understood. Initial studies dating back to the 1960s characterized changes in metabolites, enzymes, and ATP over the course of lactation [104, 105, 284-286]. Many of these studies focused on mitochondrial processes and observed alterations in mitochondrial morphology and output during mammary gland development. Mitochondrial density, oxidative capacity, and the total number of mitochondria per secretory cell increase with the onset of lactation [92, 283, 287-289]. These observations suggest that mitochondria are actively engaged to enable massive synthesis and secretion of proteins, lipids, and carbohydrates during lactation.

Technological advances have improved our ability to analyze the function and importance of mitochondria. As a result, our understanding of the dynamic control of mitochondrial homeostasis has expanded to include the processes of fission, fusion, biogenesis, and mitophagy, the targeted macroautophagy/autophagy of mitochondria [106]. Mitophagy plays tissue-specific roles in cell survival, differentiation, and function [102, 103, 107, 113]. Moreover, a growing number of studies now support the role of mitophagy during tissue development as well as during cellular differentiation and have termed this process 'programmed mitophagy' [103, 290]. Programmed mitophagy differs from other forms of starvation- or chemically-induced mitophagy in that it occurs in response to developmental stimuli. The most dramatic examples of programmed mitophagy include the complete removal of mitochondria during erythroid differentiation [111] and from sperm after fertilization [291]; however, numerous studies in other cell types have suggested that removal and subsequent replacement of mitochondria, collectively termed mitochondrial turnover, is required for functional differentiation. For example, Gong et al. demonstrated that the development of mature cardiac mitochondria that support the metabolic function of adult cardiomyocytes in mice requires PRKN/parkin-mediated mitophagy. Disruption of PRKN-mediated mitophagy resulted in the retention of fetal cardiomyocyte mitochondria and early post-natal death. The authors concluded that mitochondrial turnover is required for metabolic transitioning in the heart [113].

The idea that a metabolic transition accompanies programmed mitophagy is also supported in other tissues. In skeletal muscle, myogenic differentiation relies on mitochondrial turnover, which is accompanied by a metabolic transition towards an oxidative state [102]. Conversely, a mitophagy-dependent metabolic transition towards glycolytic metabolism occurs during neuroblast differentiation into retinal ganglion cells [103]. Although metabolic transitions clearly occur during mammary gland development, particularly between gestation and lactation, the precise contribution of mitochondria to this transition is undefined. Of note, mitochondrial turnover is one of two hypotheses reached by Rosano and Jones to explain the morphological and functional differences in mitochondria between gestation and lactation in the mouse mammary gland [105]. Their alternative hypothesis was that mitochondria underwent differentiation along with mammary epithelial cells (MECs); however, neither hypothesis has been addressed. Therefore, we sought to further investigate the importance and contribution of mitochondria, potentially involving programmed mitophagy, using an *in vitro* model of MEC differentiation.

The purpose of these studies was to expand our understanding of the bioenergetic control of metabolic transitions in the mammary gland to provide new insight into the establishment and maintenance of lactation and how metabolic disruption may lead to disease and breast cancer in particular.

HC11 MECs undergo a metabolic transition during functional differentiation

To address the bioenergetic adaptation of the mammary gland during development, we first needed to establish a functional baseline of MEC differentiation.

As the primary function of the terminally differentiated lactating mammary gland is to provide nutritional support to the neonate(s) in the form of proteins, lipids, and carbohydrates, the production of milk proteins is often used as a marker of MEC functional differentiation. Therefore, we evaluated the expression of the milk protein CSN2 (casein beta) across differentiation in the HC11 mouse MEC line using a previously validated differentiation protocol [240]. Differentiation-dependent expression of *Csn2* increased starting 4 h into differentiation and peaked from 24 to 96 h (Figure 14A). Consistent with gene expression, protein levels of CSN2 increased across differentiation and persisted to 96 h. As cell viability is another factor that affects cell function, we evaluated the expression of the cell apoptosis marker PARP1 (poly[ADP-ribose] polymerase 1) and the mammary gland involution marker STAT3 (signal transducer and activator of transcription 3) across differentiation. Both markers were increasingly activated (cleaved PARP1 and p-STAT3) from 12 to 96 h and peaked at 96 h and 72 h, respectively, suggesting that HC11 cells begin to undergo cell death at later differentiation time points (Figure 14B). This observation is consistent with a previous report that demonstrated p-STAT3 induction and subsequent cell death during lysosomal-mediated programmed cell death in an EpH4 mouse MEC involution-like model after treatment with OSM (oncostatin M), a cytokine that activates STAT3 [78]. Moreover, we observed a transient elevation of p-STAT3 at priming. This expression pattern is similar to that of the mammary gland during the transition from gestation to lactation (Figure 13) and may be associated with the production of phagophore membranes. These results suggest that peak differentiation, indicated by maximal

expression of milk protein genes and low levels of cell death makers, occurs between 24 and 48 h in HC11 cells.

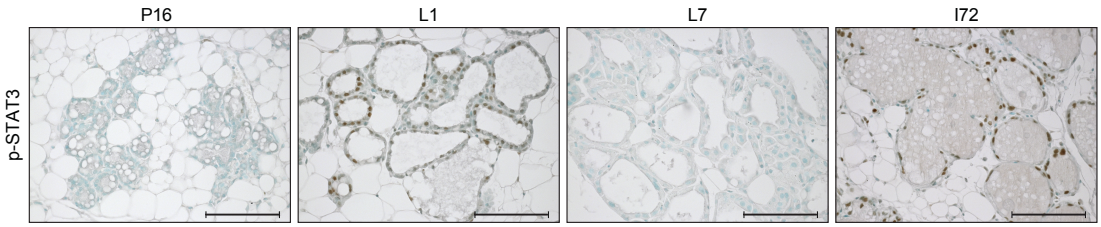

Figure 13 STAT3 is transiently activated in early lactation in the mouse mammary gland.
Immunohistochemical staining of p-STAT3 in the mouse mammary gland at pregnancy day 16 (P16), lactation day 1 (L1), lactation day 7 (L7), and 72 h of involution (I72). I72 was included as a positive control. Two mice were evaluated for each time point, and two sections from each mouse were stained for comparisons. Scale bars: 100 μm.

As we were interested in using this model of MEC differentiation to examine the contribution of mitochondria to the function of the mammary gland, we next measured cellular respiration and glycolysis to establish a baseline for mitochondrial function during HC11 MEC differentiation. The oxygen consumption rate (OCR) and extracellular acidification rate (ECAR) were analyzed on a Seahorse Extracellular Flux Bioanalyzer using the mitochondrial stress test, which employs sequential addition of oligomycin, trifluoromethoxy carbonylcyanide phenylhydrazone (FCCP), and antimycin A + rotenone (A+R) to measure basal, maximal, and reserve respiration (Figure 14C). We found that both basal and maximal OCRs were significantly elevated with differentiation, peaking at 48 h (Figure 14D-E). We then compared the relative energy phenotypes of differentiating cells by pairing the OCR with the ECAR to separate energy phenotypes into quadrants: quiescent, glycolytic, aerobic, and energetic. Using differentiation as a stressor in our model, we found that basal OCRs gradually increased

from the lowest basal values in undifferentiated cells up to 24 h of differentiation. At 48 h, a dramatic increase in ECAR shifted the energy phenotype to a more energetic state, suggesting that engagement of glycolysis transiently assists at a peak functional state. Finally, in the later hours of differentiation when cells appear to undergo an involution-like event (72 to 96 h), ECARs and OCRs fell back to early differentiation levels (Figure 14F). Altogether, these findings suggest that mitochondrial function attains a highly energetic state that coincides with the functional differentiation baseline established above in differentiating HC11 cells, peaking at 48 h of differentiation.

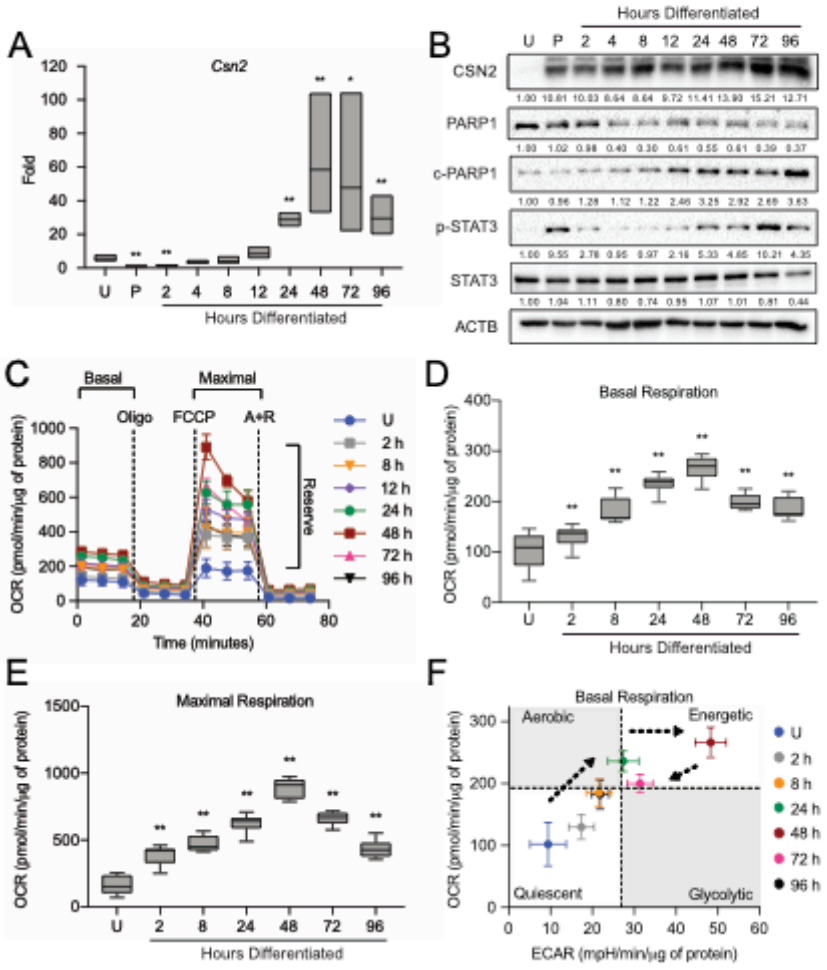

Figure 14 Functional differentiation of HC11 mouse mammary epithelial cells. (**A**) Differentiation-dependent expression of *Csn2* in HC11 mouse MECs (n=3). (**B**) Expression of differentiation and cell death markers during HC11 MEC differentiation. Levels of PARP1, c-PARP1, p-STAT3, and STAT3 are indicated below each lane after normalization to ACTB. The undifferentiated sample was set to 1.00, and all other time points are presented relative to 1.00. (**C**) Seahorse Extracellular Flux oxygen consumption rates (OCRs) in differentiating HC11 cells. (**D**) Basal OCRs and (**E**) maximal OCRs show progressive metabolic transition that regresses at 72 h and 96 h. (**F**) Energy phenotype comparison of OCRs and extracellular acidification rates (ECARs) in differentiating HC11 cells further demonstrating a dynamic metabolic transition. (n=4, ≥9 replicates per experiment) U: undifferentiated; P: 24 h primed; h: hours differentiated; oligo: oligomycin; A+R: antimycin a + rotenone. Data are presented as mean ± standard deviation. Box and whisker plots are presented from the 25th to 75th percentile, with the line at the median and the whiskers extending to the minimum and maximum values. Statistical significance was evaluated with multiple student t-tests relative to the undifferentiated time point (U). *p<0.05, **p<0.01.

Autophagy occurs during a window of functional differentiation

Recent studies have suggested that the ultrastructure of mitochondria, including the length, cristae association, and cristae number, contribute to their function [144]. Therefore, we evaluated mitochondrial ultrastructure in HC11 cells across differentiation by transmission electron microscopy (TEM). Based on our energy phenotype results, we expected mitochondria to exhibit distinct morphologies between an undifferentiated state and those leading up to peak differentiation. Although mitochondria were visibly more electron-dense in differentiated cells, we did not observe significant differences in mitochondrial structure or length up to 24 h of differentiation (data not shown). Unexpectedly, we did observe an abundance of autophagic vesicles that exhibited progressive maturation with differentiation (Figure 15A-B). Beginning at 2 h, we found lighter autophagosomes throughout the cytoplasm, and these vesicles appeared increasingly more electron-dense from 8 to 24 h, suggesting lysosome fusion and maturation of autolysosomes (Figure 15B-C). Another marker of autophagic flux, microtubule-associated protein 1 light chain 3 beta (LC3B), showed a transient increase of both the nonlipidated (LC3B-I) and lipidated (LC3B-II) forms at priming, suggesting induction of phagophore biogenesis and subsequent lysosomal degradation at the time points thereafter (Figure 15D). As elevated LCB-II levels can indicate both blockage and induction of autophagic flux [292], we treated differentiating HC11 cells with the vacuolar-type H^+-ATPase inhibitor bafilomycin A_1 (BAF), which inhibits autophagosome-lysosome fusion, for 4 h prior to protein isolation. Indeed, we found that

LC3B-II accumulated in the presence of BAF (Figure 15E), suggesting that autophagic flux is occurring. TEM analysis of mouse mammary glands during the transition from gestation to lactation also exhibited autophagic vesicles and the presence of phagophore membranes (Figure 16A). Moreover, the autophagy receptor SQSTM1 (sequestosome 1) showed higher levels of expression at late pregnancy (P16) and early lactation (L1) compared to mid-lactation (L10) (Figure 16B), which is indicative of macroautophagy during the transition from gestation to lactation. Together, these data suggest that autophagy occurs during an important functional transition in MEC differentiation.

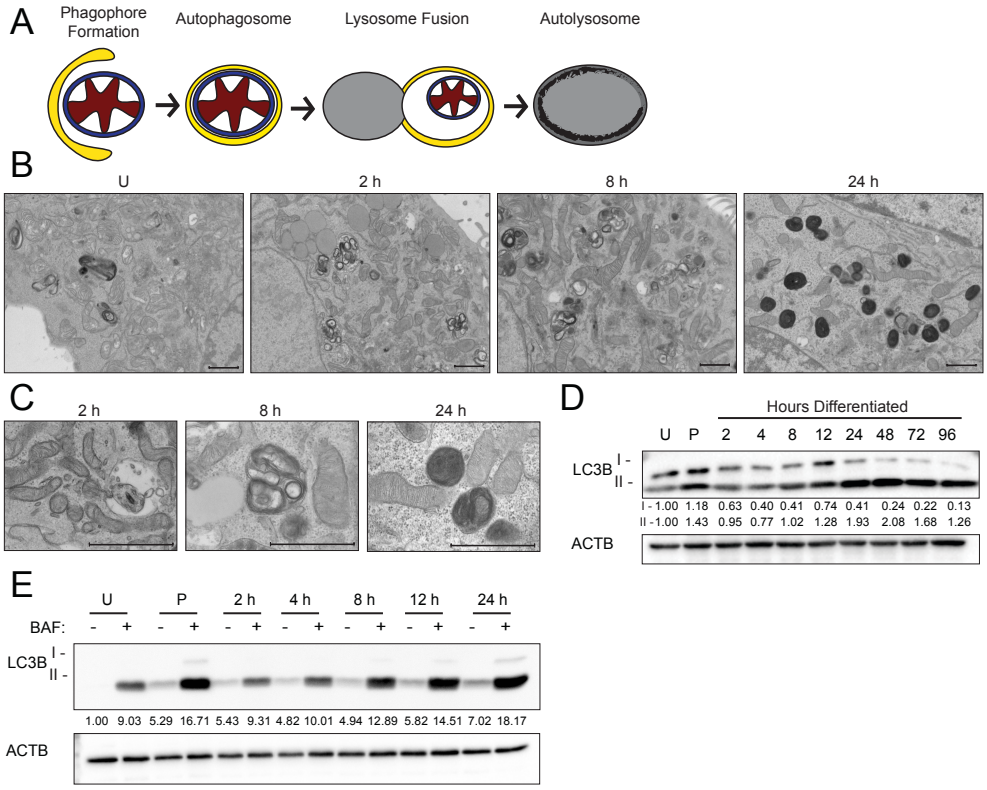

Figure 15 Autophagic membrane formation during HC11 cell differentiation. (A) Model of autophagic flux. (B) Transmission electron microscopy (TEM) images of HC11 cells at progressive stages of differentiation, showing the accumulation of autophagic membranes. (C) Higher magnification TEM images demonstrate vesicle content at each stage of differentiation. Three sections each were evaluated from two independent samples for TEM analysis. (D) LC3B levels across differentiation in HC11 cells. Levels of LC3B-I and -II are indicated below each lane after normalization to ACTB. The undifferentiated time point was set to 1.00, and all other time points are presented relative to 1.00. (E) LC3B accumulation after treatment with 100 nM bafilomycin A_1 (BAF) for 4 h to prevent phagophore degradation. The level of LC3B-II was normalized to ACTB and is indicated below the blot relative to the undifferentiated and untreated time point. U: undifferentiated; P: 24 h primed; h: hours differentiated. Scale bars: 1 μm.

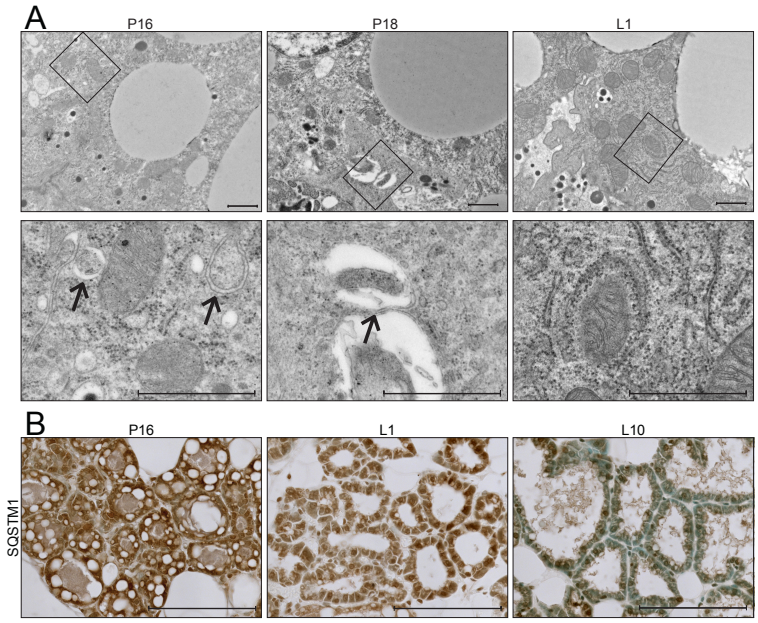

Figure 16 Transition from gestation to lactation in the mouse mammary gland. (A) Transmission electron microscopy (TEM) images of mouse mammary glands at pregnancy day 16 (P16), pregnancy day 18 (P18), and lactation day 1 (L1). Boxed regions are shown below at higher magnification. Scale bars: 1 μm. Three sections from three independent mice were evaluated by TEM. (B) Immunohistochemical staining for sequestosome 1 (SQSTM1) at P16, L1, and L10. Scale bars: 100 μm. Two mice were evaluated for each time point, and two sections from each mouse were stained for comparisons.

Inhibition of autophagy impairs HC11 MEC differentiation and energy phenotype

To evaluate the necessity of autophagy during HC11 cell differentiation, we inhibited autophagosome-lysosome fusion with BAF. Initial evaluation of *Csn2* expression at 48 h of differentiation revealed that even low concentrations of BAF substantially reduced induction of differentiation-dependent *Csn2* expression in HC11 cells (Figure 17A), suggesting that the inhibition of autophagy indeed impaired differentiation. At these low doses of BAF, HC11 cells were still viable, as evidenced by similar levels of CASP3 (caspase 3) activity between vehicle- and BAF-treated cells

(Figure 17B). However, when we increased the concentration of BAF treatment, cell death and involution markers, cleaved-PARP1 and p-STAT3, were present throughout differentiation (Figure 18A). Induction of cell death was confirmed by the significant elevation of CASP3 activity in BAF-treated cells compared to vehicle-treated cells at 48 h of differentiation (Figure 18B). Although differentiation appears impaired with BAF treatment, other indicators of functional differentiation, such as elevated mitochondrial respiration, may persist. Therefore, we treated differentiating HC11 cells with BAF and analyzed the resulting OCRs (Figure 17C). Compared to vehicle-treated cells, cells treated with 12.5 nM BAF had significantly reduced basal and maximal respiration at 24 h of differentiation (Figure 17D-E). A trend towards reduced respiration with BAF treatment was observed at 48 h but was not significant.

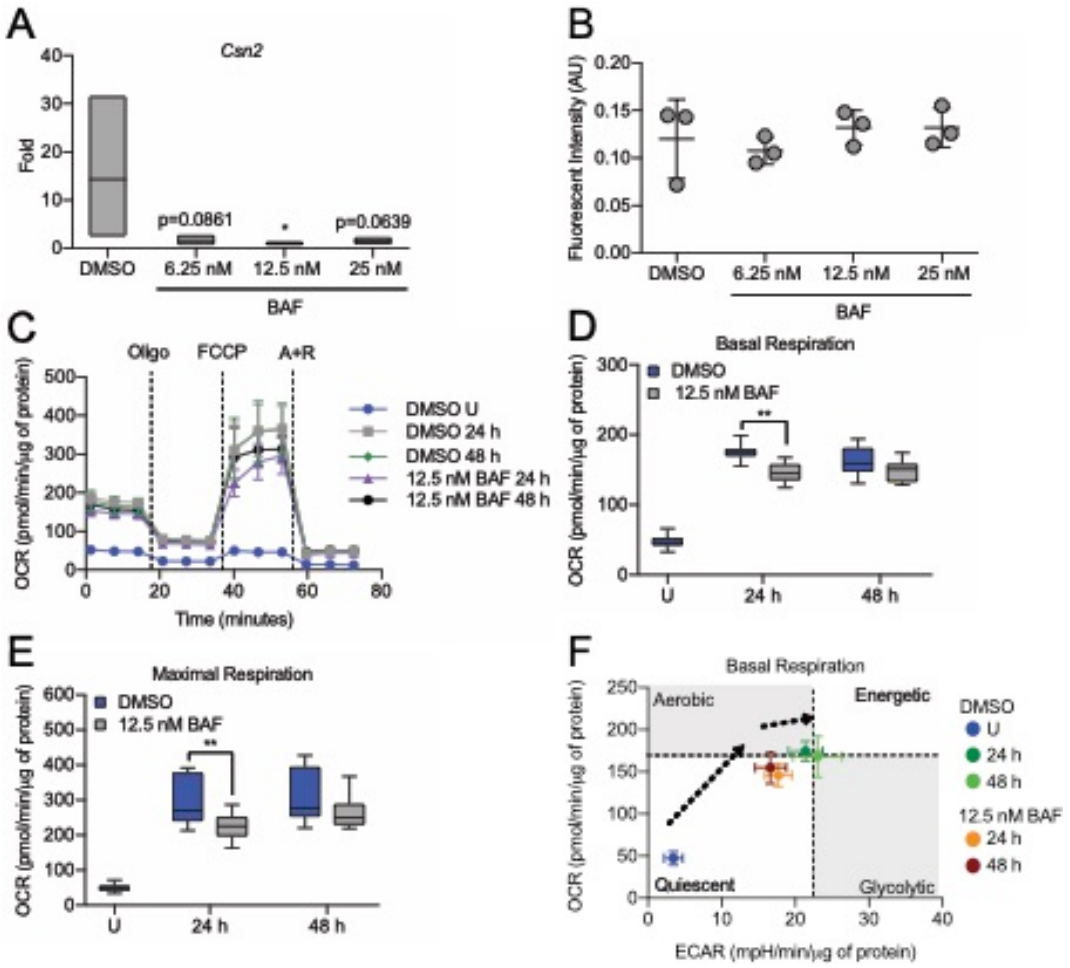

Figure 17 Inhibition of autophagy impairs HC11 cell differentiation.
(A) Differentiation-dependent *Csn2* expression in HC11 cells at 48 h of differentiation is inhibited by treatment with bafilomycin A_1 (BAF) at low concentrations. BAF treatment was applied in the priming medium and maintained throughout differentiation (n=3). (B) CASP3 activity in DMSO- or BAF-treated HC11 cells at 48 h of differentiation. BAF treatment was applied in the priming medium and maintained throughout differentiation (n=3). (C) OCRs of DMSO- or BAF-treated differentiating HC11 cells. BAF treatment was applied in the priming medium and maintained throughout differentiation. (D) Basal OCRs and (E) maximal OCRs are impaired by BAF treatment at 24 and 48 h of differentiation. (F) Energy phenotypes of BAF-treated cells are also reduced compared to DMSO-treated HC11 cells (n=2, ≥9 replicates per experiment). U: undifferentiated; P: 24 h primed; h: hours differentiated; oligo: oligomycin; A+R: antimycin a + rotenone. Data are presented as mean ± standard deviation. Box and whisker plots are presented from the 25th to 75th percentile, with the line at the median and the whiskers extending to the minimum and maximum values. Statistical significance was evaluated with student t-tests and compared to the appropriate DMSO-treated control. *p<0.05, **p<0.01.

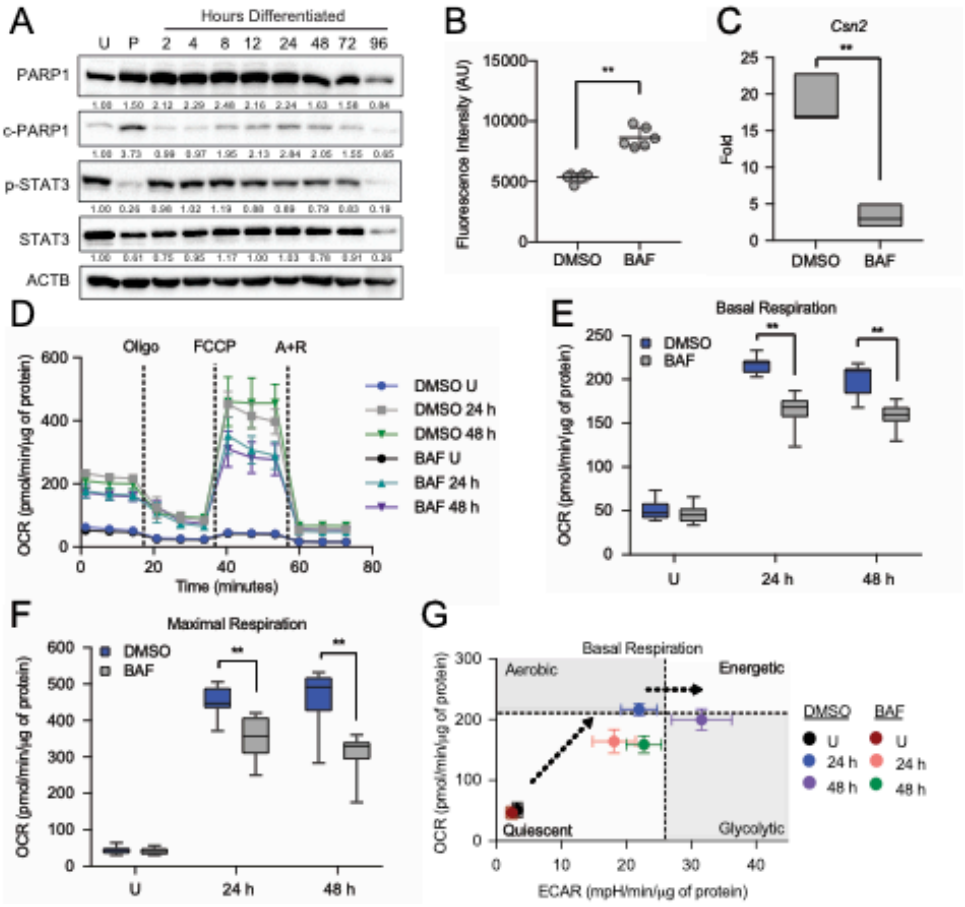

Figure 18 Bafilomycin A_1 inhibition of autophagy impairs HC11 cell differentiation. (A) Cell death markers during differentiation of BAF-treated HC11 cells. Cells were treated with 100 nM of BAF at priming, and the treatment was maintained through differentiation. Undifferentiated cells were treated for 24 h prior to collection. Levels of PARP1, c-PARP1, p-STAT3, and STAT3 are indicated below each lane after normalization to ACTB. (B) CASP3 activity in DMSO- or BAF-treated HC11 cells at 48 h of differentiation (n=3). (C) Differentiation-dependent *Csn2* expression in HC11 cells at 48 h of differentiation is inhibited by treatment with 100 nM BAF (n=3). (D) OCRs of DMSO- or BAF-treated differentiating HC11 cells. (E) Basal OCRs and (F) maximal OCRs are impaired by BAF treatment at 24 and 48 h of differentiation. (G) Energy phenotypes of BAF-treated cells are also reduced compared to DMSO-treated HC11 cells (n=2, ≥9 replicates per experiment). U: undifferentiated; P: 24 h primed; h: hours differentiated; oligo: oligomycin; A+R: antimycin a + rotenone. Data are presented as mean ± standard deviation. Box and whisker plots are presented from the 25th to 75th percentile, with the line at the median and the whiskers extending to the minimum and maximum values. Statistical significance was evaluated with student t-tests relative to the undifferentiated or untreated sample, as indicated. **p<0.01.

Moreover, the energy phenotype of BAF-treated cells was reduced compared to vehicle-treated cells (Figure 17F), indicating that the inhibition of autophagy negatively impacts both differentiation-dependent gene expression and mitochondrial function. Of note, differentiation-dependent *Csn2* expression (48 h), mitochondrial respiration (24 and 48 h), and energy phenotypes (24 and 48 h) were even more significantly reduced when cells were treated with 100 nM BAF compared to vehicle-treated cells (Figure 18C-G). Although we observed cell death at this concentration of BAF, the cells we assayed were viable and were normalized in their respective assays. In further confirmation of these results, we treated HC11 cells with chloroquine (CQ), which elevates the pH of lysosomes, ultimately preventing the fusion of lysosomes and autophagosomes. We found that concentrations of CQ as low as 10 and 20 nM were sufficient to reduce *Csn2* expression at 48 h of differentiation (Figure 19A). Furthermore, OCRs were reduced significantly at 48 h in response to 20 nM CQ treatment (Figure 19B-D). Together, these data strongly suggest that autophagy is vital to HC11 MEC differentiation.

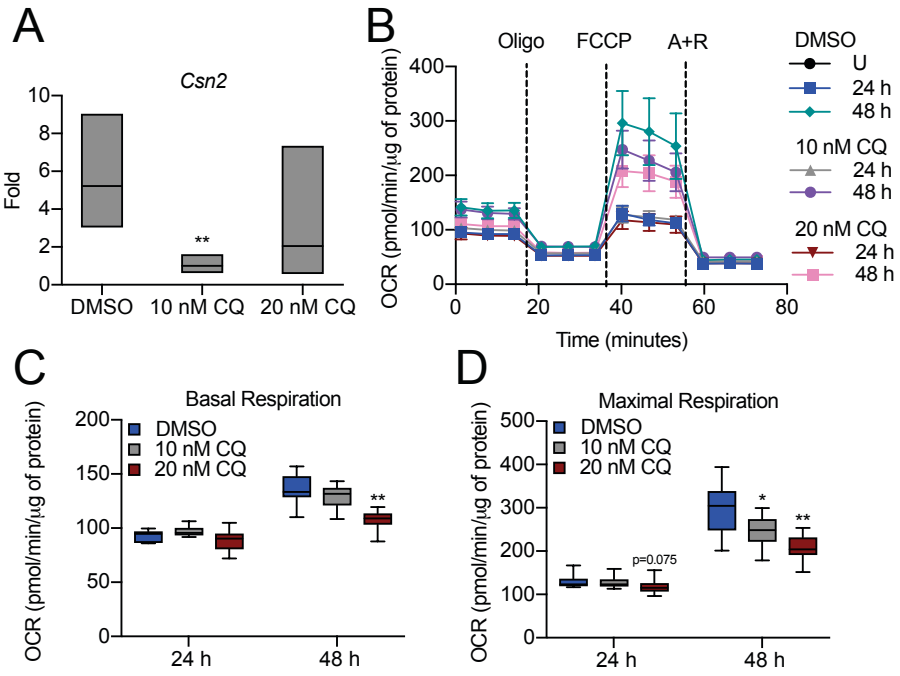

Figure 19 Chloroquine inhibition of autophagy impairs HC11 cell differentiation. (A) Differentiation-dependent expression of *Csn2* is reduced with low concentrations of chloroquine (CQ) at 48 h of differentiation. CQ treatment was applied with the addition of priming media and was maintained throughout differentiation (n=3). (B) OCRs of DMSO- and CQ-treated HC11 cells at an undifferentiated state as well as at 24 and 48 h of differentiation. (C) Basal and (D) maximal respiration in DMSO- and CQ-treated differentiating HC11 cells show a dose-dependent decline in OCR with CQ treatment (n=2, ≥12 replicates per experiment). U: undifferentiated; h: hours differentiated; oligo: oligomycin; A+R: antimycin a + rotenone. Data are presented as mean ± standard deviation. Box and whisker plots are presented from the 25th to 75th percentile, with the line at the median and the whiskers extending to the minimum and maximum values. Statistical significance was evaluated with student t-tests relative to the untreated sample. *$p<0.05$, **$p<0.01$.

ATG5 and ATG7 expression varies with MEC differentiation

To begin addressing the mechanism responsible for this autophagy, we asked whether autophagy mediators, such as the autophagy related (*Atg*) genes, exhibited expression patterns corresponding to the autophagic processes observed in

differentiating MECs. Gene expression of *Atg5* demonstrated a reduction with the onset of differentiation, whereas expression of *Atg7* was relatively consistent throughout differentiation. Both *Atg5* and *Atg7* trended towards elevated expression from 24 to 96 h of differentiation (Figure 20A). The transcript levels of these factors in the mouse mammary gland between late gestation (P16 and P18) and early lactation (L1 and L2) did not vary (Figure 20B). As many autophagy mediators are post-transcriptionally regulated, we examined protein expression by western blot and immunohistochemistry in HC11 cells and mouse mammary tissues, respectively. Interestingly, both ATG5 and ATG7 expression increased steadily with differentiation in HC11 cells and peaked at 48 h of differentiation (Figure 20C). In mouse mammary tissues, ATG5 expression was present throughout pregnancy (P16), early lactation (L1), and mid-lactation (L7) (Figure 20D). In contrast, the expression of ATG7 was generally low and only exhibited faint staining at P16 and L1 (Figure 20D). These findings suggest that autophagy factors may be developmentally regulated in MECs and that their expression coincides with the important transition between gestation and lactation in the mouse mammary gland.

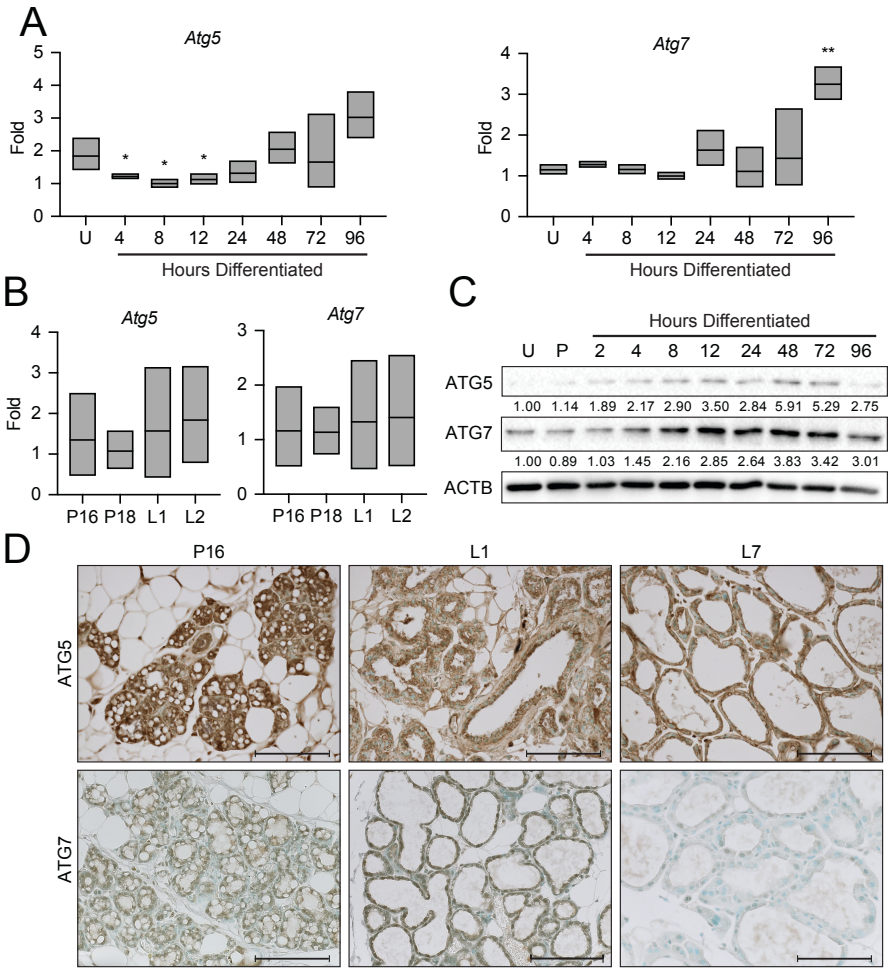

Figure 20 Expression of autophagy factors during HC11 cell differentiation and mammary gland development.
(A) *Atg5* and *Atg7* expression across differentiation in HC11 cells and (B) at pregnancy days 16 and 18 (P16, P18) and lactation days 1 and 2 (L1, L2) in the mouse mammary gland. RNA was collected from three mice per developmental time point. (C) Expression levels of ATG5 and ATG7 across differentiation in HC11 cells. Levels of ATG5 and ATG7 are indicated below each lane after normalization to ACTB. The undifferentiated time point was set to 1.00, and all other time points are presented relative to 1.00. (D) ATG5 and ATG7 expression at P16, L1, and L7 in the mouse mammary gland. Two mice were evaluated for each time point, and two sections from each mouse were stained for comparisons. U: undifferentiated; P: 24 h primed; h: hours differentiated. Scale bars: 100 μm. Data are presented as mean ± standard deviation. Statistical significance was evaluated with multiple student t-tests relative to the undifferentiated time point (U). *p<0.05, **p<0.01.

Loss of *Atg7* impairs the bioenergetic transition during HC11 MEC differentiation

Based on the reduced functional differentiation capacity observed with pharmacological inhibition of autophagy in HC11 cells, we expected genetic manipulation of the autophagy machinery to have similar effects. We targeted *Atg7* due to its role in both LC3 lipidation and ATG12–ATG5 conjugation during early phagophore membrane assembly prior to sequestration of cytoplasmic material [293]. Unexpectedly, stable shRNA-mediated knockdown of *Atg7* in HC11 cells resulted in significantly enhanced *Csn2* expression at 48 h of differentiation compared to non-targeting shRNA control (*shNT*) cells (Figure 21A), directly contrasting results seen with BAF and CQ treatment. We confirmed the loss of ATG7 in proliferating HC11 cells by preventing the degradation of phagophore membranes with BAF or by inducing mitochondrial depolarization with FCCP. Both treatments efficiently induced ATG7 expression in control cells but failed to induce substantial expression in either knockdown cell line (Figure 21B). Because *Csn2* expression is known to be regulated by STAT5 signaling in the mammary gland, we next asked whether STAT5 expression or activation of STAT5 via phosphorylation was elevated in these cells. We found that activated STAT5 (p-STAT5) was, in fact, present at higher levels in differentiated *shAtg7* cell lines (Figure 21C). Several reports have demonstrated that increased levels of reactive oxygen species (ROS) can activate the STAT family of transcription factors, and mitophagy-deficient conditions enhance ROS production [294, 295]; therefore, we sought to determine whether ROS production was altered in *Atg7* knockdown cells. More specifically, we asked whether mitochondrial ROS (mROS) was affected by the

loss of *Atg7*. To test this, we evaluated mitochondrial superoxide (mROS) production by staining HC11 cells with mitoSOX and found that *Atg7* knockdown cell lines produced significantly more mROS than control cells at 48 h of differentiation (Figure 21D). The level of mROS generated in *shAtg7* cells was comparable to control cells treated with 0.5 μM antimycin A (AA) for 1 h as a positive control. Of note, 100 nM BAF treatment for the duration of differentiation did not induce a similar elevation of mROS, presumably because mitochondria are sequestered prior to lysosomal fusion. Thus, it appears that inhibiting specific events in autophagic flux has distinct outcomes on differentiation-dependent *Csn2* expression and may explain why *Csn2* expression was reduced in response to BAF treatment (Figure 17A), which prevents fusion of autophagosomes and lysosomes, but was strongly elevated in *Atg7* knockdown cell lines (Figure 21A), where phagophore conjugation is impaired. We found that loss of *Atg5*, which is also involved in phagophore assembly, had similar effects on *Csn2* expression and mROS production (Figure 22A-C).

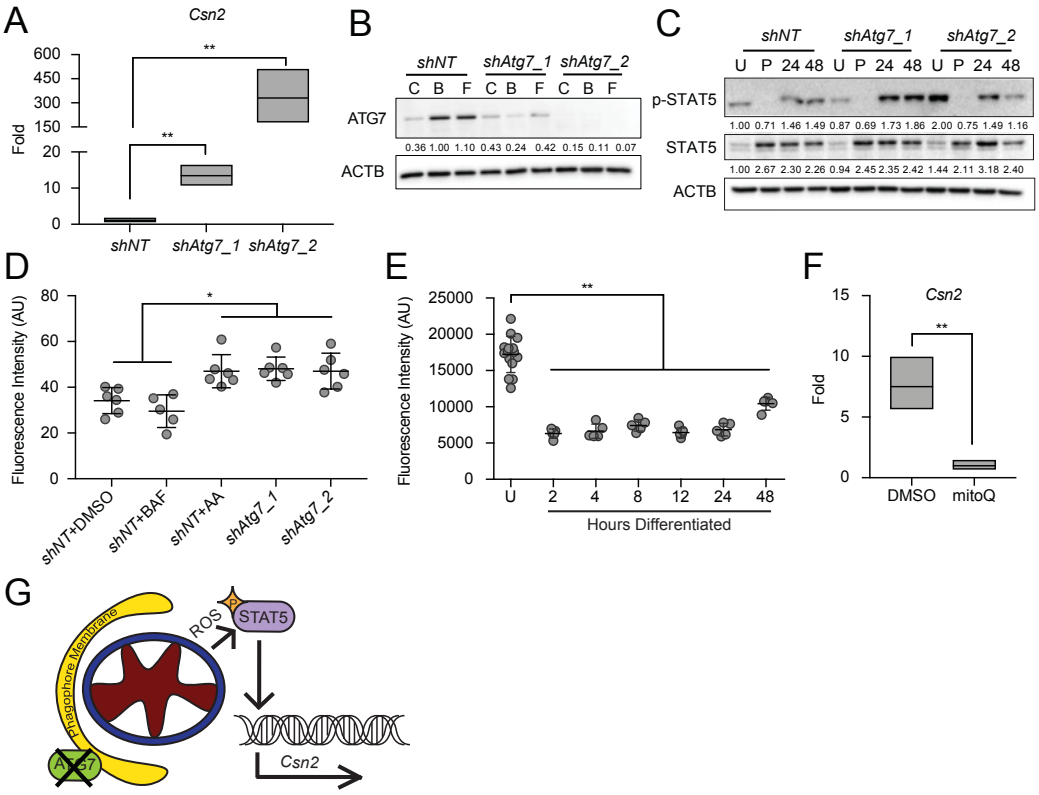

Figure 21 Knockdown of *Atg7* contributes to ROS-mediated gene expression. (A) Differentiation-dependent expression of *Csn2* in control (*shNT*) and *shAtg7* HC11 cell lines (n=3). (B) ATG7 expression in *shNT* and *shAtg7* cell lines after 4 h treatment with DMSO, 100 nM BAF, or 1 µM FCCP (C, B, or F, respectively). Levels of ATG7 are indicated below each lane after normalization to ACTB. The *shNT* sample treated with BAF was set to 1.00. (C) Activation (phosphorylation) of STAT5 during differentiation in *shNT* and *shAtg7* cell lines. Levels of p-STAT5 and STAT5 are indicated below each lane after normalization to ACTB. The undifferentiated time point was set to 1.00, and all other time points are presented relative to 1.00. (D) Mitochondrial ROS generation in *shNT* and *shAtg7* cell lines at 48 h of differentiation, measured by mitoSOX fluorescence. Control cells were treated with DMSO or 100 nM BAF beginning at priming, and treatment was maintained through differentiation. Cells were treated with 50 µM antimycin a (AA) for 1 h prior to analysis as a positive control (n=3). (E) MitoSOX fluorescence analysis in wild-type HC11 cells across differentiation (n=3). (F) Reduction of differentiation-dependent *Csn2* expression at 48 h in HC11 cells treated with mitochondrial ROS scavenger, mitoquinol (mitoQ, 1 µM) from priming through 48 h differentiation (n=3). (G) Proposed model, demonstrating how loss of ATG7 contributes to STAT5-mediated differentiation-dependent gene expression. U: undifferentiated; P: 24 h primed; h: hours differentiated. Data are presented as mean ± standard deviation. Statistical significance was evaluated with multiple student t-tests relative to the undifferentiated or untreated time point. *p<0.05, **p<0.01.

As the role of ROS as a signaling molecule in MEC differentiation is unknown, we investigated the production of mROS across differentiation. We found that proliferating, or undifferentiated (U), HC11 cells produced higher levels of mROS compared to cells that differentiated for 2 to 24 h (Figure 21E). At 48 h, mROS was elevated again and may contribute to the elevated *Csn2* expression observed at that time. Importantly, scavenging mROS during differentiation using the antioxidant mitoquinol (mitoQ, 1 μM), which accumulates specifically in mitochondria, resulted in significantly reduced *Csn2* induction at 48 h of differentiation (Figure 21F). These studies suggest that STAT5 activation and subsequent induction of *Csn2* expression may be due in part to elevated levels of ROS (Figure 21G). Of note, this activation is likely dependent on the state of the cell, as high levels of mROS in undifferentiated HC11 cells did not coincide with elevated p-STAT5 or *Csn2* expression.

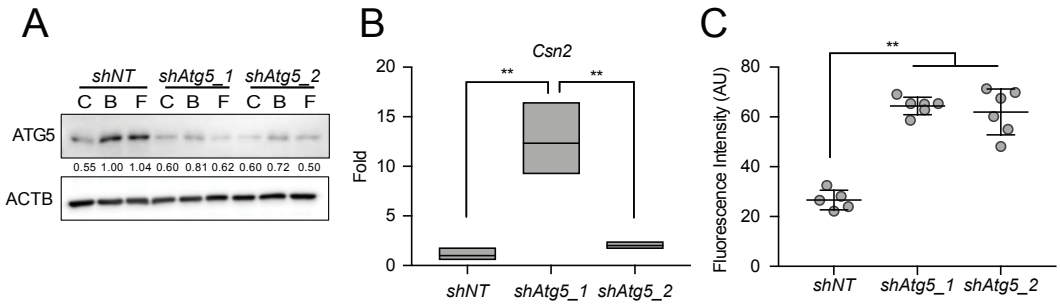

Figure 22 Loss of *Atg5* induces *Csn2* expression and ROS.
(A) ATG5 expression in *shNT* and *shAtg5* cell lines after 4 h treatment with DMSO, 100 nM BAF, or 1 μM FCCP (C, B, or F, respectively). Levels of ATG5 are indicated below each lane after normalization to ACTB. The *shNT* sample treated with BAF was set to 1.00, and all other time points are presented relative to 1.00. (B) Differentiation-dependent expression of *Csn2* at 48 h of differentiation in *shNT* and *shAtg5* HC11 cell lines (n=3). (C) Mitochondrial ROS generation in *shNT* and *shAtg5* HC11 cell lines at 48 h of differentiation (n=3). Data are presented as mean ± standard deviation. Statistical significance was evaluated with student t-tests relative to the *shNT* cell line. ** $p<0.01$.

Beyond the unexpected contribution of mROS to differentiation-dependent gene expression, we investigated the impact of *Atg7* knockdown on the bioenergetic capacity of differentiating HC11 cells. Basal respiration in undifferentiated *shAtg7* cells was significantly reduced compared to *shNT* cells, but we observed no significant differences at 24 or 48 h of differentiation (Figure 23A). In contrast, maximal respiration at 24 and 48 h of differentiation was significantly reduced with the loss of *Atg7* (Figure 23B), suggesting that mitochondria in *shAtg7* cells are less functional than those in *shNT* cells. More importantly, we found that *shAtg7* cells exhibited a reduced basal energy phenotype compared to *shNT* cells at 24 and 48 h of differentiation (Figure 23C), further suggesting that loss of *Atg7* indeed impaired the bioenergetic component of MEC differentiation. Finally, although other studies have shown that haploinsufficiency or knockdown of *Atg7* in MECs results in enhanced cell death [118, 296], we did not observe significant cell death or induction of CASP3 activity during peak differentiation time points in *shAtg7* cells (data not shown). This discrepancy could be due in part to compensation by other factors in the phagophore conjugation pathway or incomplete loss of *Atg7*. Nevertheless, the reduced functionality of mitochondria from *shAtg7* cells suggests that *Atg7* may be necessary for the metabolic transition associated with HC11 differentiation.

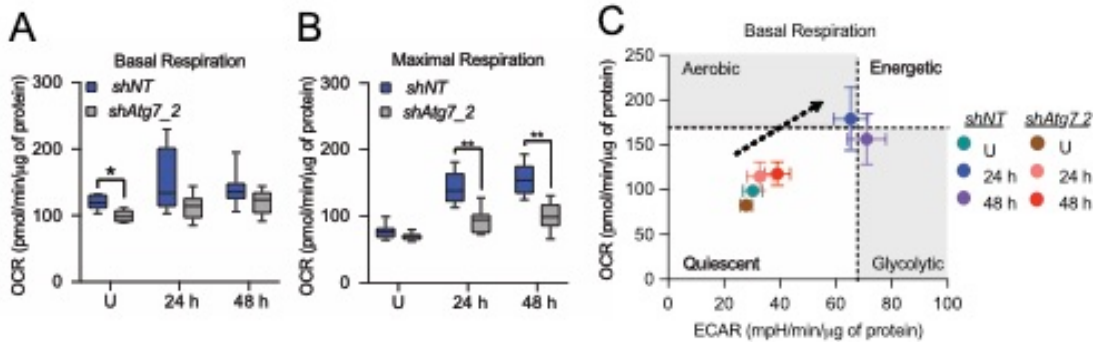

Figure 23 Metabolic transition of differentiating HC11 cells is impaired by loss of *Atg7*. (A) Basal OCRs and (B) maximal OCRs in *shNT* and *shAtg7_2* HC11 cell lines. (C) Energy phenotypes in *shNT* and *shAtg7_2* HC11 cell lines (n=2, ≥9 replicates per experiment). U: undifferentiated; h: hours differentiated. Data are presented as mean ± standard deviation. Box and whisker plots are presented from the 25th to 75th percentile, with the line at the median and the whiskers extending to the minimum and maximum values. Statistical significance was evaluated with student t-tests relative to the *shNT* cell line. * $p<0.05$, ** $p<0.01$.

Mitophagy is temporally regulated during *in vitro* differentiation

To determine whether the autophagic process observed during the differentiation of HC11 cells involved selective degradation of mitochondria, we employed the fluorescent probe, *pMitoTimer* [281]. The protein Timer is targeted to mitochondria via a COX8A (cytochrome c oxidase subunit 8A) sequence, initially fluoresces green, and shifts irreversibly to red when mitochondrial proteins are oxidized. A comparison of the ratio of mean red to green fluorescence gives a relative oxidation status, with higher values indicating increased oxidation. The use of this system allowed us to evaluate live-cell images throughout HC11 cell differentiation in real-time (Figure 24A). Quantification of the ratio of mean red to green fluorescent signal intensity revealed that mitochondrial oxidation was elevated in early differentiation (4 to 8 h) and returned to basal levels by 24 h (Figure 24B). This wave of oxidation suggests that programmed

mitophagy may be occurring, but is better evaluated by quantification of mitochondria that express only red punctate signal. Importantly, the number of red-only punctate mitochondria increased at early differentiation (2 to 8 h) and began to fall at 24 h (Figure 24C). Along with our autophagy analyses, this data suggests that autophagy, and more specifically mitophagy, is engaged early during differentiation in HC11 cells.

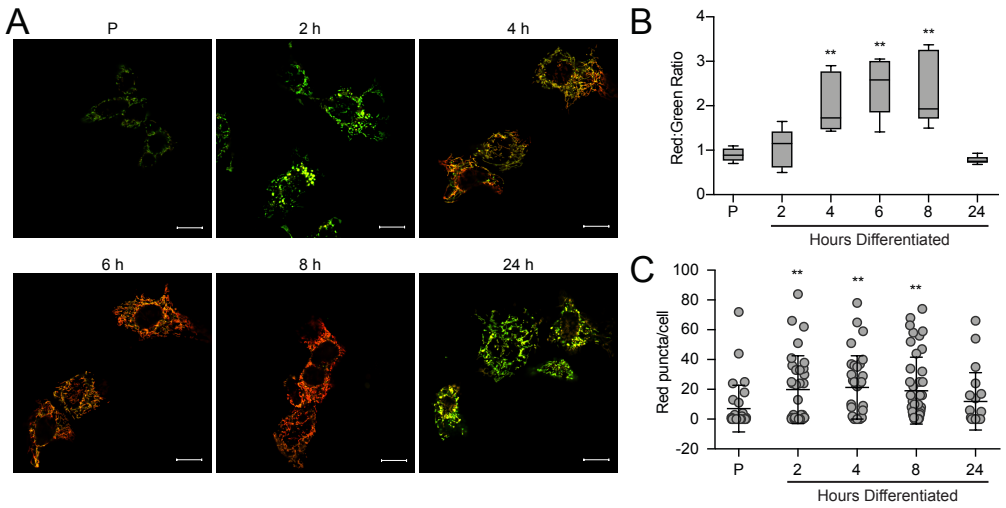

Figure 24 Mitochondria undergo progressive oxidation during HC11 cell differentiation. (A) Representative live-cell images of differentiating HC11 cells transiently transfected with *pMitoTimer*. Scale bars: 10 μm. (B) Average red to green fluorescent intensity ratio from 10 images per time point. (C) Enumeration of red-only punctate mitochondria from *pMitoTimer* images, indicating mitochondria actively undergoing mitophagy. A minimum of 10 images were evaluated per time point. Red puncta were not evaluated at 6 h of differentiation, as they were assessed from an independent experiment (n=3). P: 24 h primed; h: hours differentiated. Data are presented as mean ± standard deviation. Box and whisker plots are presented from the 25th to 75th percentile, with the line at the median and the whiskers extending to the minimum and maximum values. Statistical significance was evaluated with multiple student t-tests relative to the primed time point (P). *p<0.05, **p<0.01.

Because a balance of mitophagy and biogenesis maintains mitochondrial homeostasis, we also evaluated the expression of the transcription factors that are primarily responsible for mitochondrial protein biogenesis: *Ppargc1a* (PPARG

coactivator 1 alpha) and *Tfam* (transcription factor A, mitochondrial). The expression of both *Ppargc1a* and *Tfam* was low from 4 to 24 h and increased at 48 h (Figure 25A-B). *Ppargc1a* expression was highest at 48 h, whereas *Tfam* expression was highest in proliferating cells and from 48 to 96 h. To assess relative mitochondrial content across HC11 MEC differentiation, we normalized mitochondrial DNA to nuclear DNA using previously validated PCR primers [297]. We found that mitochondrial content rose at priming and stayed elevated until 8 h, dropping back to proliferating cell levels for the remainder of differentiation (Figure 25C). Together, these data suggest that a transitionary state exists between early (4-12 h) and peak differentiation (24-48 h) where mitochondrial turnover signals for generation of mitochondrial proteins and mitochondrial content falls back to homeostatic levels. We went on to assess mitochondrial DNA content relative to nuclear DNA in the transitionary state between gestation and lactation in the mouse mammary gland. We found that mitochondrial content was reduced at pregnancy day 18, suggesting that this could be a point of mitochondrial turnover (Figure 25D). However, we acknowledge that this bioenergetic transition may also occur outside of the investigated time frame.

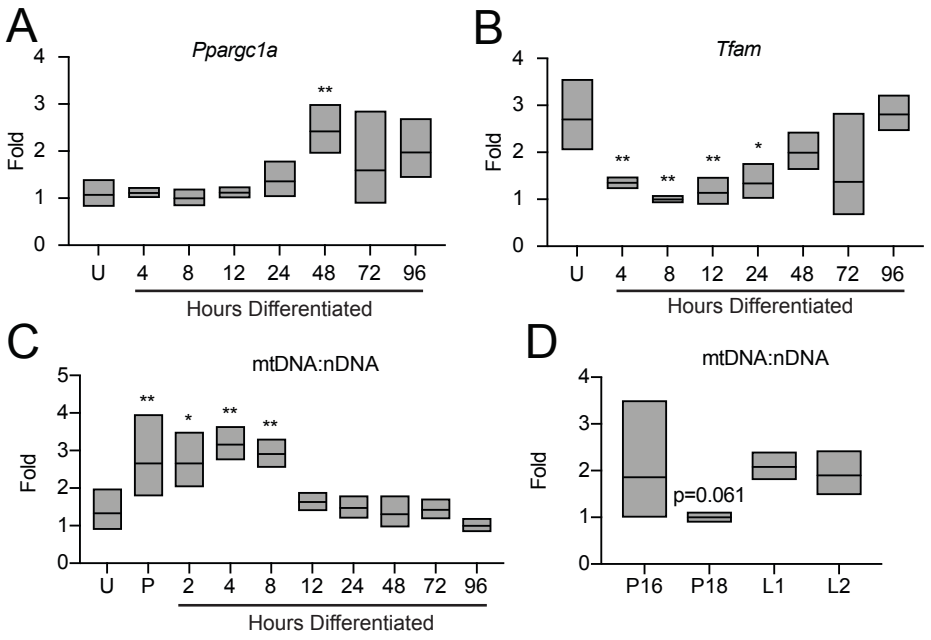

Figure 25 Mitochondrial biogenesis and content during HC11 cell differentiation and mammary gland development.
(A) *Ppargc1a* and (B) *Tfam* expression across HC11 cell differentiation (n=3). (C) Mitochondrial content was assessed by comparing mitochondrial DNA copy number to nuclear DNA copy number across HC11 cell differentiation (n=3). (D) DNA was also isolated from mouse mammary gland tissue at pregnancy days 16 and 18 (P16 and P18) as well as lactation days 1 and 2 (L1 and L2). DNA was collected from three mice per developmental time point. Statistical significance was evaluated with multiple student t-tests relative to the undifferentiated sample, as indicated. *$p<0.05$, **$p<0.01$.

PRKN localizes to the mitochondria of differentiating HC11 cells

Prior to asking whether differentiation in MECs specifically requires mitophagy, we examined the expression of mitophagy mediators during HC11 cell differentiation. As PINK1 (PTEN induced kinase 1) and PRKN are key factors in the most well-characterized mitophagy pathway [146, 298], and PRKN has recently been identified as a tumor suppressor in breast cancer [299], we began by examining PRKN expression across HC11 cell differentiation. We found that *Prkn* expression was significantly

elevated at priming in HC11 cells and continued to increase throughout differentiation (Figure 26A). Consistent with gene expression, PRKN protein expression increased dramatically with priming in HC11 cells (Figure 26B). We observed PINK1 expression throughout differentiation, with minimal variation between time points. Interestingly, PRKN expression in mouse mammary tissues was faint in late pregnancy (P16, Figure 26C) but exhibited diffuse cytoplasmic staining in early lactation (L1, Figure 26D) before returning to a reduced level in mid-lactation (L7). Similarly, PINK1 expression was observed in late pregnancy and early lactation but was largely absent in mid-lactation.

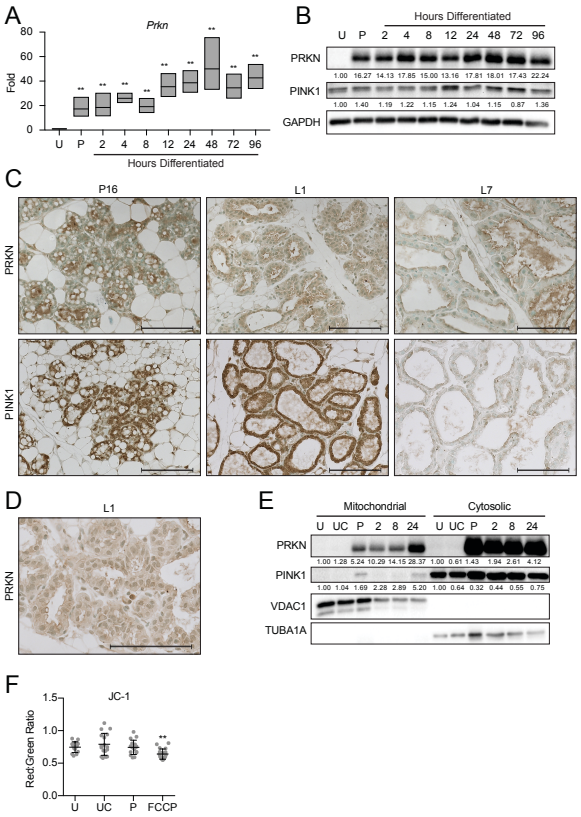

Figure 26 *Pink1* and *parkin* expression during HC11 cell differentiation and mammary gland development.
(A) Expression of *Prkn* across differentiation in HC11 cells (n=3). (B) Protein levels of PRKN and PINK1 during HC11 cell differentiation. Levels of PRKN and PINK1 are indicated below each lane after normalization to GAPDH. The undifferentiated sample was set to 1.00. (C) Immunohistochemical expression of PRKN and PINK1 at pregnancy day 16 (P16), lactation day 1 (L1), and lactation day 7 (L7) in the mouse mammary gland. (D) Higher magnification of cytoplasmic PRKN staining at L1. Two mice were evaluated for each time point, and two sections from each mouse were stained for comparisons. (E) Fractionation of HC11 cell lysates into mitochondrial and cytosolic components and expression of PRKN and PINK1. VDAC1 and TUBA1A expression confirm mitochondrial and cytosolic fraction purity, respectively. Levels of PRKN and PINK1 are indicated below each lane after normalization to VDAC1 for mitochondrial fractions and to TUBA1A for cytosolic fractions. The undifferentiated sample for each fraction was set to 1.00. (F) JC-1 was used to assess mitochondrial membrane polarization. A minimum of 10 images were evaluated for red and green fluorescent intensity for each time point. FCCP was used as a positive control for membrane depolarization (n=3). U: undifferentiated; UC: undifferentiated confluent; P: 24 h primed; h: hours differentiated Scale bars: 100 μm. Data are presented as mean ± standard deviation. Statistical significance was evaluated with multiple student t-tests relative to the undifferentiated time point (U). **p<0.01.

As the upregulation of PRKN and PINK1 expression does not necessarily indicate induction of mitophagy, we fractioned HC11 cells into mitochondrial and cytosolic components at several differentiation time points to observe accumulation of the mitophagy factors at the mitochondria, which would more clearly indicate active mitophagy. Interestingly, PRKN was strongly expressed in both fractions at priming and every differentiation time point. In contrast, although PINK1 was strongly expressed at every time point in the cytosolic fraction, it was only present in the mitochondrial fraction at priming and again at 24 h of differentiation (Figure 26E). Of note, mitochondrial membrane potential remained unaltered during early MEC differentiation between proliferating, confluent, and primed cell states, as evidenced by JC-1 staining (Figure 26F). The addition of FCCP confirmed that membrane depolarization could be detected by a significant reduction of the JC-1 red:green fluorescent signal. This result suggests that PRKN loading at mitochondria does not occur in response to the canonical depolarization-induced accumulation of PINK1 at damaged mitochondria and may instead respond to a developmental signaling cascade. These data suggest that non-canonical PRKN driven mitophagy may be involved in the autophagy initiated during early MEC differentiation.

PRKN is required for HC11 MEC differentiation

Finally, to assess the necessity of the mitophagy factor PRKN in HC11 MEC differentiation, we stably knocked down *Prkn* using two shRNAs. As proliferating HC11 cells did not substantially express PRKN (Figure 26B), we primed cells for 24 h to confirm the loss of PRKN protein (Figure 27A). Unexpectedly, *shPrkn* cell lines

exhibited apoptotic cell morphology during priming, which we did not observe if we maintained the cells in growth medium for the same length of time. One of the *shPrkn* cell lines, *shPrkn_1*, consistently underwent cell death during priming, whereas *shPrkn_2* cells survived until peak differentiation time points. This observation was quantified and confirmed by significant induction of CASP3 activity at 24 h of priming in *shPrkn_1* cells (Figure 27B) and at 24 h of differentiation in *shPrkn_2* cells (Figure 27C), each compared to *shNT* cells at the appropriate time point. To determine whether mitochondrial function was affected by the loss of *Prkn*, we first measured the OCR in proliferating control and *shPrkn* cell lines. We found that OCRs were significantly reduced in *shPrkn* cell lines compared to control cells (Figure 27D). As we were interested in the differentiation ability of these cells, we subjected surviving *shPrkn_2* cells to extracellular flux analysis at 24 h of differentiation. We found that *shPrkn_2* cells had significantly reduced basal respiration at 24 h but exhibited maximal respiration rates comparable to those of *shNT* cells (Figure 27E-G).

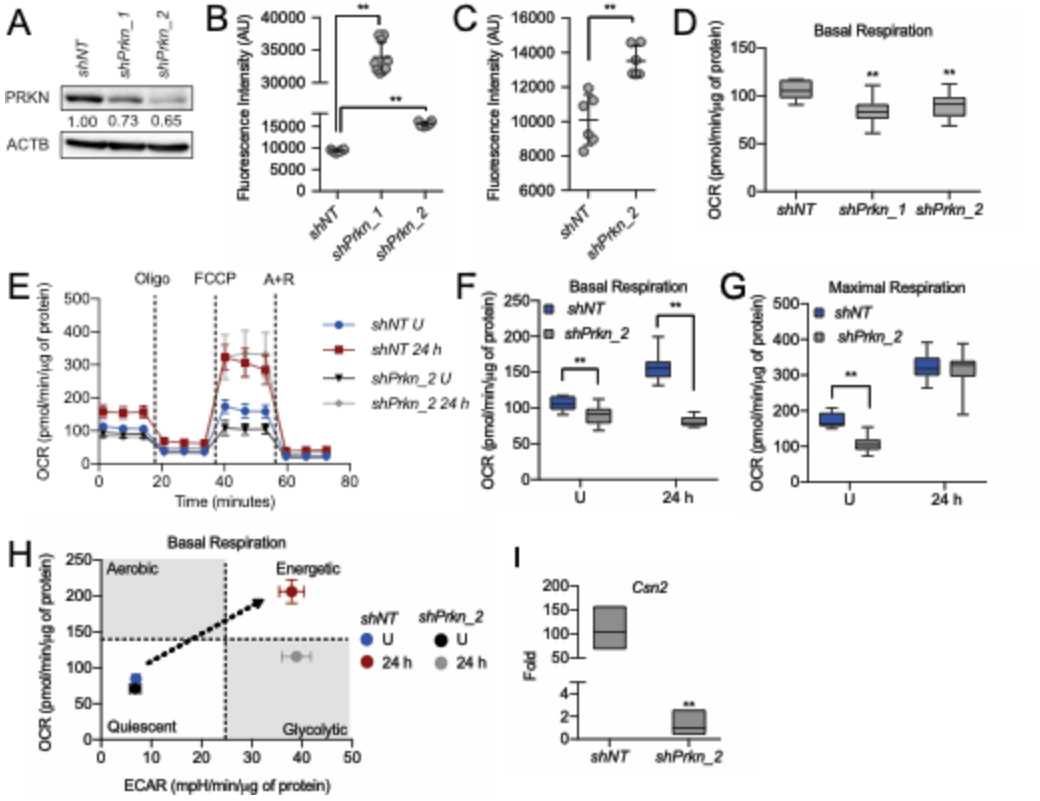

Figure 27 Loss of *Prkn* impairs HC11 cell differentiation.
(A) PRKN expression in *shNT* and *shPrkn* HC11 cell lines at 24 h of priming. Levels of PRKN are indicated below each lane after normalization to ACTB. The *shNT* sample was set to 1.00, and all other time points are presented relative to 1.00. (B) CASP3 activity in *shNT* and *shPrkn* HC11 cell lines at 24 h priming, showing induction of caspase activity in the *shPrkn_1* cell line (n=3). (C) CASP3 activity in *shNT* and *shPrkn_2* cell lines at 24 h of differentiation (n=3). (D) Basal OCRs in proliferating *shNT* and *shPrkn* HC11 cell lines. (E) Basal OCRs in *shNT* and *shPrkn* HC11 cell lines at a proliferative (U) state and at 24 h of differentiation. (F) Breakdown of basal and (G) maximal respiration in *shNT* and *shPrkn* HC11 cell lines at a proliferative (U) state and at 24 h of differentiation. (H) Energy phenotype profile of basal state *shNT* and *shPrkn* HC11 cell lines (n=2, ≥9 replicates per experiment). (I) Differentiation-dependent *Csn2* expression after loss of *Prkn* in HC11 cells at 24 h of differentiation (n=3). Data are presented as mean ± standard deviation. Box and whisker plots are presented from the 25th to 75th percentile, with the line at the median and the whiskers extending to the minimum and maximum values. Statistical significance was evaluated with student t-tests relative to the *shNT* cell line. **p<0.01.

Interestingly, the energy phenotype of these cells revealed that although *shPrkn_2* cells were significantly stunted in OCR, ECAR still increased with differentiation (Figure 27H). These results suggest that the loss of *Prkn* impaired full bioenergetic adaptation and further highlights the complexity of programmed mitophagy. Although we have established that differentiation-dependent gene expression can be uncoupled from other markers of differentiation, we analyzed *Csn2* expression with loss of *Prkn* at 24 h of differentiation. We found that *Csn2* expression was significantly reduced in *shPrkn_2* cells compared to *shNT* cells, further suggesting that loss of *Prkn* impaired total differentiation (Figure 27I). Together, these results suggest that PRKN is a key factor in MEC differentiation and likely contributes to the mitophagy observed during this important bioenergetic transition (Figure 28).

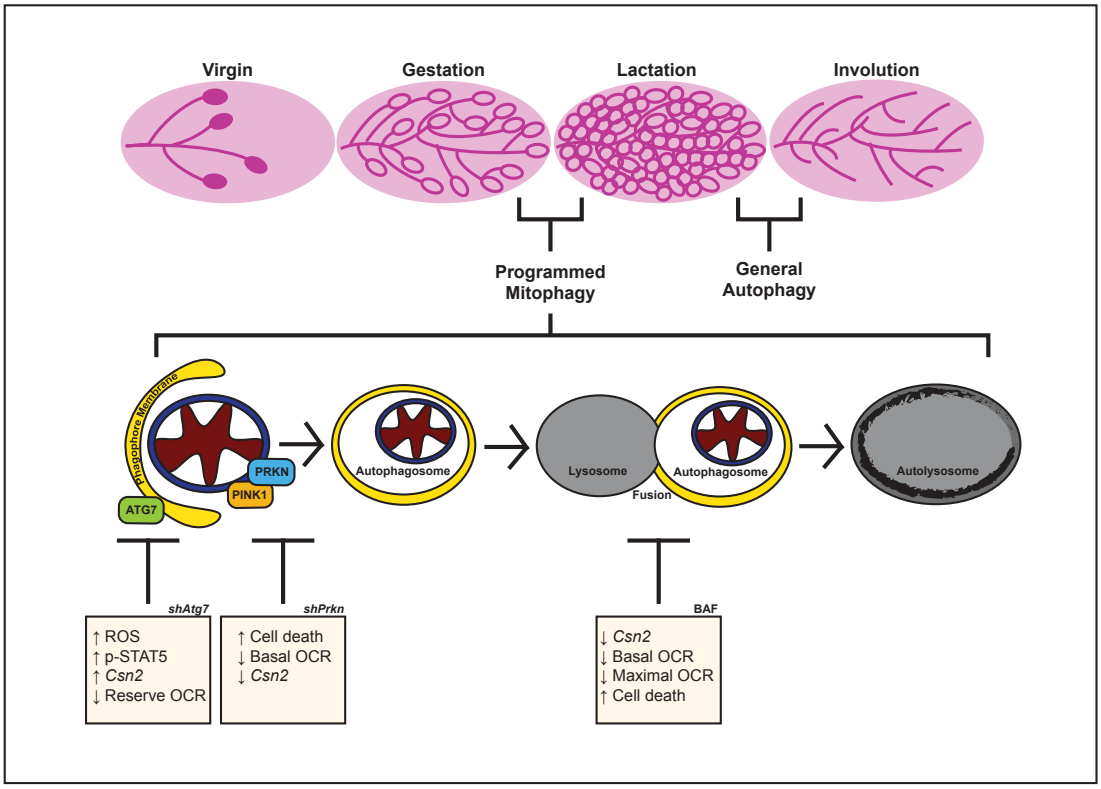

Figure 28 Model of mammary epithelial cell functional differentiation.
Our results suggest that the transition from gestation to lactation in the mammary gland involves programmed mitophagy. This process relies on the autophagy machinery as well as the mitophagy factor PRKN. The boxes depict the outcomes of *Atg7* knockdown, *Prkn* knockdown, and pharmacological inhibition of autophagy with bafilomycin A_1 (BAF). Notably, this form of mitophagy is distinct from the general autophagy that occurs during involution to reset the mammary gland for subsequent rounds of gestation and lactation.

CHAPTER IV

SIM2S REGULATES THE DIFFERENTIATION AND SURVIVAL OF MAMMARY EPITHELIAL CELLS BY ENHANCING MITOPHAGY

Introduction

Achieving and maintaining a differentiated cell state is vital to tissue function and the prevention of disease. In fact, cancer has been referred to as a "disease of differentiation" [100, 300]. This theory is supported by the observation that many low-grade malignancies demonstrate well-differentiated morphology, whereas higher-grades are associated with hallmarks of de-differentiation or undifferentiated cell states. Importantly, differentiation is tightly linked to metabolic function, and dramatic metabolic reprogramming is a hallmark of tumor cells [101]. Despite these clear associations, it is unknown whether metabolic adaptations instruct or respond to differentiation. Therefore, understanding the regulatory biology of achieving and maintaining terminal differentiation will provide important insights for therapeutic advances.

Terminal differentiation can be studied very effectively during the post-natal development of the mammary gland. During development, mammary epithelial cells (MECs) respond to integrated hormonal, transcriptional, and metabolic signaling to enable a range of cellular programs. Of key interest is the transition from gestation to lactation when MECs undergo dramatic metabolic reprogramming. During this transition, MECs switch from proliferative centers of catabolism to post-mitotic anabolism factories that generate copious amounts of proteins, fats, and carbohydrates,

which are secreted into milk. This dramatic reprogramming has been largely attributed to hormonal and transcriptional regulation, but recent insight into the signaling roles of metabolites and mitochondria suggest that this transition may also be informed by metabolism. Factors that are activated or suppressed specifically during this transition are of key interest as potential master regulators of metabolic reprogramming.

Our lab has previously established that single-minded 2s (SIM2s) plays an important role in the onset and maintenance of mammary gland differentiation [240, 241, 243]. SIM2s is a member of the bHLH-PAS family of transcription factors, which classically function as environmental sensors. bHLH-PAS proteins can bind DNA, proteins, and small molecules, allowing them to respond to environmental stimuli, such as oxygen stress and dioxin, by enacting transcriptional or protein binding functions. In comparison to other bHLH-PAS proteins, relatively little is known about the activation of SIM2s. We have recently shown that DNA damage stimulates the phosphorylation of SIM2s in an ATM-dependent manner, and we expect that ATM-mediated activation of SIM2s has additional implications for novel SIM2s function.

Several lines of evidence suggest that modulating the level of SIM2 may have important functional outcomes for MECs. First, loss of SIM2 is associated with progression of breast cancer and malignant transformation in the developing mammary gland. Moreover, the SIM2 gene is located on human chromosome 21 in the Down Syndrome critical region (DSCR), which indicates that SIM2 is overexpressed in Down Syndrome patients. Although Down Syndrome patients are at increased risk of metabolic syndrome, their risk of breast cancer is surprisingly low and is thought to be linked to a

breast tumor suppressor located in the DSCR. Beyond these observations, we sought to address the functional outcome of gain and loss of *Sim2* in the mammary gland. To do so, we developed tissue-specific mouse models of *Sim2s* gain and loss. Using these models, we demonstrate that SIM2s regulates the differentiation and survival of MECs by enhancing mitophagy. This work integrates the study of the transcriptional and metabolic mechanisms that culminate in the terminal differentiation of MECs and provides important insight into achieving and maintaining cell differentiation and tissue function.

SIM2s promotes mammary gland function *in vivo*

Terminally differentiated MECs perform a highly specialized and temporary function that is essential for the survival of mammalian neonates. Uniquely, MEC differentiation can be monitored by lactation efficiency, and is measured indirectly by pup weight gain in cross-fostered experiments. To determine the effect of SIM2s on MEC functional differentiation, we performed cross-foster experiments in mice that over-express *Sim2s* or that express a conditionally excised *Sim2* allele.

We have previously established a transgenic mouse model of *Sim2s* over-expression driven by the mouse mammary tumor virus (MMTV-*Sim2s*) [240]. To further characterize the functional role of SIM2s in the mammary gland, we have also engineered tissue-specific conditional knockout mice via a floxed *Sim2* allele (Figure 29A). *Sim2* is conditionally deleted by crossing mice bearing the floxed *Sim2* allele with mice that express cre recombinase under control of the whey acidic protein (*Wap*) promoter ($Wap^{Cre/+}$). *Wap* is specifically expressed in mammary alveolar epithelial cells

from mid-pregnancy through lactation, and thus allows for mammary gland-specific deletion of *Sim2* shortly before and during lactation. Due to mosaic cre recombinase activity, we used the genetic tag Gt(ROSA)26Sor$^{tm4(ACTB-tdTomato,-EGFP)luo}$/J (*mTmG*) [301] to distinguish recombined and non-recombined cells (Figure 29B). Using this model, non-recombined cells express tdTomato, whereas recombined cells express EGFP, indicating loss of *Sim2* in floxed *Sim2* mice. To this end, *Sim2*$^{fl/+}$;*Wap*$^{Cre/+}$ mice were crossed to *Sim2*$^{fl/+}$;*mTmG/mTmG* mice to produce *Sim2*$^{fl/fl}$;*Wap*$^{Cre/+}$;*mTmG* mice (*Sim2*$^{fl/fl}$) and littermate *Wap*$^{Cre/+}$;*mTmG* (control) mice. *Sim2s* expression was confirmed to be reduced in the mammary glands of lactating *Sim2*$^{fl/fl}$ mice compared to control mice in a previous study [262].

Figure 29 *Sim2* conditional knockout allele and fluorescent genetic tag.

To examine the functional effect of SIM2s on milk composition and subsequent pup growth, we cross-fostered and measured the weight gain of the first litters of wild-type (WT), MMTV-*Sim2s*, *Sim2*$^{fl/fl}$, and control mice. We found that by day 10 of lactation, MMTV-*Sim2s* dams nursed litters with significantly higher weight gain, whereas *Sim2*$^{fl/fl}$ dams nursed litters with significantly lower weight gain compared to their respective controls (Figure 30A-B). Histological characterization of mammary glands from these mice revealed that whereas MMTV-*Sim2s* glands appeared similar to WT (Figure 30C), *Sim2*$^{fl/fl}$ glands exhibited reduced epithelial filling and suppressed

CSN2 expression (Figure 30C-D). The expression of *Csn2* is differentiation-dependent and has been widely used as a marker for functional differentiation in MECs [67, 302]. Whole slide scans of hematoxylin and eosin (H&E) stained sections highlight the reduced epithelial cell occupancy by day 10 of lactation in $Sim2^{fl/fl}$ mice. Together, these results suggest that SIM2s is required for functional differentiation of MECs.

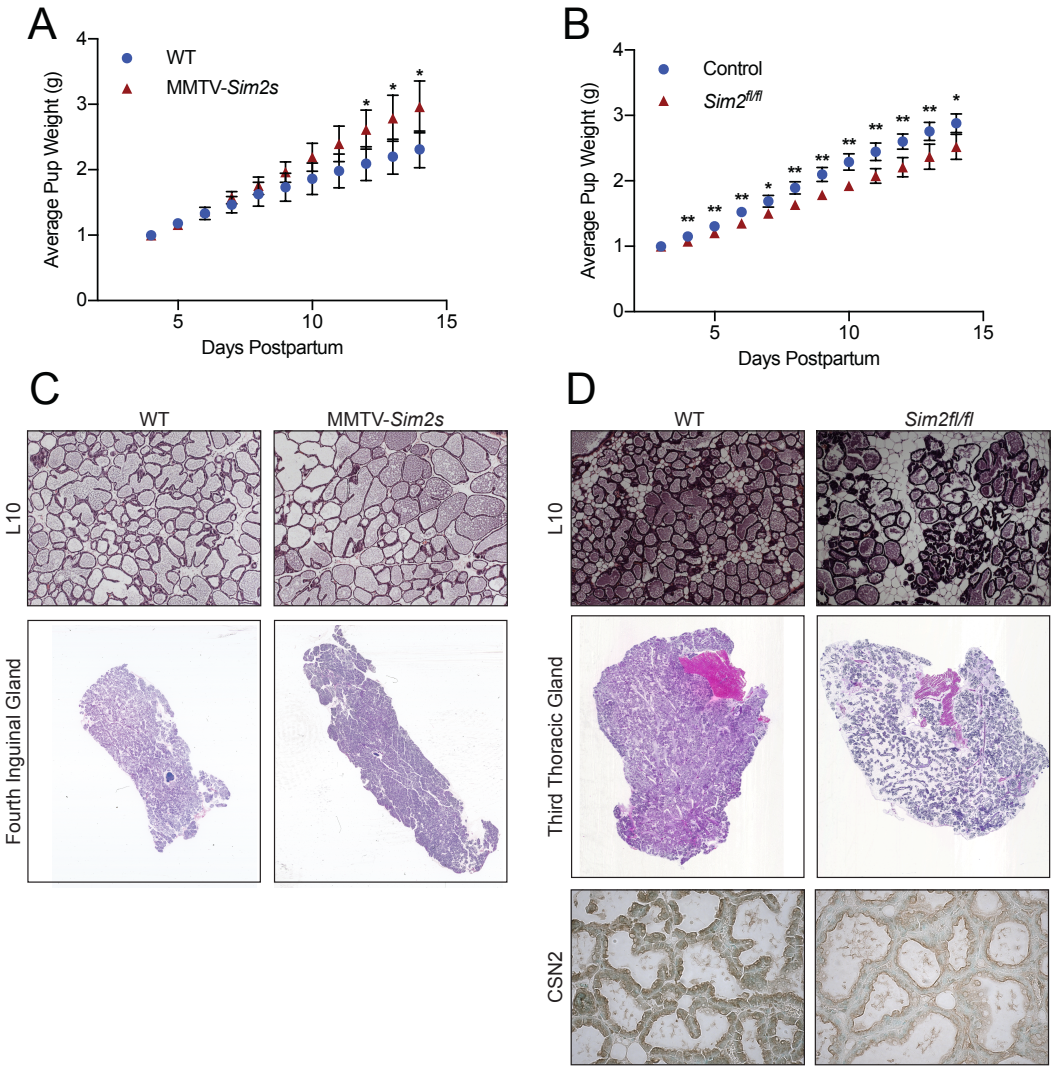

Figure 30 Gain and loss of *Sim2* in the mouse mammary gland.
(A) The first litters of WT and MMTV-*Sim2s* females were cross-fostered with 10 ICR pups each. Litter weights were recorded daily for two weeks and normalized to day one of fostering. (B) The first litters of control and *Sim2*$^{fl/fl}$ females were cross-fostered with 10 ICR pups each. Litter weights were recorded daily for two weeks and normalized to day one of fostering. (C) Representative H&E images and whole slide scans of FVB and MMTV-*Sim2s* mammary glands at lactation day 10. (D) Representative H&E images and whole slide scans of WT and *Sim2*$^{fl/fl}$ mammary glands at lactation day 10. Immunohistochemistry for CSN2 in WT and *Sim2*$^{fl/fl}$ mammary glands at lactation day 10. Two mice were evaluated for each time point, and two sections from each mouse were stained for comparisons. Data are presented as mean ± standard deviation. Statistical significance was evaluated with multiple student t-tests relative to the WT or control group. *p<0.05, **p<0.01.

SIM2s enhances mitochondrial energetic phenotype

As the functional differentiation of MECs necessarily requires a metabolic reprogramming event, we next investigated the impact of SIM2s on mitochondrial respiration and glycolysis, which together generate the energy required to power anabolic processes, such as those engaged during lactation. We interrogated the energetic potential of MECs using the established differentiation protocol of the HC11 mouse mammary epithelial cell line [303] and Seahorse Extracellular Flux technology. This technology allowed us to simultaneously compare the efficiency of oxidative phosphorylation, via oxygen consumption rate (OCR), and the capacity for induction of glycolysis, via extracellular acidification rate (ECAR) [304]. Addition of the mitochondrial uncoupler FCCP (carbonyl cyanide-4 (trifluoromethoxy) phenylhydrazone) disconnects electron transport from ATP synthase, allowing for unchecked, or maximal, oxygen consumption. This maximal oxygen consumption provides a measure of the oxidative potential that can be achieved (Figure 31A). Finally, when OCR is paired with ECAR, a relative energy phenotype of cells can be compared to a stressed state to separate energy phenotypes into quadrants: quiescent, glycolytic, aerobic, and energetic [305].

We then asked whether *Sim2s* affected the energy phenotype of differentiating mammary epithelial cells. Indeed, we found that overexpression of *Sim2s* enhanced both basal and maximal respiration compared to control HC11 cells (Figure 31 B-C). Further, HC11-*Sim2s* cells were substantially more energetic compared to control cells (Figure 31D). Surprisingly, *Sim2s* cells maintained this energetic phenotype out to 96 hours of

differentiation at a level that was not different from that of 48 hours. These results suggest that *Sim2s* is required for metabolic reprogramming during MEC differentiation *in vitro*, and this reprogramming event may be linked to the functional capability of MECs.

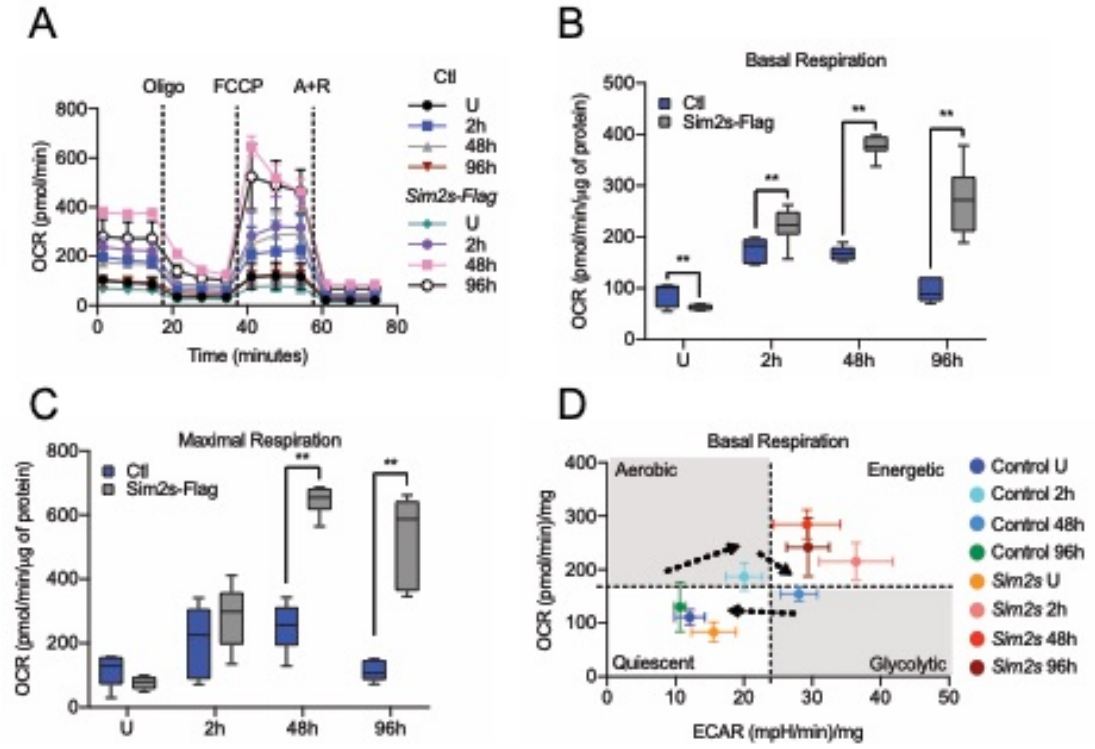

Figure 31 *Sim2s* enhances and prolongs the differentiation-dependent energetic phenotype in HC11 cells.
(A) Seahorse Extracellular Flux oxygen consumption rates (OCRs) in differentiating HC11 cells. (B) Basal OCRs and (C) maximal OCRs show enhanced respiration in *Sim2s* cells. (D) Energy phenotype comparison of OCRs and extracellular acidification rates (ECARs) in differentiating HC11 cells further demonstrating an enhanced energetic state in *Sim2s* cells. (n=2, ≥12 replicates per experiment) U: undifferentiated; h: hours differentiated; oligo: oligomycin; A+R: antimycin a + rotenone. Data are presented as mean ± standard deviation. Box and whisker plots are presented from the 25th to 75th percentile, with the line at the median and the whiskers extending to the minimum and maximum values. Statistical significance was evaluated with multiple student t-tests relative to the control group. *p<0.05, **p<0.01.

Mitochondrial homeostasis is altered by SIM2s

Based on the dramatic differences in mitochondrial respiration and energy potential with gain of *Sim2s*, we sought to determine whether mitochondrial morphology was affected by *Sim2s*. Mitochondrial morphology is known to indicate function; fused mitochondrial networks are generally associated with differentiated cell states and higher mitochondrial respiration, whereas fragmented mitochondria are generally associated with proliferating cells and tend to be more glycolytic. To first evaluate mitochondrial morphology over the course of differentiation, HC11 control and *Sim2s* cells were fixed for transmission electron microscopy (TEM) at an undifferentiated state (U) and at 2-, 8-, and 24-hours differentiated (Figure 32A). By 24 h, clear differences in mitochondrial morphology were apparent between control and *Sim2s* cells (Figure 32B). Mitochondria in *Sim2s* cells were visibly elongated, and measurement of mitochondrial lengths revealed a significant increase in length compared to control cells at 24 h of differentiation (Figure 32C).

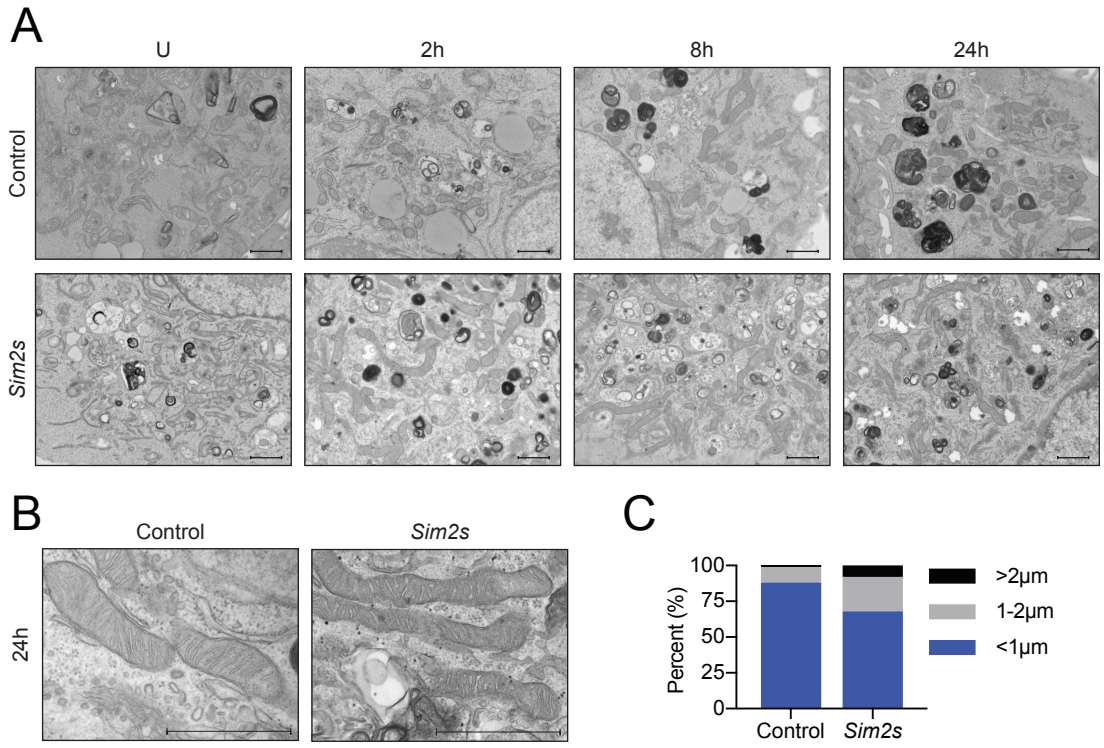

Figure 32 Differentiated HC11-*Sim2s* cells contain elongated mitochondria. (A) Transmission electron microscopy (TEM) images of HC11 cells at progressive stages of differentiation. (B) Higher magnification TEM images demonstrate mitochondrial morphology at 24h of differentiation. Three sections each were evaluated from two independent samples for TEM analysis. (C) Mitochondrial lengths were measured and categorized into short (<1μm), medium (1-2μm), and long (>2μm) length groups. *Sim2s* cells contained a higher percentage of medium and long mitochondria. U: undifferentiated; h: hours differentiated. Scale bars: 1 μm.

Mitochondrial dynamics refer to the homeostatic alterations in mitochondrial number, size, and shape that are generated by fusion and fission. Mitochondrial fusion is regulated by the mitofusins and OPA1 (optic atrophy 1), whereas mitochondrial division is controlled by FIS1 (fission, mitochondrial 1) and DNM1L (dynamin 1 like). As we observed significant elongation of the mitochondrial network in *Sim2s* cells, we evaluated mitochondrial dynamics factors by western blot and gene expression.

Although we did not observe significant changes in gene expression of *Opa1* with differentiation or *Sim2s* (Figure 33A), we did find alterations at the protein level. OPA1 increased across differentiation in control HC11 cells, concomitant with a decrease in DNM1L expression (Figure 33B). Interestingly, total mitochondrial content, indicated by expression of TOMM70 (translocase of outer mitochondrial membrane 70), appeared to increase during differentiation as well. In contrast, OPA1 was expressed at higher levels in HC11-*Sim2s* cells compared to control cells, and OPA1 levels did not change throughout differentiation. HC11-*Sim2s* cells demonstrated an opposite pattern of DNM1L expression. Further, total mitochondrial content was generally lower in HC11-*Sim2s* cells at every time point. The difference in mitochondrial content was confirmed in our mouse models by immunostaining tissue sections for cytochrome c oxidase subunit 4 (COX4), which is a mitochondrial inner membrane protein. COX4 immunostaining revealed a stark contrast of mitochondrial accumulation with loss of *Sim2s* and reduced mitochondrial mass with over expression of *Sim2s* (Figure 33C). These results suggest that *Sim2s* impacts mitochondrial dynamics as well as total mitochondrial number.

The contrast in mitochondrial accumulation between MMTV-*Sim2s* and *Sim2*$^{fl/fl}$ mammary glands could logically be explained by alterations in either mitochondrial biogenesis or mitophagy. Interestingly, our TEM analysis revealed that control cells accumulated autophagosome structures during differentiation that progressed to late-stage autolysosomes by 24 h (Figure 32A). In contrast, *Sim2s* cells exhibited a dramatic increase in autophagosome and autolysosome structures as early as 2 h. These

observations suggest that mitophagy may be enhanced by *Sim2s*. To corroborate this hypothesis, we evaluated the protein expression of microtubule-associated protein 1 light chain 3 (LC3), which is a standard method of monitoring phagophore formation [292]. We again observed induction of autophagy during differentiation, which was enhanced in *Sim2s* cells (Figure 33D). An important caveat to these observations is that autophagy does not necessarily involve the degradation of mitochondria, which is termed mitophagy.

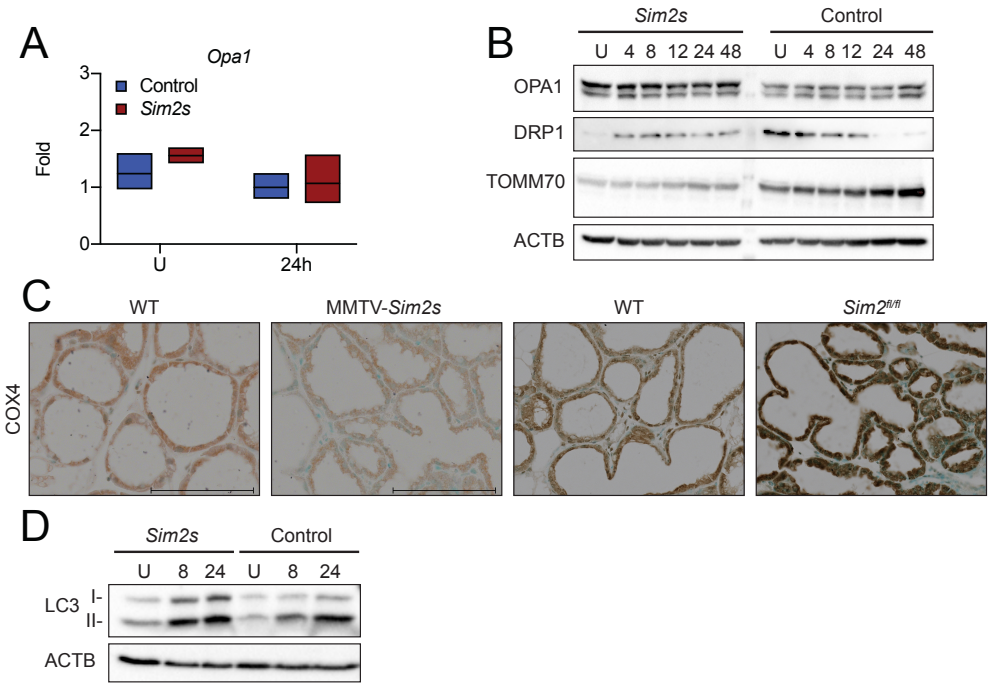

Figure 33 *Sim2s* alters mitochondrial homeostasis.
(A) Expression of *Opa1* in HC11 cells at an undifferentiated and 24h differentiated state (n=3). (B) Expression of mitochondrial markers during HC11 cell differentiation. Levels of OPA1, DRP1/DNML1, TOMM70, and ACTB are indicated. (C) Immunohistochemistry analysis of the inner mitochondrial membrane protein COX4 in the mammary glands of transgenic mice at lactation day 10. (D) Levels of LC3 in control and *Sim2s* HC11 cells.

Mitophagy has proven difficult to confirm, leading to the development of a number of fluorescent reporter systems. Several studies have detailed the use of *MitoTimer*, a novel reporter gene, to monitor mitochondrial health and turnover [281, 306, 307]. The *pMitoTimer* construct, driven by the constitutive CMV promoter, localizes to mitochondria via a cytochrome c oxidase subunit 8 (COX8) targeting sequence, fluoresces green when newly synthesized, and shifts irreversibly to red once oxidized [306]. High ratios of red to green fluorescent intensity indicate increased mitochondrial turnover. Using this system, HC11 cells expressing *pMitoTimer* were monitored by live cell imaging over the course of differentiation. Ratiometric analysis revealed that HC11-*Sim2s* cells exhibit a higher basal turnover rate, which is maintained throughout differentiation (Figure 34A-B). Together, these data support a model where *Sim2s* promotes the normal function of the mammary gland, potentially through enhanced mitophagy.

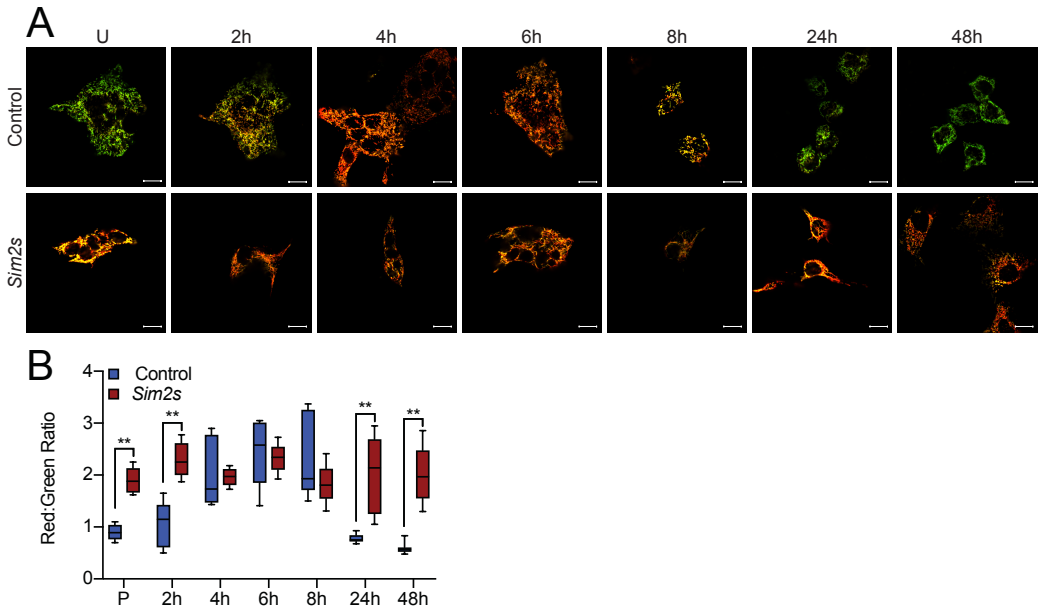

Figure 34 Mitochondrial oxidation is elevated and prolonged with *Sim2s*.
(A) Representative live-cell images of differentiating HC11 cells transiently transfected with *pMitoTimer*. Scale bars: 10 μm. (B) Average red to green fluorescent intensity ratio from 10 images per time point. P: 24 h primed; h: hours differentiated. Data are presented as mean ± standard deviation. Box and whisker plots are presented from the 25th to 75th percentile, with the line at the median and the whiskers extending to the minimum and maximum values. Statistical significance was evaluated with multiple student t-tests relative to the control group. **p<0.01.

Localization of SIM2s during MEC differentiation

SIM2s is a member of the bHLH-PAS family of transcription factors, which are known to play important roles in development and in response to environmental cues [268, 270]. Non-canonical functions of nuclear transcription factors in the mitochondria, including P53, STAT3, STAT5, NF-kB, HIF1A, and steroid receptors, have been shown to regulate numerous mitochondrial processes independent of nuclear activity [308-312]. Due to the metabolic involvement of SIM2s, we sought to determine its localization during differentiation in HC11 cells by fractionation experiments. As expected, we

found that SIM2s was strongly expressed in the nuclear fraction, but we were surprised to find that SIM2s was also present in the mitochondrial fraction (Figure 35A). The relative purity of the fractions was confirmed by the expression of a mitochondrial factor (translocase of outer mitochondrial membrane 70; TOMM70), a cytosolic factor (alpha-tubulin; TUBA), and a nuclear factor (poly[ADP-ribose] polymerase 1; PARP1). To further interrogate the mitochondrial localization of SIM2, half of a mitochondrial preparation was digested with proteinase K to degrade OMM proteins, and the other half was left intact. Digestion of OMM proteins was confirmed by the presence or absence of the OMM protein (TOMM70) or the inner mitochondrial protein COX4. Interestingly, we found that although TOMM70 was degraded in the digested (D) samples, SIM2 remained faintly present in both total (T) and digested fractions (Figure 35B). To further confirm the localization of SIM2s, we performed immunogold assays in differentiated HC11 cells and found that gold particles were indeed present in both the nucleus (data not shown) and mitochondria (Figure 35C). Together, these results suggest that SIM2s may modulate metabolic reprogramming through non-canonical and non-transcriptional mechanisms.

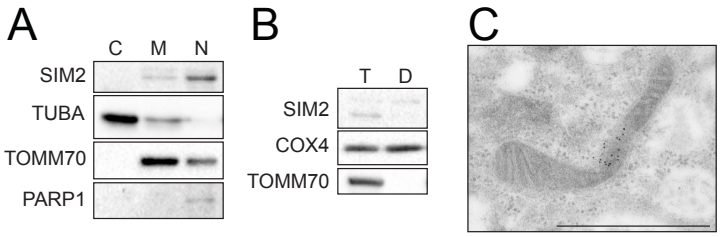

Figure 35 SIM2 localizes to the mitochondria in differentiated HC11 cells. (A) Fractionation of 24h differentiated HC11 cell lysates into cytosol, mitochondrial, and nuclear components and expression of SIM2. TOMM70 and TUBA expression confirmed mitochondrial and cytosolic fraction purity, respectively. PARP1 confirmed the nuclear fraction. (B) Mitochondrial fractions from 24h differentiated HC11 cells were split; half was subjected to proteinase K digestion, and the other half remained undigested. COX4 was used as an inner mitochondrial membrane protein, and TOMM70 was used as an outer mitochondrial protein to monitor digestion of outer mitochondrial proteins. Successful digestion was indicated by loss of TOMM70 expression in the digested fraction. SIM2 was present in two bands in the undigested fraction and in one band in the digested fraction. (C) Immunogold staining of 24h differentiated HC11 cells. SIM2 antibody detected SIM2 and is visualized by gold nanoparticles. Scale bar: 1 μm.

SIM2s interacts directly with phagophore machinery

There is increasing evidence that mitophagy is essential for promoting and maintaining differentiation [313]. Based on the direct localization of SIM2s to mitochondria and the accelerated mitophagy observed with *Sim2s* overexpression, we speculated that SIM2s may be directly involved in the mitophagy machinery. LC3 plays an active role in the formation of the autophagosome by participating in cargo-specific recruitment of adaptor proteins containing LC3 interacting region (LIR) motifs. LIR motif-containing autophagy receptors guide mitochondria to interact with LC3 containing autophagosomes and form the basis of mitophagy [313]. Analysis of the SIM2s protein identified two conserved LIR domains in the PAS-A domain at amino acids 95 and 193 (Figure 36A). To determine if SIM2s and LC3 interact, we performed

co-immunoprecipitation studies using IgG control or FLAG antibodies in control and *FLAG-Sim2s* differentiated HC11 cells. Indeed, we found that SIM2s and LC3 directly interacted in HC11 cells (Figure 36B). To further confirm the role of the SIM2s:LC3 interaction in MEC differentiation and function, we generated point mutations in both LIR domains on *Sim2* (Figure 36A). Importantly, overexpression of the mutated *Sim2s* construct failed to enhance differentiation-dependent *Csn2* gene expression (Figure 36C) or promote a more energetic phenotype when compared to *Sim2s* overexpressing cells (Figure 36D-F), suggesting that the SIM2s:LC3 interaction is essential for SIM2s-mediated mitophagy and differentiation. In summary, these data suggest that SIM2s regulates MEC differentiation through direct interaction with LC3, which may enhance mitophagy.

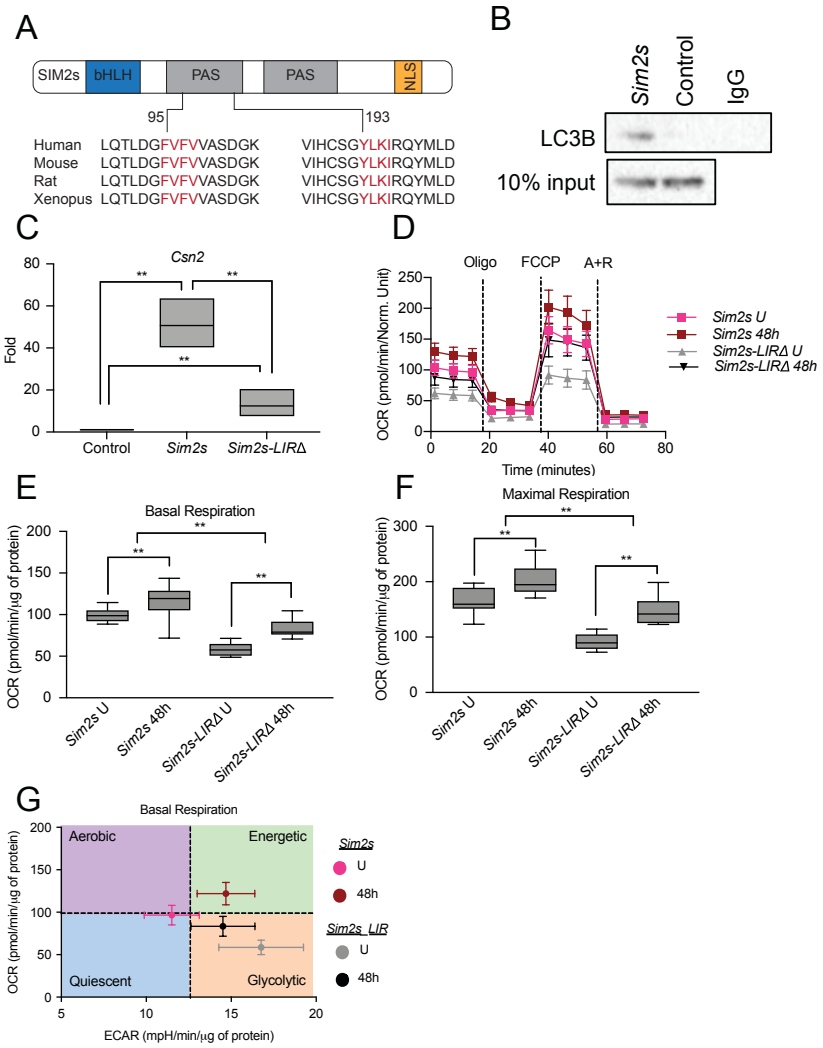

Figure 36 SIM2s interacts with autophagy machinery.
(A) Analysis of SIM2 protein for consensus LC3 interacting regions (LIRs). (B) Co-immunoprecipitation of control and FLAG-tagged *Sim2s* HC11 cells at 24 h of differentiation. SIM2 was pulled down with FLAG beads, and blotted for LC3B. (C) Differentiation-dependent *Csn2* expression in *Sim2s* and *Sim2s*-LIR mutant HC11 cells at 24 h of differentiation (n=3). (D) Seahorse extracellular flux analysis in *Sim2s* and *Sim2s*-LIR mutant HC11 cells. (E) Breakdown of basal and (F) maximal respiration in *Sim2s* and *Sim2s*-LIR mutant HC11 cell lines at a proliferative state and at 48 h of differentiation. (G) Energy phenotype profile of basal state *Sim2s* and *Sim2s*-LIR mutant HC11 cell lines (n=2, ≥9 replicates per experiment). Data are presented as mean ± standard deviation. Box and whisker plots are presented from the 25th to 75th percentile, with the line at the median and the whiskers extending to the minimum and maximum values. Statistical significance was evaluated with student t-tests relative to the control cell line. **p<0.01.

SIM2s prolongs the survival of functional mammary epithelial cell survival *in vivo*

We have previously shown that SIM2s delays involution and maintains alveolar structures after multiple pregnancies in the mouse mammary gland [243]. Although these studies suggest that SIM2s maintains a differentiated cell state, they did not indicate whether the function of the maintained cells was preserved. Therefore, to further determine if SIM2s is capable of prolonging alveolar cell survival and function, we performed an extended lactation trial using MMTV-*Sim2s* and WT mice. Lactation was prolonged in MMTV-*Sim2s* and WT mice to 42 days. Initial litters were cross-fostered with 10, weight matched, 1-day-old WT pups. Beginning on day 14, litters were replaced with 10, weight matched, 7-day old WT pups every 7 days, to maintain suckling stimulus and milk let down [283]. Litter weights were recorded every week, and pup weight gain was calculated for each 7-day period. Strikingly, MMTV-*Sim2s* dams were able to sustain litter weight gain and epithelial cell survival out to lactation day 42 better than WT dams, one and two weeks beyond normal weaning (day 28 and 35) (Figure 37A-B). Thus, over-expression of *Sim2s* provides a protective advantage in alveolar cells and supports improved lactation capacity one to two weeks beyond normal weaning.

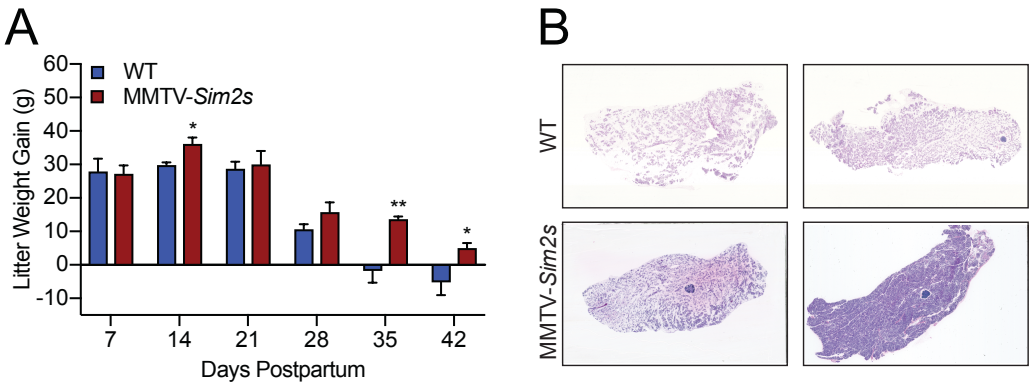

Figure 37 *Sim2s* prolongs lactation ability in mice.
(A) Lactation was extended in WT and MMTV-*Sim2s* mice by repeated cross-fostering with ICR pups. Litter weight gain was measured on a weekly basis and demonstrates that MMTV-*Sim2s* dams nurse litters that gain more weight than those nursed by WT dams. (B) Whole slide scan images of H&E-stained mammary glands from WT and MMTV-*Sim2s* mice at day 42 of lactation.

Altogether we have shown that SIM2s regulates the differentiation and survival of MECs, potentially by enhancing mitophagy through the direct interaction of SIM2s and the autophagy machinery (Figure 38). These results imply a novel regulation of MEC differentiation and of the metabolic reprogramming that occurs during the transition from gestation to lactation. We anticipate that these results will open the door for additional study of how metabolic reprogramming contributes to cell fate and differentiation decisions.

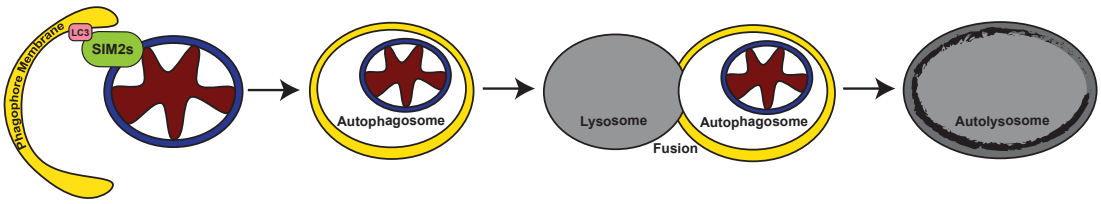

Figure 38 Model of SIM2s-mediated mitophagy.

CHAPTER V

CONCLUSIONS

Here, we show that MEC differentiation, defined by differentiation-dependent gene expression, enhanced bioenergetic capacity, and cell survival, is dependent on autophagy and SIM2s. Inhibition of autophagic flux via pharmacological treatment or knockdown of *Atg7* impaired one or more of these aspects of MEC differentiation. Moreover, we demonstrated that mitochondria undergo mitophagy during early differentiation, and loss of the mitophagy factor, PRKN, results in impairment of MEC differentiation. Together, these results suggest that mitochondria undergo mitophagy and a bioenergetic transition during early differentiation and that this process ultimately promotes the functional capacity of differentiated MECs. Upstream of autophagy, we found that the transcription factor SIM2s is required for alveolar differentiation in the mammary gland and prolongs the survival and function of MECs. Further, overexpression of *Sim2s* enhanced mitochondrial elongation and oxidation *in vitro*, and SIM2 was associated directly with mitochondria and LC3B on the phagophore membrane. These results suggest that SIM2s regulates MEC differentiation not as a traditional transcription factor, but by interacting directing with cytosolic components to finely tune the metabolic needs of MECs. Additional studies are necessary to verify and separate the transcriptional and non-transcriptional roles of SIM2s. Together, these studies increase our understanding of the metabolic reprogramming of MECs during differentiation and provide insight for future studies regarding the dysregulation that occurs with disease (Figure 39).

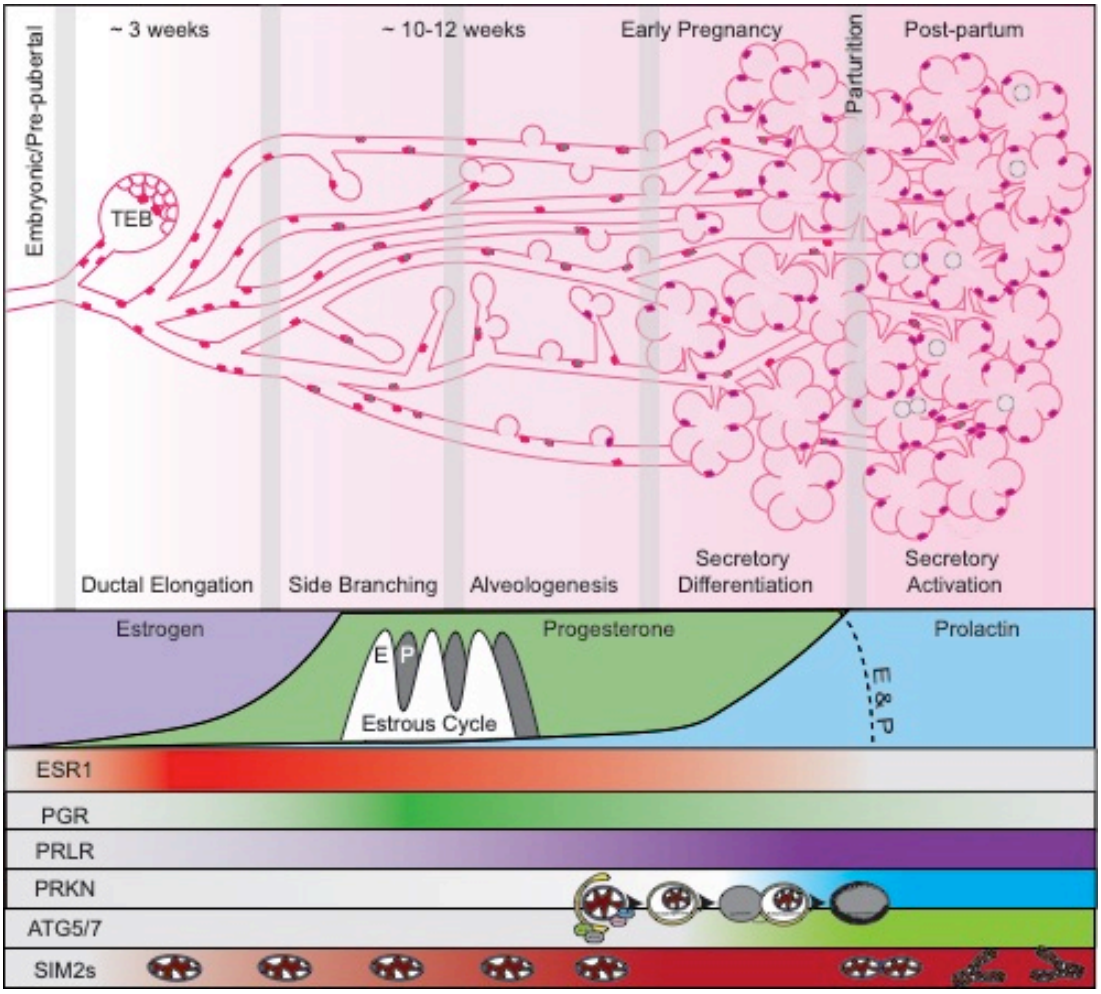

Figure 39 Model depicting the requirement of autophagy and SIM2s for MEC differentiation.

To better understand the mechanism of programmed mitophagy, it is necessary to evaluate both the targeting of mitochondria for degradation and the process of autophagic flux itself. As programmed mitophagy targeting and receptors vary widely, we began by investigating autophagic flux and autophagy factors. Autophagic flux occurs in sequential steps: biogenesis of phagophore membranes, selective or non-selective engulfment of cytoplasmic material into autophagosomes, and fusion with

lysosomes to form autolysosomes. To evaluate the requirement of autophagic flux, factors in these steps are often targeted for inhibition or deletion. Based on our findings, we suggest that the specific step targeted may have distinct functional outcomes based on the context of the cell. More specifically, inhibiting autophagic flux at early stages with depletion of ATG7 resulted in divergent gene-expression outcomes compared to late-stage inhibition with BAF or CQ.

BAF and CQ inhibit lysosomal acidification, leading to the accumulation of autophagosomes and preventing autophagic flux. We found that BAF and CQ treatment in HC11 cells completely abrogated functional differentiation. Similarly, BAF-treated myoblasts fail to differentiate [102], and CQ treatment prevents the differentiation-dependent metabolic transition of retinal ganglion cells [103] and significantly stunts the differentiation of adipocytes [110].

Returning to the autophagosome formation step, we next targeted the *Atg* genes, which are well-known and conserved factors in the autophagy conjugation machinery. Previous work has demonstrated that loss of either *Atg5* or *Atg7* results in early postnatal lethality [314, 315]. Therefore, the majority of mouse studies have utilized conditional knockout models to study specific tissues. Studies that utilize early development models, as in adipocytes and T-cells, report essential roles for ATG5 and ATG7 in reaching functionally differentiated end cell states [110, 316]. Adipose-specific loss of both *Atg5* and *Atg7* impairs adipogenesis and ultimately results in significantly reduced white adipose deposits [109, 110, 316]. Similarly, mature T lymphocytes are significantly

reduced in *Atg7* conditional knockout mice, and the naïve T-cells that do develop exhibit increased apoptosis [317].

In contrast, knockout of *Atg5* or *Atg7* in mature cell states, such as the heart [318] and muscle [319], results in phenotypes that are exacerbated when additional stress is applied; however, neuronal deletion of *Atg5* results in neurodegeneration without additional stress and suggests that basal autophagy is vital in neurons [320]. This observation is not surprising in light of the many neurodegenerative diseases with root causes arising from defects in autophagy processes. Genetic loss of *Atg5* and *Atg7* has not been specifically studied in lactation; thus, our results are the first to suggest that loss of *Atg7* impairs HC11 MEC bioenergetic capacity and implies a similar requirement for autophagy during the differentiation of these cells. It would be of interest to target these factors during postnatal mammary gland development to confirm the *in vivo* requirement of the autophagy conjugation system.

Of note, the loss of *Atg5* and *Atg7* in HC11 cells resulted in a disconnect between the differentiation-dependent gene expression and bioenergetic responses. We found that this disconnect resulted from the unexpected contribution of ROS signaling to *Csn2* expression (**Fig. 6G**). ROS production following autophagy inhibition at the early stages of autophagic flux results from the accumulation of mitochondria [129]. Moreover, ROS can mediate signaling cascades and activate the STAT family of nuclear transcription factors [294, 295]. Indeed, STAT5, a master regulator of lactation gene expression, was increasingly activated in *shAtg7* cells, and *Atg7* knockdown, but not BAF treatment, resulted in significantly elevated levels of mROS.

Further, scavenging mROS in HC11 cells with mitoquinol resulted in significantly reduced *Csn2* expression at 48 h of differentiation and did not affect cell viability (data not shown). Consistent with our findings, adipocyte differentiation enhances mitochondrial ROS production, which leads to the induction of PPARG transcriptional signaling [130]. Although ROS generation is classically regarded as a damaging event, our findings, as well as those of others, add to the notion that moderately elevated ROS serve as signaling molecules and may contribute to cellular differentiation [129].

To further define the contribution of mitophagy during MEC differentiation, we sought to address the mechanism of mitochondrial targeting. Recently, several mitophagy factors have been identified, including PINK1, PRKN, BNIP3L/NIX (BCL2 interacting protein 2 like), BNIP3 (BCL2 interacting protein 3), and FUNDC1 (FUN14 domain containing 1). Although none of these factors have been characterized in the lactating mammary gland, loss of PRKN [299] or BNIP3 [321] has been associated with breast cancer progression through the upregulation of HIF1A (hypoxia inducible factor 1 subunit alpha). Interestingly, both BNIP3 [322] and BNIP3L [150] contribute to PINK1/PRKN-mediated mitophagy. Based on these connections, we evaluated PRKN as a potential mitophagy factor during MEC differentiation. Although PRKN expression was non-existent in undifferentiated HC11 cells, strikingly similar to observations in SH-SY5Y and HeLa cell lines [150, 298], we found substantial induction of PRKN expression in both total and mitochondrial cell fractions during priming and throughout differentiation. Importantly, this localization did not coincide or follow a mitochondrial

depolarization event, as JC-1 ratios indicated no change in the accumulation of JC-1 aggregates between proliferative, confluent, and primed HC11 cell states. These observations suggest that mitochondrial localization of PRKN occurs independently of the canonical depolarization-induced accumulation of PINK1 on damaged mitochondria. Instead, we propose that a yet-to-be-identified developmental signaling cascade is responsible for PRKN loading and programmed mitophagy in this system.

To further evaluate the contribution of PRKN to HC11 MEC differentiation, we stably expressed shRNA constructs that target *Prkn* in HC11 cells. Surprisingly, knockdown of *Prkn* resulted in cell death throughout differentiation but not in cell death in confluent cells maintained for the same length of time. Similar cell death occurs with loss or mutation of *Prkn* in mouse cardiomyocytes [113] and dopaminergic neurons of Parkinson disease patients [323], respectively. We can only speculate that the observed cell death could be due to the absence of vital PRKN-mediated mitophagy or PRKN-mediated function unrelated to mitophagy that occurs during the same time frame. Nevertheless, we found a reduced bioenergetic capacity of HC11 MECs lacking *Prkn* compared to control cells, and energy phenotypes differed from those observed after loss of *Atg7*. Both OCR and ECAR were stunted in *shAtg7_2* cells, whereas *shPrkn_2* cells only exhibited reduced OCRs. This observation again points to the complexity of interpreting results following perturbation of autophagic flux and suggests that both the developmental context and stage of autophagy inhibition are important factors.

Parkin ubiquitinates outer mitochondrial proteins, including MFN2, and, surprisingly, has been shown to ubiquitinate SIM2, targeting it for degradation by the

proteasome [154]. Proteasomal degradation of bHLH-PAS proteins is a known mechanism of regulation. For example, HIF1A is hydroxylated and degraded under normoxic conditions, but is rapidly stabilized in response to low oxygen tension [155]. Thus, SIM2 degradation mediated by PRKN ubiquitination may serve to regulate SIM2 action. Indeed, we have recently shown that SIM2s is stabilized by ATM-mediated phosphorylation following ionizing radiation and DNA damage [261]; however, we did not address whether phosphorylation of SIM2s altered its ubiquitination. We have also demonstrated that SIM2s enhances alveolar differentiation and functions as a tumor suppressor in breast cancer [239-241, 243, 245]. Together, these observations suggest that SIM2s is a potential upstream regulator of MEC differentiation and may be involved directly in programmed mitophagy as well.

Similar to other master regulators of various stages of mammary gland development, including GATA3 and STAT5A, overexpression of SIM2s enhanced the functional differentiation of the mammary gland; whereas loss of SIM2s stunted full differentiation. Ectopic expression of SIM2s also prolonged differentiated MEC survival, function, and energy state as well as directly impacted the morphology and oxidation of mitochondria. The increased mitochondrial length and electron density observed in differentiated HC11-*Sim2s* cells is interesting because cristae morphology has been directly linked to respiratory efficiency [144], suggesting that the closely associated cristae in HC11-*Sim2s* cells may provide increased functionality. However, it remains unclear whether the observed mitochondrial elongation is a direct result of

SIM2 or is an adaptation made to avoid mitochondrial degradation, which has been suggested in periods of elevated autophagy [324], such as involution.

To more directly address this unanswered question, we performed fractionation and immunogold labeling experiments to determine the localization of SIM2s during MEC differentiation. We found that SIM2s localized to mitochondria, which has been observed for other transcription factors, including STAT3 [276, 310]. Interestingly, STAT3 has also been implicated indirectly and directly in mitophagy [325], and we have shown here that SIM2s interacts directly with both mitochondria and the phagophore machinery, suggesting that similar roles may be attributed to SIM2s. Although oxidative stress and ROS have been shown to induce STAT3 function [276, 325], the upstream regulators of SIM2s during MEC differentiation remain unknown. Future investigation of these regulators will provide important insight into the regulation of MEC differentiation, mitophagy, and the tumor suppressive role of SIM2s.

The mammary gland is a unique tissue that undergoes successive rounds of proliferation during gestation, nutrient production during lactation, and regression during involution. Thus far, evaluation of autophagy during MEC differentiation is limited to acinar development *in vitro* [326] and the early stages of involution both *in vivo* and *in vitro* [327-329]. Interestingly, only the early reversible phase of involution involves autophagy, whereas the later irreversible phase is associated with lysosomal-mediated cell death. Autophagy induction during early involution is hypothesized to promote cell survival if lactation stimulus recurs [118]. Induction of autophagy during the early phase involution relies on STAT3 [78]. STAT3 is expressed across mammary gland

development and is dramatically activated by tyrosine phosphorylation during involution [62]. Consistent with these studies, we did not detect activation of STAT3 during late pregnancy or mid-lactation; however, we did observe induction of nuclear p-STAT3 at lactation day 1, which has never been evaluated to our knowledge.

Moreover, HC11 cells express p-STAT3 specifically at priming, the transitional stage between undifferentiated and differentiated cells. As loss of *Stat3* results in embryonic lethality, conditional knockout models have been developed to conditionally delete *Stat3* from the mammary epithelium using *Wap* or beta-lactoglobulin (*Blg*) promoter-driven Cre recombinase expression. Conditional *Stat3* deletion in the mammary epithelium results in delayed involution and retention of mammary alveolar cells in the absence of lactational stimuli [330]. Although it was suggested that STAT3-mediated autophagy is associated with cell survival [331], the identity of the upstream signaling cascade and the effect of STAT3 deletion on autophagy remain unknown. To further complicate the delineation of the STAT3-mediated autophagy response, STAT3 has been shown to inhibit autophagy through a variety of transcriptional and non-transcriptional mechanisms in other tissues and is known to localize to the nucleus, cytoplasm, and mitochondria [325]. Thus, due to the complexity of STAT3 localization and activation, STAT3 function appears to be highly context-dependent.

Based on previous work in the mammary gland and our observation that p-STAT3 was induced during early lactation in mouse mammary tissues as well as at priming in HC11 cells, it is tempting to postulate that STAT3 may contribute to the autophagy response described here. Of note, mice lacking *Stat3* in the mammary

epithelium from mid-pregnancy through involution do not display developmental abnormalities and lactate normally [330]. Thus, if functional differentiation of MECs indeed requires programmed mitophagy, it is unlikely that STAT3 is the sole mediator of this response. The different outcomes between general autophagy during involution and the programmed mitophagy reported here point to the relevance of the developmental context in deciphering the complex mechanisms that coordinate these processes. Indeed, it is likely that the general autophagy observed during involution is distinct from the programmed mitophagy described here in terms of biological context, function, and mechanism. It is also worth noting that programmed mitophagy may be initiated much earlier in mouse mammary gland development than what has been captured in the present study or by the current *Stat3* conditional knock out models. Additional study will be necessary to fully delineate the upstream signaling responsible for the induction of autophagy during early MEC differentiation.

In summary, we propose that programmed mitophagy is the bioenergetic mechanism responsible for the necessary metabolic transition during MEC differentiation and that this process is enhanced by SIM2s. To our knowledge, this is the first work to address the dramatic differences in mitochondria and mitochondrial function in pregnant and lactating mouse mammary glands [104, 105]. Importantly, mammary gland development is largely postnatal, and our work suggests that the mammary gland provides a unique physiological model to study programmed mitophagy without the application of chemicals or nutrient starvation. Future work will be necessary to confirm the *in vivo* requirement of programmed mitophagy during

mammary gland development as well as to further define the upstream developmental signals that engage programmed mitophagy and SIM2s. Nevertheless, our results offer insight into the establishment and maintenance of lactation, with implications for future studies of mitochondrial dysfunction and disease in the mammary gland.

REFERENCES

1. Perou CM, Sorlie T, Eisen MB, van de Rijn M, Jeffrey SS, Rees CA, Pollack JR, Ross DT, Johnsen H, Akslen LA *et al*: **Molecular portraits of human breast tumours**. *Nature* 2000, **406**(6797):747-752.

2. Prat A, Parker JS, Karginova O, Fan C, Livasy C, Herschkowitz JI, He X, Perou CM: **Phenotypic and molecular characterization of the claudin-low intrinsic subtype of breast cancer**. *Breast Cancer Res* 2010, **12**(5):R68.

3. Koren S, Bentires-Alj M: **Breast Tumor Heterogeneity: Source of Fitness, Hurdle for Therapy**. *Mol Cell* 2015, **60**(4):537-546.

4. Loibl S, Treue D, Budczies J, Weber K, Stenzinger A, Schmitt WD, Weichert W, Jank P, Furlanetto J, Klauschen F *et al*: **Mutational Diversity and Therapy Response in Breast Cancer: A Sequencing Analysis in the Neoadjuvant GeparSepto Trial**. *Clin Cancer Res* 2019, **25**(13):3986-3995.

5. Marusyk A, Polyak K: **Tumor heterogeneity: causes and consequences**. *Biochim Biophys Acta* 2010, **1805**(1):105-117.

6. Wiseman BS, Werb Z: **Stromal effects on mammary gland development and breast cancer**. *Science* 2002, **296**(5570):1046-1049.

7. Bernardo GM, Lozada KL, Miedler JD, Harburg G, Hewitt SC, Mosley JD, Godwin AK, Korach KS, Visvader JE, Kaestner KH *et al*: **FOXA1 is an essential determinant of ERalpha expression and mammary ductal morphogenesis**. *Development* 2010, **137**(12):2045-2054.

8. Neville MC, McFadden TB, Forsyth I: **Hormonal regulation of mammary differentiation and milk secretion**. *J Mammary Gland Biol Neoplasia* 2002, **7**(1):49-66.

9. Brisken C, O'Malley B: **Hormone action in the mammary gland**. *Cold Spring Harb Perspect Biol* 2010, **2**(12):a003178.

10. Richert MM, Schwertfeger KL, Ryder JW, Anderson SM: **An atlas of mouse mammary gland development**. *J Mammary Gland Biol Neoplasia* 2000, **5**(2):227-241.

11. Rosen JM, Woo SL, Comstock JP: **Regulation of casein messenger RNA during the development of the rat mammary gland. 1975**. *J Mammary Gland Biol Neoplasia* 2009, **14**(3):343-351.

12. Visvader JE, Stingl J: **Mammary stem cells and the differentiation hierarchy: current status and perspectives**. *Genes & development* 2014, **28**(11):1143-1158.

13. Oakes SR, Gallego-Ortega D, Ormandy CJ: **The mammary cellular hierarchy and breast cancer**. *Cell Mol Life Sci* 2014, **71**(22):4301-4324.

14. Macias H, Hinck L: **Mammary gland development**. *Wiley Interdiscip Rev Dev Biol* 2012, **1**(4):533-557.

15. Tucker HA: **Hormones, mammary growth, and lactation: a 41-year perspective**. *Journal of dairy science* 2000, **83**(4):874-884.

16. Nandi S: **Endocrine control of mammarygland development and function in the C3H/ He Crgl mouse**. *J Natl Cancer Inst* 1958, **21**(6):1039-1063.

17. Hennighausen L, Robinson GW: **Signaling pathways in mammary gland development**. *Dev Cell* 2001, **1**(4):467-475.

18. Lubahn DB, Moyer JS, Golding TS, Couse JF, Korach KS, Smithies O: **Alteration of reproductive function but not prenatal sexual development after insertional disruption of the mouse estrogen receptor gene**. *Proc Natl Acad Sci U S A* 1993, **90**(23):11162-11166.

19. Mallepell S, Krust A, Chambon P, Brisken C: **Paracrine signaling through the epithelial estrogen receptor alpha is required for proliferation and morphogenesis in the mammary gland**. *Proc Natl Acad Sci U S A* 2006, **103**(7):2196-2201.

20. Lydon JP, DeMayo FJ, Funk CR, Mani SK, Hughes AR, Montgomery CA, Jr., Shyamala G, Conneely OM, O'Malley BW: **Mice lacking progesterone receptor exhibit pleiotropic reproductive abnormalities**. *Genes & development* 1995, **9**(18):2266-2278.

21. Brisken C, Park S, Vass T, Lydon JP, O'Malley BW, Weinberg RA: **A paracrine role for the epithelial progesterone receptor in mammary gland development**. *Proc Natl Acad Sci U S A* 1998, **95**(9):5076-5081.

22. Ormandy CJ, Camus A, Barra J, Damotte D, Lucas B, Buteau H, Edery M, Brousse N, Babinet C, Binart N *et al*: **Null mutation of the prolactin receptor gene produces multiple reproductive defects in the mouse**. *Genes & development* 1997, **11**(2):167-178.

23. Tanos T, Rojo L, Echeverria P, Brisken C: **ER and PR signaling nodes during mammary gland development**. *Breast Cancer Res* 2012, **14**(4):210.

24. Acconcia F, Kumar R: **Signaling regulation of genomic and nongenomic functions of estrogen receptors**. *Cancer Lett* 2006, **238**(1):1-14.

25. Hennighausen L, Robinson GW, Wagner KU, Liu W: **Prolactin signaling in mammary gland development**. *J Biol Chem* 1997, **272**(12):7567-7569.

26. Williams JM, Daniel CW: **Mammary ductal elongation: differentiation of myoepithelium and basal lamina during branching morphogenesis**. *Dev Biol* 1983, **97**(2):274-290.

27. Couse JF, Korach KS: **Estrogen receptor null mice: what have we learned and where will they lead us?** *Endocr Rev* 1999, **20**(3):358-417.

28. Kouros-Mehr H, Slorach EM, Sternlicht MD, Werb Z: **GATA-3 maintains the differentiation of the luminal cell fate in the mammary gland**. *Cell* 2006, **127**(5):1041-1055.

29. Asselin-Labat ML, Sutherland KD, Barker H, Thomas R, Shackleton M, Forrest NC, Hartley L, Robb L, Grosveld FG, van der Wees J *et al*: **Gata-3 is an essential regulator of mammary-gland morphogenesis and luminal-cell differentiation**. *Nat Cell Biol* 2007, **9**(2):201-209.

30. Kaestner KH, Katz J, Liu Y, Drucker DJ, Schutz G: **Inactivation of the winged helix transcription factor HNF3alpha affects glucose homeostasis and islet glucagon gene expression in vivo**. *Genes & development* 1999, **13**(4):495-504.

31. Cunha GR, Baskin L: **Use of sub-renal capsule transplantation in developmental biology**. *Differentiation* 2016, **91**(4-5):4-9.

32. Badve S, Turbin D, Thorat MA, Morimiya A, Nielsen TO, Perou CM, Dunn S, Huntsman DG, Nakshatri H: **FOXA1 expression in breast cancer--correlation with luminal subtype A and survival**. *Clin Cancer Res* 2007, **13**(15 Pt 1):4415-4421.

33. Habashy HO, Powe DG, Rakha EA, Ball G, Paish C, Gee J, Nicholson RI, Ellis IO: **Forkhead-box A1 (FOXA1) expression in breast cancer and its prognostic significance**. *Eur J Cancer* 2008, **44**(11):1541-1551.

34. Mehra R, Varambally S, Ding L, Shen R, Sabel MS, Ghosh D, Chinnaiyan AM, Kleer CG: **Identification of GATA3 as a breast cancer prognostic marker by global gene expression meta-analysis**. *Cancer Res* 2005, **65**(24):11259-11264.

35. Sorlie T, Tibshirani R, Parker J, Hastie T, Marron JS, Nobel A, Deng S, Johnsen H, Pesich R, Geisler S *et al*: **Repeated observation of breast tumor subtypes in**

independent gene expression data sets. *Proc Natl Acad Sci U S A* 2003, **100**(14):8418-8423.

36. Early Breast Cancer Trialists' Collaborative G: **Effects of chemotherapy and hormonal therapy for early breast cancer on recurrence and 15-year survival: an overview of the randomised trials**. *Lancet* 2005, **365**(9472):1687-1717.

37. Usary J, Llaca V, Karaca G, Presswala S, Karaca M, He X, Langerod A, Karesen R, Oh DS, Dressler LG *et al*: **Mutation of GATA3 in human breast tumors**. *Oncogene* 2004, **23**(46):7669-7678.

38. Carroll JS, Liu XS, Brodsky AS, Li W, Meyer CA, Szary AJ, Eeckhoute J, Shao W, Hestermann EV, Geistlinger TR *et al*: **Chromosome-wide mapping of estrogen receptor binding reveals long-range regulation requiring the forkhead protein FoxA1**. *Cell* 2005, **122**(1):33-43.

39. Laganiere J, Deblois G, Lefebvre C, Bataille AR, Robert F, Giguere V: **From the Cover: Location analysis of estrogen receptor alpha target promoters reveals that FOXA1 defines a domain of the estrogen response**. *Proc Natl Acad Sci U S A* 2005, **102**(33):11651-11656.

40. Carroll JS, Meyer CA, Song J, Li W, Geistlinger TR, Eeckhoute J, Brodsky AS, Keeton EK, Fertuck KC, Hall GF *et al*: **Genome-wide analysis of estrogen receptor binding sites**. *Nat Genet* 2006, **38**(11):1289-1297.

41. Eeckhoute J, Keeton EK, Lupien M, Krum SA, Carroll JS, Brown M: **Positive cross-regulatory loop ties GATA-3 to estrogen receptor alpha expression in breast cancer**. *Cancer Res* 2007, **67**(13):6477-6483.

42. Fendrick JL, Raafat AM, Haslam SZ: **Mammary gland growth and development from the postnatal period to postmenopause: ovarian steroid receptor ontogeny and regulation in the mouse**. *J Mammary Gland Biol Neoplasia* 1998, **3**(1):7-22.

43. Silberstein GB, Van Horn K, Shyamala G, Daniel CW: **Progesterone receptors in the mouse mammary duct: distribution and developmental regulation**. *Cell Growth Differ* 1996, **7**(7):945-952.

44. Haslam SZ, Nummy KA: **The ontogeny and cellular distribution of estrogen receptors in normal mouse mammary gland**. *J Steroid Biochem Mol Biol* 1992, **42**(6):589-595.

45. Fata JE, Kong YY, Li J, Sasaki T, Irie-Sasaki J, Moorehead RA, Elliott R, Scully S, Voura EB, Lacey DL *et al*: **The osteoclast differentiation factor**

osteoprotegerin-ligand is essential for mammary gland development. *Cell* 2000, **103**(1):41-50.

46. Beleut M, Rajaram RD, Caikovski M, Ayyanan A, Germano D, Choi Y, Schneider P, Brisken C: **Two distinct mechanisms underlie progesterone-induced proliferation in the mammary gland**. *Proc Natl Acad Sci U S A* 2010, **107**(7):2989-2994.

47. Mulac-Jericevic B, Lydon JP, DeMayo FJ, Conneely OM: **Defective mammary gland morphogenesis in mice lacking the progesterone receptor B isoform**. *Proc Natl Acad Sci U S A* 2003, **100**(17):9744-9749.

48. Schramek D, Leibbrandt A, Sigl V, Kenner L, Pospisilik JA, Lee HJ, Hanada R, Joshi PA, Aliprantis A, Glimcher L *et al*: **Osteoclast differentiation factor RANKL controls development of progestin-driven mammary cancer**. *Nature* 2010, **468**(7320):98-102.

49. Gonzalez-Suarez E, Jacob AP, Jones J, Miller R, Roudier-Meyer MP, Erwert R, Pinkas J, Branstetter D, Dougall WC: **RANK ligand mediates progestin-induced mammary epithelial proliferation and carcinogenesis**. *Nature* 2010, **468**(7320):103-107.

50. Oscar Riddle RWB, and Simon W. Dykshorn: **The preparation, identification, and assay of prolactin - a hormone of the anterior pituitary**. *American Journal of Physiology-Legacy Content* 1933, **105**(1):191-216.

51. Stricker P, Grueter F: **Action du lobe ant6rieur de l'hypophyse sur la mont6e laiteuse.** *C R Soc Biol* 1928, **99**:1978-1980.

52. Benedek-Jaszmann LJ, Sternthal V: **Late suppression of lactation with bromocriptine**. *Practitioner* 1976, **216**(1294):450-454.

53. Flint DJ, Vernon RG: **Effects of food restriction on the responses of the mammary gland and adipose tissue to prolactin and growth hormone in the lactating rat**. *J Endocrinol* 1998, **156**(2):299-305.

54. Brisken C: **Hormonal control of alveolar development and its implications for breast carcinogenesis**. *J Mammary Gland Biol Neoplasia* 2002, **7**(1):39-48.

55. Brisken C, Kaur S, Chavarria TE, Binart N, Sutherland RL, Weinberg RA, Kelly PA, Ormandy CJ: **Prolactin controls mammary gland development via direct and indirect mechanisms**. *Dev Biol* 1999, **210**(1):96-106.

56. Ormandy CJ, Naylor M, Harris J, Robertson F, Horseman ND, Lindeman GJ, Visvader J, Kelly PA: **Investigation of the transcriptional changes underlying**

functional defects in the mammary glands of prolactin receptor knockout mice. *Recent Prog Horm Res* 2003, **58**:297-323.

57. Shillingford JM, Miyoshi K, Robinson GW, Grimm SL, Rosen JM, Neubauer H, Pfeffer K, Hennighausen L: **Jak2 is an essential tyrosine kinase involved in pregnancy-mediated development of mammary secretory epithelium**. *Mol Endocrinol* 2002, **16**(3):563-570.

58. Liu X, Robinson GW, Wagner KU, Garrett L, Wynshaw-Boris A, Hennighausen L: **Stat5a is mandatory for adult mammary gland development and lactogenesis**. *Genes & development* 1997, **11**(2):179-186.

59. Groner B, Hennighausen L: **Linear and cooperative signaling: roles for Stat proteins in the regulation of cell survival and apoptosis in the mammary epithelium**. *Breast Cancer Res* 2000, **2**(3):149-153.

60. Yamaji D, Na R, Feuermann Y, Pechhold S, Chen W, Robinson GW, Hennighausen L: **Development of mammary luminal progenitor cells is controlled by the transcription factor STAT5A**. *Genes & development* 2009, **23**(20):2382-2387.

61. Cui Y, Riedlinger G, Miyoshi K, Tang W, Li C, Deng CX, Robinson GW, Hennighausen L: **Inactivation of Stat5 in mouse mammary epithelium during pregnancy reveals distinct functions in cell proliferation, survival, and differentiation**. *Molecular and cellular biology* 2004, **24**(18):8037-8047.

62. Philp JA, Burdon TG, Watson CJ: **Differential activation of STATs 3 and 5 during mammary gland development**. *FEBS Lett* 1996, **396**(1):77-80.

63. Hughes K, Watson CJ: **The Multifaceted Role of STAT3 in Mammary Gland Involution and Breast Cancer**. *Int J Mol Sci* 2018, **19**(6).

64. Zhou J, Chehab R, Tkalcevic J, Naylor MJ, Harris J, Wilson TJ, Tsao S, Tellis I, Zavarsek S, Xu D *et al*: **Elf5 is essential for early embryogenesis and mammary gland development during pregnancy and lactation**. *EMBO J* 2005, **24**(3):635-644.

65. Oakes SR, Naylor MJ, Asselin-Labat ML, Blazek KD, Gardiner-Garden M, Hilton HN, Kazlauskas M, Pritchard MA, Chodosh LA, Pfeffer PL *et al*: **The Ets transcription factor Elf5 specifies mammary alveolar cell fate**. *Genes & development* 2008, **22**(5):581-586.

66. Choi YS, Chakrabarti R, Escamilla-Hernandez R, Sinha S: **Elf5 conditional knockout mice reveal its role as a master regulator in mammary alveolar**

development: failure of Stat5 activation and functional differentiation in the absence of Elf5. *Dev Biol* 2009, **329**(2):227-241.

67. Siegel PM, Muller WJ: **Transcription factor regulatory networks in mammary epithelial development and tumorigenesis**. *Oncogene* 2010, **29**(19):2753-2759.

68. Lee HJ, Ormandy CJ: **Interplay between progesterone and prolactin in mammary development and implications for breast cancer**. *Mol Cell Endocrinol* 2012, **357**(1-2):101-107.

69. Frend HT, Watson CJ: **Elf5 - breast cancer's little helper**. *Breast Cancer Res* 2013, **15**(2):307.

70. Kalyuga M, Gallego-Ortega D, Lee HJ, Roden DL, Cowley MJ, Caldon CE, Stone A, Allerdice SL, Valdes-Mora F, Launchbury R *et al*: **ELF5 suppresses estrogen sensitivity and underpins the acquisition of antiestrogen resistance in luminal breast cancer**. *PLoS Biol* 2012, **10**(12):e1001461.

71. Monks J, Henson PM: **Differentiation of the mammary epithelial cell during involution: implications for breast cancer**. *J Mammary Gland Biol Neoplasia* 2009, **14**(2):159-170.

72. Li M, Liu X, Robinson G, Bar-Peled U, Wagner KU, Young WS, Hennighausen L, Furth PA: **Mammary-derived signals activate programmed cell death during the first stage of mammary gland involution**. *Proc Natl Acad Sci U S A* 1997, **94**(7):3425-3430.

73. Marti A, Feng Z, Altermatt HJ, Jaggi R: **Milk accumulation triggers apoptosis of mammary epithelial cells**. *Eur J Cell Biol* 1997, **73**(2):158-165.

74. Creamer BA, Sakamoto K, Schmidt JW, Triplett AA, Moriggl R, Wagner KU: **Stat5 promotes survival of mammary epithelial cells through transcriptional activation of a distinct promoter in Akt1**. *Molecular and cellular biology* 2010, **30**(12):2957-2970.

75. Schwertfeger KL, Richert MM, Anderson SM: **Mammary gland involution is delayed by activated Akt in transgenic mice**. *Mol Endocrinol* 2001, **15**(6):867-881.

76. Kritikou EA, Sharkey A, Abell K, Came PJ, Anderson E, Clarkson RW, Watson CJ: **A dual, non-redundant, role for LIF as a regulator of development and STAT3-mediated cell death in mammary gland**. *Development* 2003, **130**(15):3459-3468.

77. Ning Y, Hoang B, Schuller AG, Cominski TP, Hsu MS, Wood TL, Pintar JE: **Delayed mammary gland involution in mice with mutation of the insulin-like growth factor binding protein 5 gene**. *Endocrinology* 2007, **148**(5):2138-2147.

78. Kreuzaler PA, Staniszewska AD, Li W, Omidvar N, Kedjouar B, Turkson J, Poli V, Flavell RA, Clarkson RW, Watson CJ: **Stat3 controls lysosomal-mediated cell death in vivo**. *Nat Cell Biol* 2011, **13**(3):303-309.

79. Chapman RS, Lourenco PC, Tonner E, Flint DJ, Selbert S, Takeda K, Akira S, Clarke AR, Watson CJ: **Suppression of epithelial apoptosis and delayed mammary gland involution in mice with a conditional knockout of Stat3**. *Genes & development* 1999, **13**(19):2604-2616.

80. Clarkson RW, Boland MP, Kritikou EA, Lee JM, Freeman TC, Tiffen PG, Watson CJ: **The genes induced by signal transducer and activators of transcription (STAT)3 and STAT5 in mammary epithelial cells define the roles of these STATs in mammary development**. *Mol Endocrinol* 2006, **20**(3):675-685.

81. Meier-Abt F, Bentires-Alj M: **How pregnancy at early age protects against breast cancer**. *Trends Mol Med* 2014, **20**(3):143-153.

82. Schedin P: **Pregnancy-associated breast cancer and metastasis**. *Nat Rev Cancer* 2006, **6**(4):281-291.

83. Lactation IoMUCoNSDPa. In: *Nutrition During Lactation.* edn. Washington (DC); 1991.

84. Anderson SM, Rudolph MC, McManaman JL, Neville MC: **Key stages in mammary gland development. Secretory activation in the mammary gland: it's not just about milk protein synthesis!** *Breast Cancer Res* 2007, **9**(1):204.

85. Hartmann PE, Trevethan P, Shelton JN: **Progesterone and oestrogen and the initiation of lactation in ewes**. *J Endocrinol* 1973, **59**(2):249-259.

86. Deis RP, Delouis C: **Lactogenesis induced by ovariectomy in pregnant rats and its regulation by oestrogen and progesterone**. *J Steroid Biochem* 1983, **18**(6):687-690.

87. Rudolph MC, McManaman JL, Hunter L, Phang T, Neville MC: **Functional development of the mammary gland: use of expression profiling and trajectory clustering to reveal changes in gene expression during pregnancy, lactation, and involution**. *J Mammary Gland Biol Neoplasia* 2003, **8**(3):287-307.

88. Phang TL, Neville MC, Rudolph M, Hunter L: **Trajectory clustering: a non-parametric method for grouping gene expression time courses, with applications to mammary development**. *Pac Symp Biocomput* 2003:351-362.

89. Camps M, Vilaro S, Testar X, Palacin M, Zorzano A: **High and polarized expression of GLUT1 glucose transporters in epithelial cells from mammary gland: acute down-regulation of GLUT1 carriers by weaning**. *Endocrinology* 1994, **134**(2):924-934.

90. Nemeth BA, Tsang SW, Geske RS, Haney PM: **Golgi targeting of the GLUT1 glucose transporter in lactating mouse mammary gland**. *Pediatr Res* 2000, **47**(4 Pt 1):444-450.

91. Kaselonis GL, McCabe ER, Gray SM: **Expression of hexokinase 1 and hexokinase 2 in mammary tissue of nonlactating and lactating rats: evaluation by RT-PCR**. *Mol Genet Metab* 1999, **68**(3):371-374.

92. Rudolph MC, McManaman JL, Phang T, Russell T, Kominsky DJ, Serkova NJ, Stein T, Anderson SM, Neville MC: **Metabolic regulation in the lactating mammary gland: a lipid synthesizing machine**. *Physiol Genomics* 2007, **28**(3):323-336.

93. Matsuda M, Lockefeer JA, Horseman ND: **Aldolase C/zebrin gene regulation by prolactin during pregnancy and lactation**. *Endocrine* 2003, **20**(1-2):91-100.

94. Horton JD, Goldstein JL, Brown MS: **SREBPs: transcriptional mediators of lipid homeostasis**. *Cold Spring Harb Symp Quant Biol* 2002, **67**:491-498.

95. Horton JD, Goldstein JL, Brown MS: **SREBPs: activators of the complete program of cholesterol and fatty acid synthesis in the liver**. *J Clin Invest* 2002, **109**(9):1125-1131.

96. Berwick DC, Hers I, Heesom KJ, Moule SK, Tavare JM: **The identification of ATP-citrate lyase as a protein kinase B (Akt) substrate in primary adipocytes**. *J Biol Chem* 2002, **277**(37):33895-33900.

97. Porstmann T, Griffiths B, Chung YL, Delpuech O, Griffiths JR, Downward J, Schulze A: **PKB/Akt induces transcription of enzymes involved in cholesterol and fatty acid biosynthesis via activation of SREBP**. *Oncogene* 2005, **24**(43):6465-6481.

98. Boxer RB, Stairs DB, Dugan KD, Notarfrancesco KL, Portocarrero CP, Keister BA, Belka GK, Cho H, Rathmell JC, Thompson CB *et al*: **Isoform-specific requirement for Akt1 in the developmental regulation of cellular metabolism during lactation**. *Cell Metab* 2006, **4**(6):475-490.

99. Miyazawa H, Aulehla A: **Revisiting the role of metabolism during development**. *Development* 2018, **145**(19).

100. Agathocleous M, Harris WA: **Metabolism in physiological cell proliferation and differentiation**. *Trends Cell Biol* 2013, **23**(10):484-492.

101. Warburg O, Wind F, Negelein E: **The Metabolism of Tumors in the Body**. *J Gen Physiol* 1927, **8**(6):519-530.

102. Sin J, Andres AM, Taylor DJ, Weston T, Hiraumi Y, Stotland A, Kim BJ, Huang C, Doran KS, Gottlieb RA: **Mitophagy is required for mitochondrial biogenesis and myogenic differentiation of C2C12 myoblasts**. *Autophagy* 2016, **12**(2):369-380.

103. Esteban-Martinez L, Sierra-Filardi E, McGreal RS, Salazar-Roa M, Marino G, Seco E, Durand S, Enot D, Grana O, Malumbres M *et al*: **Programmed mitophagy is essential for the glycolytic switch during cell differentiation**. *EMBO J* 2017, **36**(12):1688-1706.

104. Rosano TG, Jones DH: **Developmental changes in mitochondria during the transition into lactation in the mouse mammary gland**. *J Cell Biol* 1976, **69**(3):573-580.

105. Rosano TG, Lee SK, Jones DH: **Developmental changes in mitochondria during the transition into lactation in the mouse mammary gland. II. Membrane marker enzymes and membrane ultrastructure**. *J Cell Biol* 1976, **69**(3):581-588.

106. Friedman JR, Nunnari J: **Mitochondrial form and function**. *Nature* 2014, **505**(7483):335-343.

107. Altshuler-Keylin S, Shinoda K, Hasegawa Y, Ikeda K, Hong H, Kang Q, Yang Y, Perera RM, Debnath J, Kajimura S: **Beige Adipocyte Maintenance Is Regulated by Autophagy-Induced Mitochondrial Clearance**. *Cell Metab* 2016, **24**(3):402-419.

108. Shiau MY, Lee PS, Huang YJ, Yang CP, Hsiao CW, Chang KY, Chen HW, Chang YH: **Role of PARL-PINK1-Parkin pathway in adipocyte differentiation**. *Metabolism* 2017, **72**:1-17.

109. Zhang Y, Goldman S, Baerga R, Zhao Y, Komatsu M, Jin S: **Adipose-specific deletion of autophagy-related gene 7 (atg7) in mice reveals a role in adipogenesis**. *Proc Natl Acad Sci U S A* 2009, **106**(47):19860-19865.

110. Baerga R, Zhang Y, Chen PH, Goldman S, Jin S: **Targeted deletion of autophagy-related 5 (atg5) impairs adipogenesis in a cellular model and in mice**. *Autophagy* 2009, **5**(8):1118-1130.

111. Sandoval H, Thiagarajan P, Dasgupta SK, Schumacher A, Prchal JT, Chen M, Wang J: **Essential role for Nix in autophagic maturation of erythroid cells**. *Nature* 2008, **454**(7201):232-235.

112. Ito K, Turcotte R, Cui J, Zimmerman SE, Pinho S, Mizoguchi T, Arai F, Runnels JM, Alt C, Teruya-Feldstein J *et al*: **Self-renewal of a purified Tie2+ hematopoietic stem cell population relies on mitochondrial clearance**. *Science* 2016, **354**(6316):1156-1160.

113. Gong G, Song M, Csordas G, Kelly DP, Matkovich SJ, Dorn GW, 2nd: **Parkin-mediated mitophagy directs perinatal cardiac metabolic maturation in mice**. *Science* 2015, **350**(6265):aad2459.

114. Kasahara A, Cipolat S, Chen Y, Dorn GW, 2nd, Scorrano L: **Mitochondrial fusion directs cardiomyocyte differentiation via calcineurin and Notch signaling**. *Science* 2013, **342**(6159):734-737.

115. Buck MD, O'Sullivan D, Klein Geltink RI, Curtis JD, Chang CH, Sanin DE, Qiu J, Kretz O, Braas D, van der Windt GJ *et al*: **Mitochondrial Dynamics Controls T Cell Fate through Metabolic Programming**. *Cell* 2016, **166**(1):63-76.

116. Prieto J, Leon M, Ponsoda X, Sendra R, Bort R, Ferrer-Lorente R, Raya A, Lopez-Garcia C, Torres J: **Early ERK1/2 activation promotes DRP1-dependent mitochondrial fission necessary for cell reprogramming**. *Nat Commun* 2016, **7**:11124.

117. Liu K, Zhao Q, Liu P, Cao J, Gong J, Wang C, Wang W, Li X, Sun H, Zhang C *et al*: **ATG3-dependent autophagy mediates mitochondrial homeostasis in pluripotency acquirement and maintenance**. *Autophagy* 2016, **12**(11):2000-2008.

118. Warri A, Cook KL, Hu R, Jin L, Zwart A, Soto-Pantoja DR, Liu J, Finkel T, Clarke R: **Autophagy and unfolded protein response (UPR) regulate mammary gland involution by restraining apoptosis-driven irreversible changes**. *Cell Death Discov* 2018, **4**:40.

119. Elswood J, Pearson SJ, Payne HR, Barhoumi R, Rijnkels M, W WP: **Autophagy regulates functional differentiation of mammary epithelial cells**. *Autophagy* 2020.

120. Baechler BL, Bloemberg D, Quadrilatero J: **Mitophagy regulates mitochondrial network signaling, oxidative stress, and apoptosis during myoblast differentiation**. *Autophagy* 2019, **15**(9):1606-1619.

121. Mishra P, Varuzhanyan G, Pham AH, Chan DC: **Mitochondrial Dynamics is a Distinguishing Feature of Skeletal Muscle Fiber Types and Regulates Organellar Compartmentalization**. *Cell Metab* 2015, **22**(6):1033-1044.

122. Xing F, Luan Y, Cai J, Wu S, Mai J, Gu J, Zhang H, Li K, Lin Y, Xiao X *et al*: **The Anti-Warburg Effect Elicited by the cAMP-PGC1alpha Pathway Drives Differentiation of Glioblastoma Cells into Astrocytes**. *Cell Rep* 2017, **18**(2):468-481.

123. Serasinghe MN, Wieder SY, Renault TT, Elkholi R, Asciolla JJ, Yao JL, Jabado O, Hoehn K, Kageyama Y, Sesaki H *et al*: **Mitochondrial division is requisite to RAS-induced transformation and targeted by oncogenic MAPK pathway inhibitors**. *Mol Cell* 2015, **57**(3):521-536.

124. Nunnari J, Suomalainen A: **Mitochondria: in sickness and in health**. *Cell* 2012, **148**(6):1145-1159.

125. Trifunovic A, Wredenberg A, Falkenberg M, Spelbrink JN, Rovio AT, Bruder CE, Bohlooly YM, Gidlof S, Oldfors A, Wibom R *et al*: **Premature ageing in mice expressing defective mitochondrial DNA polymerase**. *Nature* 2004, **429**(6990):417-423.

126. Trifunovic A, Hansson A, Wredenberg A, Rovio AT, Dufour E, Khvorostov I, Spelbrink JN, Wibom R, Jacobs HT, Larsson NG: **Somatic mtDNA mutations cause aging phenotypes without affecting reactive oxygen species production**. *Proc Natl Acad Sci U S A* 2005, **102**(50):17993-17998.

127. Seo AY, Joseph AM, Dutta D, Hwang JC, Aris JP, Leeuwenburgh C: **New insights into the role of mitochondria in aging: mitochondrial dynamics and more**. *J Cell Sci* 2010, **123**(Pt 15):2533-2542.

128. Carey BW, Finley LW, Cross JR, Allis CD, Thompson CB: **Intracellular alpha-ketoglutarate maintains the pluripotency of embryonic stem cells**. *Nature* 2015, **518**(7539):413-416.

129. Hamanaka RB, Chandel NS: **Mitochondrial reactive oxygen species regulate cellular signaling and dictate biological outcomes**. *Trends Biochem Sci* 2010, **35**(9):505-513.

130. Tormos KV, Anso E, Hamanaka RB, Eisenbart J, Joseph J, Kalyanaraman B, Chandel NS: **Mitochondrial complex III ROS regulate adipocyte differentiation**. *Cell Metab* 2011, **14**(4):537-544.

131. Detmer SA, Chan DC: **Functions and dysfunctions of mitochondrial dynamics**. *Nat Rev Mol Cell Biol* 2007, **8**(11):870-879.

132. Wanet A, Arnould T, Najimi M, Renard P: **Connecting Mitochondria, Metabolism, and Stem Cell Fate**. *Stem Cells Dev* 2015, **24**(17):1957-1971.

133. Sesaki H, Jensen RE: **Division versus fusion: Dnm1p and Fzo1p antagonistically regulate mitochondrial shape**. *J Cell Biol* 1999, **147**(4):699-706.

134. Atkins K, Dasgupta A, Chen KH, Mewburn J, Archer SL: **The role of Drp1 adaptor proteins MiD49 and MiD51 in mitochondrial fission: implications for human disease**. *Clin Sci (Lond)* 2016, **130**(21):1861-1874.

135. Boutant M, Kulkarni SS, Joffraud M, Ratajczak J, Valera-Alberni M, Combe R, Zorzano A, Canto C: **Mfn2 is critical for brown adipose tissue thermogenic function**. *EMBO J* 2017.

136. Jahani-Asl A, Cheung EC, Neuspiel M, MacLaurin JG, Fortin A, Park DS, McBride HM, Slack RS: **Mitofusin 2 protects cerebellar granule neurons against injury-induced cell death**. *J Biol Chem* 2007, **282**(33):23788-23798.

137. Ramonet D, Perier C, Recasens A, Dehay B, Bove J, Costa V, Scorrano L, Vila M: **Optic atrophy 1 mediates mitochondria remodeling and dopaminergic neurodegeneration linked to complex I deficiency**. *Cell Death Differ* 2013, **20**(1):77-85.

138. Westermann B: **Mitochondrial fusion and fission in cell life and death**. *Nat Rev Mol Cell Biol* 2010, **11**(12):872-884.

139. Delettre C, Lenaers G, Griffoin JM, Gigarel N, Lorenzo C, Belenguer P, Pelloquin L, Grosgeorge J, Turc-Carel C, Perret E *et al*: **Nuclear gene OPA1, encoding a mitochondrial dynamin-related protein, is mutated in dominant optic atrophy**. *Nat Genet* 2000, **26**(2):207-210.

140. Zuchner S, Mersiyanova IV, Muglia M, Bissar-Tadmouri N, Rochelle J, Dadali EL, Zappia M, Nelis E, Patitucci A, Senderek J *et al*: **Mutations in the mitochondrial GTPase mitofusin 2 cause Charcot-Marie-Tooth neuropathy type 2A**. *Nat Genet* 2004, **36**(5):449-451.

141. Ploumi C, Daskalaki I, Tavernarakis N: **Mitochondrial biogenesis and clearance: a balancing act**. *FEBS J* 2017, **284**(2):183-195.

142. Song M, Gong G, Burelle Y, Gustafsson AB, Kitsis RN, Matkovich SJ, Dorn GW, 2nd: **Interdependence of Parkin-Mediated Mitophagy and Mitochondrial Fission in Adult Mouse Hearts**. *Circ Res* 2015, **117**(4):346-351.

143. Frank S, Gaume B, Bergmann-Leitner ES, Leitner WW, Robert EG, Catez F, Smith CL, Youle RJ: **The role of dynamin-related protein 1, a mediator of mitochondrial fission, in apoptosis**. *Dev Cell* 2001, **1**(4):515-525.

144. Cogliati S, Frezza C, Soriano ME, Varanita T, Quintana-Cabrera R, Corrado M, Cipolat S, Costa V, Casarin A, Gomes LC *et al*: **Mitochondrial cristae shape determines respiratory chain supercomplexes assembly and respiratory efficiency**. *Cell* 2013, **155**(1):160-171.

145. Gatica D, Lahiri V, Klionsky DJ: **Cargo recognition and degradation by selective autophagy**. *Nat Cell Biol* 2018, **20**(3):233-242.

146. Youle RJ, Narendra DP: **Mechanisms of mitophagy**. *Nat Rev Mol Cell Biol* 2011, **12**(1):9-14.

147. Shintani T, Klionsky DJ: **Autophagy in health and disease: a double-edged sword**. *Science* 2004, **306**(5698):990-995.

148. Vives-Bauza C, Zhou C, Huang Y, Cui M, de Vries RL, Kim J, May J, Tocilescu MA, Liu W, Ko HS *et al*: **PINK1-dependent recruitment of Parkin to mitochondria in mitophagy**. *Proc Natl Acad Sci U S A* 2010, **107**(1):378-383.

149. Deng H, Dodson MW, Huang H, Guo M: **The Parkinson's disease genes pink1 and parkin promote mitochondrial fission and/or inhibit fusion in Drosophila**. *Proc Natl Acad Sci U S A* 2008, **105**(38):14503-14508.

150. Ding WX, Ni HM, Li M, Liao Y, Chen X, Stolz DB, Dorn GW, 2nd, Yin XM: **Nix is critical to two distinct phases of mitophagy, reactive oxygen species-mediated autophagy induction and Parkin-ubiquitin-p62-mediated mitochondrial priming**. *J Biol Chem* 2010, **285**(36):27879-27890.

151. Liu L, Feng D, Chen G, Chen M, Zheng Q, Song P, Ma Q, Zhu C, Wang R, Qi W *et al*: **Mitochondrial outer-membrane protein FUNDC1 mediates hypoxia-induced mitophagy in mammalian cells**. *Nat Cell Biol* 2012, **14**(2):177-185.

152. Lampert MA, Orogo AM, Najor RH, Hammerling BC, Leon LJ, Wang BJ, Kim T, Sussman MA, Gustafsson AB: **BNIP3L/NIX and FUNDC1-mediated**

mitophagy is required for mitochondrial network remodeling during cardiac progenitor cell differentiation. *Autophagy* 2019, **15**(7):1182-1198.

153. Wong YC, Holzbaur EL: **Temporal dynamics of PARK2/parkin and OPTN/optineurin recruitment during the mitophagy of damaged mitochondria**. *Autophagy* 2015, **11**(2):422-424.

154. Okui M, Yamaki A, Takayanagi A, Kudoh J, Shimizu N, Shimizu Y: **Transcription factor single-minded 2 (SIM2) is ubiquitinated by the RING-IBR-RING-type E3 ubiquitin ligases**. *Exp Cell Res* 2005, **309**(1):220-228.

155. Crews ST, Fan CM: **Remembrance of things PAS: regulation of development by bHLH-PAS proteins**. *Curr Opin Genet Dev* 1999, **9**(5):580-587.

156. Kewley RJ, Whitelaw ML, Chapman-Smith A: **The mammalian basic helix-loop-helix/PAS family of transcriptional regulators**. *Int J Biochem Cell Biol* 2004, **36**(2):189-204.

157. Taylor BL, Zhulin IB: **PAS domains: internal sensors of oxygen, redox potential, and light**. *Microbiol Mol Biol Rev* 1999, **63**(2):479-506.

158. Sullivan AE, Raimondo A, Schwab TA, Bruning JB, Froguel P, Farooqi IS, Peet DJ, Whitelaw ML: **Characterization of human variants in obesity-related SIM1 protein identifies a hot-spot for dimerization with the partner protein ARNT2**. *Biochem J* 2014, **461**(3):403-412.

159. Kolonko M, Greb-Markiewicz B: **bHLH-PAS Proteins: Their Structure and Intrinsic Disorder**. *Int J Mol Sci* 2019, **20**(15).

160. Moffett P, Pelletier J: **Different transcriptional properties of mSim-1 and mSim-2**. *FEBS Lett* 2000, **466**(1):80-86.

161. Moffett P, Reece M, Pelletier J: **The murine Sim-2 gene product inhibits transcription by active repression and functional interference**. *Molecular and cellular biology* 1997, **17**(9):4933-4947.

162. Franks RG, Crews ST: **Transcriptional activation domains of the single-minded bHLH protein are required for CNS midline cell development**. *Mech Dev* 1994, **45**(3):269-277.

163. Ward MP, Mosher JT, Crews ST: **Regulation of bHLH-PAS protein subcellular localization during Drosophila embryogenesis**. *Development* 1998, **125**(9):1599-1608.

164. Ema M, Morita M, Ikawa S, Tanaka M, Matsuda Y, Gotoh O, Saijoh Y, Fujii H, Hamada H, Kikuchi Y *et al*: **Two new members of the murine Sim gene family are transcriptional repressors and show different expression patterns during mouse embryogenesis**. *Molecular and cellular biology* 1996, **16**(10):5865-5875.

165. Wu D, Rastinejad F: **Structural characterization of mammalian bHLH-PAS transcription factors**. *Curr Opin Struct Biol* 2017, **43**:1-9.

166. Ryan HE, Lo J, Johnson RS: **HIF-1 alpha is required for solid tumor formation and embryonic vascularization**. *EMBO J* 1998, **17**(11):3005-3015.

167. Peng J, Zhang L, Drysdale L, Fong GH: **The transcription factor EPAS-1/hypoxia-inducible factor 2alpha plays an important role in vascular remodeling**. *Proc Natl Acad Sci U S A* 2000, **97**(15):8386-8391.

168. Compernolle V, Brusselmans K, Acker T, Hoet P, Tjwa M, Beck H, Plaisance S, Dor Y, Keshet E, Lupu F *et al*: **Loss of HIF-2alpha and inhibition of VEGF impair fetal lung maturation, whereas treatment with VEGF prevents fatal respiratory distress in premature mice**. *Nat Med* 2002, **8**(7):702-710.

169. Michaud JL, Rosenquist T, May NR, Fan CM: **Development of neuroendocrine lineages requires the bHLH-PAS transcription factor SIM1**. *Genes & development* 1998, **12**(20):3264-3275.

170. Goshu E, Jin H, Fasnacht R, Sepenski M, Michaud JL, Fan CM: **Sim2 mutants have developmental defects not overlapping with those of Sim1 mutants**. *Molecular and cellular biology* 2002, **22**(12):4147-4157.

171. Shamblott MJ, Bugg EM, Lawler AM, Gearhart JD: **Craniofacial abnormalities resulting from targeted disruption of the murine Sim2 gene**. *Dev Dyn* 2002, **224**(4):373-380.

172. Epstein DJ, Martinu L, Michaud JL, Losos KM, Fan C, Joyner AL: **Members of the bHLH-PAS family regulate Shh transcription in forebrain regions of the mouse CNS**. *Development* 2000, **127**(21):4701-4709.

173. Kozak KR, Abbott B, Hankinson O: **ARNT-deficient mice and placental differentiation**. *Dev Biol* 1997, **191**(2):297-305.

174. Maltepe E, Schmidt JV, Baunoch D, Bradfield CA, Simon MC: **Abnormal angiogenesis and responses to glucose and oxygen deprivation in mice lacking the protein ARNT**. *Nature* 1997, **386**(6623):403-407.

175. Shi S, Hida A, McGuinness OP, Wasserman DH, Yamazaki S, Johnson CH: **Circadian clock gene Bmal1 is not essential; functional replacement with its paralog, Bmal2**. *Curr Biol* 2010, **20**(4):316-321.

176. Bunger MK, Walisser JA, Sullivan R, Manley PA, Moran SM, Kalscheur VL, Colman RJ, Bradfield CA: **Progressive arthropathy in mice with a targeted disruption of the Mop3/Bmal-1 locus**. *Genesis (New York, NY : 2000)* 2005, **41**(3):122-132.

177. Bunger MK, Wilsbacher LD, Moran SM, Clendenin C, Radcliffe LA, Hogenesch JB, Simon MC, Takahashi JS, Bradfield CA: **Mop3 is an essential component of the master circadian pacemaker in mammals**. *Cell* 2000, **103**(7):1009-1017.

178. Laposky A, Easton A, Dugovic C, Walisser J, Bradfield C, Turek F: **Deletion of the mammalian circadian clock gene BMAL1/Mop3 alters baseline sleep architecture and the response to sleep deprivation**. *Sleep* 2005, **28**(4):395-409.

179. McDearmon EL, Patel KN, Ko CH, Walisser JA, Schook AC, Chong JL, Wilsbacher LD, Song EJ, Hong HK, Bradfield CA *et al*: **Dissecting the functions of the mammalian clock protein BMAL1 by tissue-specific rescue in mice**. *Science* 2006, **314**(5803):1304-1308.

180. Debruyne JP, Noton E, Lambert CM, Maywood ES, Weaver DR, Reppert SM: **A clock shock: mouse CLOCK is not required for circadian oscillator function**. *Neuron* 2006, **50**(3):465-477.

181. DeBruyne JP, Weaver DR, Reppert SM: **CLOCK and NPAS2 have overlapping roles in the suprachiasmatic circadian clock**. *Nat Neurosci* 2007, **10**(5):543-545.

182. DeBruyne JP, Weaver DR, Reppert SM: **Peripheral circadian oscillators require CLOCK**. *Curr Biol* 2007, **17**(14):R538-539.

183. Mimura J, Yamashita K, Nakamura K, Morita M, Takagi TN, Nakao K, Ema M, Sogawa K, Yasuda M, Katsuki M *et al*: **Loss of teratogenic response to 2,3,7,8-tetrachlorodibenzo-p-dioxin (TCDD) in mice lacking the Ah (dioxin) receptor**. *Genes Cells* 1997, **2**(10):645-654.

184. Schmidt JV, Su GH, Reddy JK, Simon MC, Bradfield CA: **Characterization of a murine Ahr null allele: involvement of the Ah receptor in hepatic growth and development**. *Proc Natl Acad Sci U S A* 1996, **93**(13):6731-6736.

185. Fernandez-Salguero P, Pineau T, Hilbert DM, McPhail T, Lee SS, Kimura S, Nebert DW, Rudikoff S, Ward JM, Gonzalez FJ: **Immune system impairment and hepatic fibrosis in mice lacking the dioxin-binding Ah receptor**. *Science* 1995, **268**(5211):722-726.

186. McIntosh BE, Hogenesch JB, Bradfield CA: **Mammalian Per-Arnt-Sim proteins in environmental adaptation**. *Annu Rev Physiol* 2010, **72**:625-645.

187. Swanson HI, Chan WK, Bradfield CA: **DNA binding specificities and pairing rules of the Ah receptor, ARNT, and SIM proteins**. *J Biol Chem* 1995, **270**(44):26292-26302.

188. Crews ST: **Control of cell lineage-specific development and transcription by bHLH-PAS proteins**. *Genes & development* 1998, **12**(5):607-620.

189. McGuire J, Coumailleau P, Whitelaw ML, Gustafsson JA, Poellinger L: **The basic helix-loop-helix/PAS factor Sim is associated with hsp90. Implications for regulation by interaction with partner factors**. *J Biol Chem* 1995, **270**(52):31353-31357.

190. Probst MR, Fan CM, Tessier-Lavigne M, Hankinson O: **Two murine homologs of the Drosophila single-minded protein that interact with the mouse aryl hydrocarbon receptor nuclear translocator protein**. *J Biol Chem* 1997, **272**(7):4451-4457.

191. Taipale M, Krykbaeva I, Koeva M, Kayatekin C, Westover KD, Karras GI, Lindquist S: **Quantitative analysis of HSP90-client interactions reveals principles of substrate recognition**. *Cell* 2012, **150**(5):987-1001.

192. Dougherty EJ, Pollenz RS: **ARNT: A Key bHLH/PAS Regulatory Protein Across Multiple Pathways**. *Comprehensive Toxicology, Vol 2: Cellular and Molecular Toxicology, 2nd Edition* 2010:231-252.

193. Ema M, Suzuki M, Morita M, Hirose K, Sogawa K, Matsuda Y, Gotoh O, Saijoh Y, Fujii H, Hamada H *et al*: **cDNA cloning of a murine homologue of Drosophila single-minded, its mRNA expression in mouse development, and chromosome localization**. *Biochem Biophys Res Commun* 1996, **218**(2):588-594.

194. Woods SL, Whitelaw ML: **Differential activities of murine single minded 1 (SIM1) and SIM2 on a hypoxic response element. Cross-talk between basic helix-loop-helix/per-Arnt-Sim homology transcription factors**. *J Biol Chem* 2002, **277**(12):10236-10243.

195. Woods S, Farrall A, Procko C, Whitelaw ML: **The bHLH/Per-Arnt-Sim transcription factor SIM2 regulates muscle transcript myomesin2 via a novel, non-canonical E-box sequence**. *Nucleic Acids Res* 2008, **36**(11):3716-3727.

196. Farrall AL, Whitelaw ML: **The HIF1alpha-inducible pro-cell death gene BNIP3 is a novel target of SIM2s repression through cross-talk on the hypoxia response element**. *Oncogene* 2009, **28**(41):3671-3680.

197. Havis E, Coumailleau P, Bonnet A, Bismuth K, Bonnin MA, Johnson R, Fan CM, Relaix F, Shi DL, Duprez D: **Sim2 prevents entry into the myogenic program by repressing MyoD transcription during limb embryonic myogenesis**. *Development* 2012, **139**(11):1910-1920.

198. Letourneau A, Cobellis G, Fort A, Santoni F, Garieri M, Falconnet E, Ribaux P, Vannier A, Guipponi M, Carninci P *et al*: **HSA21 Single-Minded 2 (Sim2) Binding Sites Co-Localize with Super-Enhancers and Pioneer Transcription Factors in Pluripotent Mouse ES Cells**. *PloS one* 2015, **10**(5):e0126475.

199. Hilliker AJ, Clark SH, Chovnick A, Gelbart WM: **Cytogenetic analysis of the chromosomal region immediately adjacent to the rosy locus in Drosophila melanogaster**. *Genetics* 1980, **95**(1):95-110.

200. Thomas JB, Crews ST, Goodman CS: **Molecular genetics of the single-minded locus: a gene involved in the development of the Drosophila nervous system**. *Cell* 1988, **52**(1):133-141.

201. Nambu JR, Lewis JO, Wharton KA, Jr., Crews ST: **The Drosophila single-minded gene encodes a helix-loop-helix protein that acts as a master regulator of CNS midline development**. *Cell* 1991, **67**(6):1157-1167.

202. Lewis JO, Crews ST: **Genetic analysis of the Drosophila single-minded gene reveals a central nervous system influence on muscle development**. *Mech Dev* 1994, **48**(2):81-91.

203. Coumailleau P, Penrad-Mobayed M, Lecomte C, Bollerot K, Simon F, Poellinger L, Angelier N: **Characterization and developmental expression of xSim, a Xenopus bHLH/PAS gene related to the Drosophila neurogenic master gene single-minded**. *Mech Dev* 2000, **99**(1-2):163-166.

204. Coumailleau P, Bollerot K, Lecomte C, Angelier N: **Xenopus single-minded (xSim) is a nuclear factor allowing nuclear translocation of its cytoplasmic partner xArnt**. *Exp Cell Res* 2003, **287**(2):237-248.

205. Caqueret A, Coumailleau P, Michaud JL: **Regionalization of the anterior hypothalamus in the chick embryo**. *Dev Dyn* 2005, **233**(2):652-658.

206. Li KL, Lu TM, Yu JK: **Genome-wide survey and expression analysis of the bHLH-PAS genes in the amphioxus Branchiostoma floridae reveal both conserved and diverged expression patterns between cephalochordates and vertebrates**. *Evodevo* 2014, **5**:20.

207. Linne V, Eriksson BJ, Stollewerk A: **Single-minded and the evolution of the ventral midline in arthropods**. *Dev Biol* 2012, **364**(1):66-76.

208. Morita S, Shiga Y, Tokishita S, Ohta T: **Analysis of spatiotemporal expression and function of the single-minded homolog in the branchiopod crustacean Daphnia magna**. *Gene* 2015, **555**(2):335-345.

209. Crews ST, Thomas JB, Goodman CS: **The Drosophila single-minded gene encodes a nuclear protein with sequence similarity to the per gene product**. *Cell* 1988, **52**(1):143-151.

210. Nambu JR, Franks RG, Hu S, Crews ST: **The single-minded gene of Drosophila is required for the expression of genes important for the development of CNS midline cells**. *Cell* 1990, **63**(1):63-75.

211. Muralidhar MG, Callahan CA, Thomas JB: **Single-minded regulation of genes in the embryonic midline of the Drosophila central nervous system**. *Mech Dev* 1993, **41**(2-3):129-138.

212. Xiao H, Hrdlicka LA, Nambu JR: **Alternate functions of the single-minded and rhomboid genes in development of the Drosophila ventral neuroectoderm**. *Mech Dev* 1996, **58**(1-2):65-74.

213. Pielage J, Steffes G, Lau DC, Parente BA, Crews ST, Strauss R, Klambt C: **Novel behavioral and developmental defects associated with Drosophila single-minded**. *Dev Biol* 2002, **249**(2):283-299.

214. Mai CT, Isenburg JL, Canfield MA, Meyer RE, Correa A, Alverson CJ, Lupo PJ, Riehle-Colarusso T, Cho SJ, Aggarwal D *et al*: **National population-based estimates for major birth defects, 2010-2014**. *Birth Defects Res* 2019, **111**(18):1420-1435.

215. Delabar JM, Theophile D, Rahmani Z, Chettouh Z, Blouin JL, Prieur M, Noel B, Sinet PM: **Molecular mapping of twenty-four features of Down syndrome on chromosome 21**. *Eur J Hum Genet* 1993, **1**(2):114-124.

216. Rahmani Z, Blouin JL, Creau-Goldberg N, Watkins PC, Mattei JF, Poissonnier M, Prieur M, Chettouh Z, Nicole A, Aurias A *et al*: **Critical role of the D21S55 region on chromosome 21 in the pathogenesis of Down syndrome**. *Proc Natl Acad Sci U S A* 1989, **86**(15):5958-5962.

217. McCormick MK, Schinzel A, Petersen MB, Stetten G, Driscoll DJ, Cantu ES, Tranebjaerg L, Mikkelsen M, Watkins PC, Antonarakis SE: **Molecular genetic approach to the characterization of the "Down syndrome region" of chromosome 21**. *Genomics* 1989, **5**(2):325-331.

218. Chatterjee A, Dutta S, Sinha S, Mukhopadhyay K: **Exploratory investigation on functional significance of ETS2 and SIM2 genes in Down syndrome**. *Dis Markers* 2011, **31**(5):247-257.

219. Hasle H, Clemmensen IH, Mikkelsen M: **Risks of leukaemia and solid tumours in individuals with Down's syndrome**. *Lancet* 2000, **355**(9199):165-169.

220. Chatterjee A, Dutta S, Mukherjee S, Mukherjee N, Dutta A, Mukherjee A, Sinha S, Panda CK, Chaudhuri K, Roy AL *et al*: **Potential contribution of SIM2 and ETS2 functional polymorphisms in Down syndrome associated malignancies**. *BMC Med Genet* 2013, **14**:12.

221. Chen H, Chrast R, Rossier C, Gos A, Antonarakis SE, Kudoh J, Yamaki A, Shindoh N, Maeda H, Minoshima S *et al*: **Single-minded and Down syndrome?** *Nat Genet* 1995, **10**(1):9-10.

222. Dahmane N, Charron G, Lopes C, Yaspo ML, Maunoury C, Decorte L, Sinet PM, Bloch B, Delabar JM: **Down syndrome-critical region contains a gene homologous to Drosophila sim expressed during rat and human central nervous system development**. *Proc Natl Acad Sci U S A* 1995, **92**(20):9191-9195.

223. Chrast R, Scott HS, Chen H, Kudoh J, Rossier C, Minoshima S, Wang Y, Shimizu N, Antonarakis SE: **Cloning of two human homologs of the Drosophila single-minded gene SIM1 on chromosome 6q and SIM2 on 21q within the Down syndrome chromosomal region**. *Genome Res* 1997, **7**(6):615-624.

224. Fan CM, Kuwana E, Bulfone A, Fletcher CF, Copeland NG, Jenkins NA, Crews S, Martinez S, Puelles L, Rubenstein JL *et al*: **Expression patterns of two murine homologs of Drosophila single-minded suggest possible roles in embryonic patterning and in the pathogenesis of Down syndrome**. *Mol Cell Neurosci* 1996, **7**(1):1-16.

225. Yamaki A, Noda S, Kudoh J, Shindoh N, Maeda H, Minoshima S, Kawasaki K, Shimizu Y, Shimizu N: **The mammalian single-minded (SIM) gene: mouse cDNA structure and diencephalic expression indicate a candidate gene for Down syndrome**. *Genomics* 1996, **35**(1):136-143.

226. Moffett P, Dayo M, Reece M, McCormick MK, Pelletier J: **Characterization of msim, a murine homologue of the Drosophila sim transcription factor**. *Genomics* 1996, **35**(1):144-155.

227. Goshu E, Jin H, Lovejoy J, Marion JF, Michaud JL, Fan CM: **Sim2 contributes to neuroendocrine hormone gene expression in the anterior hypothalamus**. *Mol Endocrinol* 2004, **18**(5):1251-1262.

228. Rachidi M, Lopes C, Charron G, Delezoide AL, Paly E, Bloch B, Delabar JM: **Spatial and temporal localization during embryonic and fetal human development of the transcription factor SIM2 in brain regions altered in Down syndrome**. *Int J Dev Neurosci* 2005, **23**(5):475-484.

229. Kola I, Hertzog PJ: **Down syndrome and mouse models**. *Curr Opin Genet Dev* 1998, **8**(3):316-321.

230. Epstein CJ, Cox DR, Epstein LB: **Mouse trisomy 16: an animal model of human trisomy 21 (Down syndrome)**. *Ann N Y Acad Sci* 1985, **450**:157-168.

231. Reeves RH, Irving NG, Moran TH, Wohn A, Kitt C, Sisodia SS, Schmidt C, Bronson RT, Davisson MT: **A mouse model for Down syndrome exhibits learning and behaviour deficits**. *Nat Genet* 1995, **11**(2):177-184.

232. Demas GE, Nelson RJ, Krueger BK, Yarowsky PJ: **Impaired spatial working and reference memory in segmental trisomy (Ts65Dn) mice**. *Behav Brain Res* 1998, **90**(2):199-201.

233. Sago H, Carlson EJ, Smith DJ, Kilbridge J, Rubin EM, Mobley WC, Epstein CJ, Huang TT: **Ts1Cje, a partial trisomy 16 mouse model for Down syndrome, exhibits learning and behavioral abnormalities**. *Proc Natl Acad Sci U S A* 1998, **95**(11):6256-6261.

234. Ema M, Ikegami S, Hosoya T, Mimura J, Ohtani H, Nakao K, Inokuchi K, Katsuki M, Fujii-Kuriyama Y: **Mild impairment of learning and memory in mice overexpressing the mSim2 gene located on chromosome 16: an animal model of Down's syndrome**. *Hum Mol Genet* 1999, **8**(8):1409-1415.

235. Chrast R, Scott HS, Madani R, Huber L, Wolfer DP, Prinz M, Aguzzi A, Lipp HP, Antonarakis SE: **Mice trisomic for a bacterial artificial chromosome with the single-minded 2 gene (Sim2) show phenotypes similar to some of those**

present in the partial trisomy 16 mouse models of Down syndrome. *Hum Mol Genet* 2000, **9**(12):1853-1864.

236. Meng X, Peng B, Shi J, Zheng Y, Chen H, Zhang J, Li L, Zhang C: **Effects of overexpression of Sim2 on spatial memory and expression of synapsin I in rat hippocampus**. *Cell Biol Int* 2006, **30**(10):841-847.

237. Chen KJ, Lizaso A, Lee YH: **SIM2 maintains innate host defense of the small intestine**. *Am J Physiol Gastrointest Liver Physiol* 2014, **307**(11):G1044-1056.

238. Metz RP, Kwak HI, Gustafson T, Laffin B, Porter WW: **Differential transcriptional regulation by mouse single-minded 2s**. *J Biol Chem* 2006, **281**(16):10839-10848.

239. Kwak HI, Gustafson T, Metz RP, Laffin B, Schedin P, Porter WW: **Inhibition of breast cancer growth and invasion by single-minded 2s**. *Carcinogenesis* 2007, **28**(2):259-266.

240. Wellberg E, Metz RP, Parker C, Porter WW: **The bHLH/PAS transcription factor singleminded 2s promotes mammary gland lactogenic differentiation**. *Development* 2010, **137**(6):945-952.

241. Laffin B, Wellberg E, Kwak HI, Burghardt RC, Metz RP, Gustafson T, Schedin P, Porter WW: **Loss of singleminded-2s in the mouse mammary gland induces an epithelial-mesenchymal transition associated with up-regulation of slug and matrix metalloprotease 2**. *Molecular and cellular biology* 2008, **28**(6):1936-1946.

242. Meng X, Tian X, Wang X, Gao P, Zhang C: **A novel binding protein of single-minded 2: the mitotic arrest-deficient protein MAD2B**. *Neurogenetics* 2012, **13**(3):251-260.

243. Scribner KC, Wellberg EA, Metz RP, Porter WW: **Singleminded-2s (Sim2s) promotes delayed involution of the mouse mammary gland through suppression of Stat3 and NFkappaB**. *Mol Endocrinol* 2011, **25**(4):635-644.

244. Vander Jagt CJ, Whitley JC, Cocks BG, Goddard ME: **Gene expression in the mammary gland of the tammar wallaby during the lactation cycle reveals conserved mechanisms regulating mammalian lactation**. *Reprod Fertil Dev* 2015.

245. Scribner KC, Behbod F, Porter WW: **Regulation of DCIS to invasive breast cancer progression by Singleminded-2s (SIM2s)**. *Oncogene* 2013, **32**(21):2631-2639.

246. Gustafson TL, Wellberg E, Laffin B, Schilling L, Metz RP, Zahnow CA, Porter WW: **Ha-Ras transformation of MCF10A cells leads to repression of Singleminded-2s through NOTCH and C/EBPbeta**. *Oncogene* 2009, **28**(12):1561-1568.

247. Rosa-Rosa JM, Pita G, Urioste M, Llort G, Brunet J, Lazaro C, Blanco I, Ramon y Cajal T, Diez O, de la Hoya M *et al*: **Genome-wide linkage scan reveals three putative breast-cancer-susceptibility loci**. *Am J Hum Genet* 2009, **84**(2):115-122.

248. Wyatt GL, Crump LS, Young CM, Wessells VM, McQueen CM, Wall SW, Gustafson TL, Fan YY, Chapkin RS, Porter WW *et al*: **Cross-talk between SIM2s and NFkappaB regulates cyclooxygenase 2 expression in breast cancer**. *Breast Cancer Res* 2019, **21**(1):131.

249. Sullivan AE, Peet DJ, Whitelaw ML: **MAGED1 is a novel regulator of a select subset of bHLH PAS transcription factors**. *FEBS J* 2016, **283**(18):3488-3502.

250. Deyoung MP, Scheurle D, Damania H, Zylberberg C, Narayanan R: **Down's syndrome-associated single minded gene as a novel tumor marker**. *Anticancer Res* 2002, **22**(6A):3149-3157.

251. Halvorsen OJ, Rostad K, Oyan AM, Puntervoll H, Bo TH, Stordrange L, Olsen S, Haukaas SA, Hood L, Jonassen I *et al*: **Increased expression of SIM2-s protein is a novel marker of aggressive prostate cancer**. *Clin Cancer Res* 2007, **13**(3):892-897.

252. Arredouani MS, Lu B, Bhasin M, Eljanne M, Yue W, Mosquera JM, Bubley GJ, Li V, Rubin MA, Libermann TA *et al*: **Identification of the transcription factor single-minded homologue 2 as a potential biomarker and immunotherapy target in prostate cancer**. *Clin Cancer Res* 2009, **15**(18):5794-5802.

253. Lu B, Asara JM, Sanda MG, Arredouani MS: **The role of the transcription factor SIM2 in prostate cancer**. *PloS one* 2011, **6**(12):e28837.

254. DeYoung MP, Tress M, Narayanan R: **Identification of Down's syndrome critical locus gene SIM2-s as a drug therapy target for solid tumors**. *Proc Natl Acad Sci U S A* 2003, **100**(8):4760-4765.

255. Aleman MJ, DeYoung MP, Tress M, Keating P, Perry GW, Narayanan R: **Inhibition of Single Minded 2 gene expression mediates tumor-selective apoptosis and differentiation in human colon cancer cells**. *Proc Natl Acad Sci U S A* 2005, **102**(36):12765-12770.

256. Jin X, Liu G, Zhang X, Du N: **Long noncoding RNA TMEM75 promotes colorectal cancer progression by activation of SIM2**. *Gene* 2018, **675**:80-87.

257. DeYoung MP, Tress M, Narayanan R: **Down's syndrome-associated Single Minded 2 gene as a pancreatic cancer drug therapy target**. *Cancer Lett* 2003, **200**(1):25-31.

258. He Q, Li G, Su Y, Shen J, Liu Q, Ma X, Zhao P, Zhang J: **Single minded 2-s (SIM2-s) gene is expressed in human GBM cells and involved in GBM invasion**. *Cancer Biol Ther* 2010, **9**(6):430-436.

259. Su Y, He Q, Deng L, Wang J, Liu Q, Wang D, Huang Q, Li G: **MiR-200a impairs glioma cell growth, migration, and invasion by targeting SIM2-s**. *Neuroreport* 2014, **25**(1):12-17.

260. Tamaoki M, Komatsuzaki R, Komatsu M, Minashi K, Aoyagi K, Nishimura T, Chiwaki F, Hiroki T, Daiko H, Morishita K *et al*: **Multiple roles of single-minded 2 in esophageal squamous cell carcinoma and its clinical implications**. *Cancer Sci* 2018, **109**(4):1121-1134.

261. Pearson SJ, Roy Sarkar T, McQueen CM, Elswood J, Schmitt EE, Wall SW, Scribner KC, Wyatt G, Barhoumi R, Behbod F *et al*: **ATM-dependent activation of SIM2s regulates homologous recombination and epithelial-mesenchymal transition**. *Oncogene* 2019, **38**(14):2611-2626.

262. Pearson SJ, Elswood J, Barhoumi R, Ming-Whitfield B, Rijnkels M, Porter WW: **Loss of SIM2s inhibits RAD51 binding and leads to unresolved replication stress**. *Breast Cancer Res* 2019, **21**(1):125.

263. Wang J, Ding Q, Fujimori H, Motegi A, Miki Y, Masutani M: **Loss of CtIP disturbs homologous recombination repair and sensitizes breast cancer cells to PARP inhibitors**. *Oncotarget* 2016, **7**(7):7701-7714.

264. Du Y, Yamaguchi H, Wei Y, Hsu JL, Wang HL, Hsu YH, Lin WC, Yu WH, Leonard PG, Lee GRt *et al*: **Blocking c-Met-mediated PARP1 phosphorylation enhances anti-tumor effects of PARP inhibitors**. *Nat Med* 2016, **22**(2):194-201.

265. Bryant HE, Schultz N, Thomas HD, Parker KM, Flower D, Lopez E, Kyle S, Meuth M, Curtin NJ, Helleday T: **Specific killing of BRCA2-deficient tumours with inhibitors of poly(ADP-ribose) polymerase**. *Nature* 2005, **434**(7035):913-917.

266. Tutt A, Robson M, Garber JE, Domchek SM, Audeh MW, Weitzel JN, Friedlander M, Arun B, Loman N, Schmutzler RK *et al*: **Oral poly(ADP-ribose)**

polymerase inhibitor olaparib in patients with BRCA1 or BRCA2 mutations and advanced breast cancer: a proof-of-concept trial. *Lancet* 2010, **376**(9737):235-244.

267. Farmer H, McCabe N, Lord CJ, Tutt AN, Johnson DA, Richardson TB, Santarosa M, Dillon KJ, Hickson I, Knights C *et al*: **Targeting the DNA repair defect in BRCA mutant cells as a therapeutic strategy**. *Nature* 2005, **434**(7035):917-921.

268. Briston T, Yang J, Ashcroft M: **HIF-1alpha localization with mitochondria: a new role for an old favorite?** *Cell Cycle* 2011, **10**(23):4170-4171.

269. Rane S, He M, Sayed D, Vashistha H, Malhotra A, Sadoshima J, Vatner DE, Vatner SF, Abdellatif M: **Downregulation of miR-199a derepresses hypoxia-inducible factor-1alpha and Sirtuin 1 and recapitulates hypoxia preconditioning in cardiac myocytes**. *Circ Res* 2009, **104**(7):879-886.

270. Hwang HJ, Dornbos P, Steidemann M, Dunivin TK, Rizzo M, LaPres JJ: **Mitochondrial-targeted aryl hydrocarbon receptor and the impact of 2,3,7,8-tetrachlorodibenzo-p-dioxin on cellular respiration and the mitochondrial proteome**. *Toxicol Appl Pharmacol* 2016, **304**:121-132.

271. Li HS, Zhou YN, Li L, Li SF, Long D, Chen XL, Zhang JB, Feng L, Li YP: **HIF-1alpha protects against oxidative stress by directly targeting mitochondria**. *Redox Biol* 2019, **25**:101109.

272. Ogita K, Okuda H, Kitano M, Fujinami Y, Ozaki K, Yoneda Y: **Localization of activator protein-1 complex with DNA binding activity in mitochondria of murine brain after in vivo treatment with kainate**. *J Neurosci* 2002, **22**(7):2561-2570.

273. Cogswell PC, Kashatus DF, Keifer JA, Guttridge DC, Reuther JY, Bristow C, Roy S, Nicholson DW, Baldwin AS, Jr.: **NF-kappa B and I kappa B alpha are found in the mitochondria. Evidence for regulation of mitochondrial gene expression by NF-kappa B**. *J Biol Chem* 2003, **278**(5):2963-2968.

274. Ryu H, Lee J, Impey S, Ratan RR, Ferrante RJ: **Antioxidants modulate mitochondrial PKA and increase CREB binding to D-loop DNA of the mitochondrial genome in neurons**. *Proc Natl Acad Sci U S A* 2005, **102**(39):13915-13920.

275. Wegrzyn J, Potla R, Chwae YJ, Sepuri NB, Zhang Q, Koeck T, Derecka M, Szczepanek K, Szelag M, Gornicka A *et al*: **Function of mitochondrial Stat3 in cellular respiration**. *Science* 2009, **323**(5915):793-797.

276. Mohammed F, Gorla M, Bisoyi V, Tammineni P, Sepuri NBV: **Rotenone-induced reactive oxygen species signal the recruitment of STAT3 to mitochondria**. *FEBS Lett* 2020.

277. Lozoya OA, Wang T, Grenet D, Wolfgang TC, Sobhany M, Ganini da Silva D, Riadi G, Chandel N, Woychik RP, Santos JH: **Mitochondrial acetyl-CoA reversibly regulates locus-specific histone acetylation and gene expression**. *Life Sci Alliance* 2019, **2**(1).

278. Yang D, Kim J: **Mitochondrial Retrograde Signalling and Metabolic Alterations in the Tumour Microenvironment**. *Cells* 2019, **8**(3).

279. Fukuda R, Zhang H, Kim JW, Shimoda L, Dang CV, Semenza GL: **HIF-1 regulates cytochrome oxidase subunits to optimize efficiency of respiration in hypoxic cells**. *Cell* 2007, **129**(1):111-122.

280. Staskiewicz L, Thorburn J, Morgan MJ, Thorburn A: **Inhibiting autophagy by shRNA knockdown: cautions and recommendations**. *Autophagy* 2013, **9**(10):1449-1450.

281. Laker RC, Xu P, Ryall KA, Sujkowski A, Kenwood BM, Chain KH, Zhang M, Royal MA, Hoehn KL, Driscoll M *et al*: **A novel MitoTimer reporter gene for mitochondrial content, structure, stress, and damage in vivo**. *J Biol Chem* 2014, **289**(17):12005-12015.

282. McQueen CM, Schmitt EE, Sarkar TR, Elswood J, Metz RP, Earnest D, Rijnkels M, Porter WW: **PER2 regulation of mammary gland development**. *Development* 2018, **145**(6).

283. Hadsell DL, Torres D, George J, Capuco AV, Ellis SE, Fiorotto ML: **Changes in secretory cell turnover, and mitochondrial oxidative damage in the mouse mammary gland during a single prolonged lactation cycle suggest the possibility of accelerated cellular aging**. *Exp Gerontol* 2006, **41**(3):271-281.

284. Watson JA, Lowenstein JM: **Citrate and the conversion of carbohydrate into fat. Fatty acid synthesis by a combination of cytoplasm and mitochondria**. *J Biol Chem* 1970, **245**(22):5993-6002.

285. Shipman LJ, Docherty AH, Knight CH, Wilde CJ: **Metabolic adaptations in mouse mammary gland during a normal lactation cycle and in extended lactation**. *Q J Exp Physiol* 1987, **72**(3):303-311.

286. Nelson WL, Butow RA, Ciaccio EI: **Oxidative phosphorylation in guinea pig mammary gland mitochondria during various functional states**. *Arch Biochem Biophys* 1962, **96**:500-505.

287. Alex AP, Collier JL, Hadsell DL, Collier RJ: **Milk yield differences between 1x and 4x milking are associated with changes in mammary mitochondrial number and milk protein gene expression, but not mammary cell apoptosis or SOCS gene expression**. *Journal of dairy science* 2015, **98**(7):4439-4448.

288. Hadsell DL, Olea W, Wei J, Fiorotto ML, Matsunami RK, Engler DA, Collier RJ: **Developmental regulation of mitochondrial biogenesis and function in the mouse mammary gland during a prolonged lactation cycle**. *Physiol Genomics* 2011, **43**(6):271-285.

289. Mowry AV, Donoviel ZS, Kavazis AN, Hood WR: **Mitochondrial function and bioenergetic trade-offs during lactation in the house mouse (Mus musculus)**. *Ecol Evol* 2017, **7**(9):2994-3005.

290. Rodger CE, McWilliams TG, Ganley IG: **Mammalian mitophagy - from in vitro molecules to in vivo models**. *FEBS J* 2018, **285**(7):1185-1202.

291. Song WH, Yi YJ, Sutovsky M, Meyers S, Sutovsky P: **Autophagy and ubiquitin-proteasome system contribute to sperm mitophagy after mammalian fertilization**. *Proc Natl Acad Sci U S A* 2016, **113**(36):E5261-5270.

292. Klionsky DJ, Abdalla FC, Abeliovich H, Abraham RT, Acevedo-Arozena A, Adeli K, Agholme L, Agnello M, Agostinis P, Aguirre-Ghiso JA *et al*: **Guidelines for the use and interpretation of assays for monitoring autophagy**. *Autophagy* 2012, **8**(4):445-544.

293. Cecconi F, Levine B: **The role of autophagy in mammalian development: cell makeover rather than cell death**. *Dev Cell* 2008, **15**(3):344-357.

294. Nakajima H, Takenaka M, Kaimori JY, Hamano T, Iwatani H, Sugaya T, Ito T, Hori M, Imai E: **Activation of the signal transducer and activator of transcription signaling pathway in renal proximal tubular cells by albumin**. *J Am Soc Nephrol* 2004, **15**(2):276-285.

295. Simon AR, Rai U, Fanburg BL, Cochran BH: **Activation of the JAK-STAT pathway by reactive oxygen species**. *Am J Physiol* 1998, **275**(6):C1640-1652.

296. Fung C, Lock R, Gao S, Salas E, Debnath J: **Induction of autophagy during extracellular matrix detachment promotes cell survival**. *Mol Biol Cell* 2008, **19**(3):797-806.

297. Yamamoto T, Takabatake Y, Kimura T, Takahashi A, Namba T, Matsuda J, Minami S, Kaimori JY, Matsui I, Kitamura H *et al*: **Time-dependent dysregulation of autophagy: Implications in aging and mitochondrial homeostasis in the kidney proximal tubule**. *Autophagy* 2016, **12**(5):801-813.

298. Narendra D, Tanaka A, Suen DF, Youle RJ: **Parkin is recruited selectively to impaired mitochondria and promotes their autophagy**. *J Cell Biol* 2008, **183**(5):795-803.

299. Liu J, Zhang C, Zhao Y, Yue X, Wu H, Huang S, Chen J, Tomsky K, Xie H, Khella CA *et al*: **Parkin targets HIF-1alpha for ubiquitination and degradation to inhibit breast tumor progression**. *Nat Commun* 2017, **8**(1):1823.

300. Harris H: **A long view of fashions in cancer research**. *Bioessays* 2005, **27**(8):833-838.

301. Muzumdar MD, Tasic B, Miyamichi K, Li L, Luo L: **A global double-fluorescent Cre reporter mouse**. *Genesis (New York, NY : 2000)* 2007, **45**(9):593-605.

302. Visvader JE: **Keeping abreast of the mammary epithelial hierarchy and breast tumorigenesis**. *Genes Dev* 2009, **23**(22):2563-2577.

303. Ball RK, Friis RR, Schoenenberger CA, Doppler W, Groner B: **Prolactin regulation of beta-casein gene expression and of a cytosolic 120-kd protein in a cloned mouse mammary epithelial cell line**. *EMBO J* 1988, **7**(7):2089-2095.

304. van der Windt GJ, Chang CH, Pearce EL: **Measuring Bioenergetics in T Cells Using a Seahorse Extracellular Flux Analyzer**. *Curr Protoc Immunol* 2016, **113**:3 16B 11-13 16B 14.

305. Nicholls DG, Darley-Usmar VM, Wu M, Jensen PB, Rogers GW, Ferrick DA: **Bioenergetic profile experiment using C2C12 myoblast cells**. *J Vis Exp* 2010(46).

306. Hernandez G, Thornton C, Stotland A, Lui D, Sin J, Ramil J, Magee N, Andres A, Quarato G, Carreira RS *et al*: **MitoTimer: a novel tool for monitoring mitochondrial turnover**. *Autophagy* 2013, **9**(11):1852-1861.

307. Stotland A, Gottlieb RA: **alpha-MHC MitoTimer mouse: In vivo mitochondrial turnover model reveals remarkable mitochondrial heterogeneity in the heart**. *J Mol Cell Cardiol* 2016, **90**:53-58.

308. Gavrilova-Jordan LP, Price TM: **Actions of steroids in mitochondria**. *Semin Reprod Med* 2007, **25**(3):154-164.

309. Green DR, Kroemer G: **Cytoplasmic functions of the tumour suppressor p53**. *Nature* 2009, **458**(7242):1127-1130.

310. Kramer AH, Kadye R, Houseman PS, Prinsloo E: **Mitochondrial STAT3 and reactive oxygen species: A fulcrum of adipogenesis?** *JAKSTAT* 2015, **4**(2):e1084084.

311. Maiuri MC, Galluzzi L, Morselli E, Kepp O, Malik SA, Kroemer G: **Autophagy regulation by p53**. *Curr Opin Cell Biol* 2010, **22**(2):181-185.

312. Price TM, Dai Q: **The Role of a Mitochondrial Progesterone Receptor (PR-M) in Progesterone Action**. *Semin Reprod Med* 2015, **33**(3):185-194.

313. Naik PP, Birbrair A, Bhutia SK: **Mitophagy-driven metabolic switch reprograms stem cell fate**. *Cell Mol Life Sci* 2018.

314. Kuma A, Hatano M, Matsui M, Yamamoto A, Nakaya H, Yoshimori T, Ohsumi Y, Tokuhisa T, Mizushima N: **The role of autophagy during the early neonatal starvation period**. *Nature* 2004, **432**(7020):1032-1036.

315. Komatsu M, Waguri S, Ueno T, Iwata J, Murata S, Tanida I, Ezaki J, Mizushima N, Ohsumi Y, Uchiyama Y *et al*: **Impairment of starvation-induced and constitutive autophagy in Atg7-deficient mice**. *J Cell Biol* 2005, **169**(3):425-434.

316. Singh R, Kaushik S, Wang Y, Xiang Y, Novak I, Komatsu M, Tanaka K, Cuervo AM, Czaja MJ: **Autophagy regulates lipid metabolism**. *Nature* 2009, **458**(7242):1131-1135.

317. Pua HH, Guo J, Komatsu M, He YW: **Autophagy is essential for mitochondrial clearance in mature T lymphocytes**. *J Immunol* 2009, **182**(7):4046-4055.

318. Nakai A, Yamaguchi O, Takeda T, Higuchi Y, Hikoso S, Taniike M, Omiya S, Mizote I, Matsumura Y, Asahi M *et al*: **The role of autophagy in cardiomyocytes in the basal state and in response to hemodynamic stress**. *Nat Med* 2007, **13**(5):619-624.

319. Masiero E, Agatea L, Mammucari C, Blaauw B, Loro E, Komatsu M, Metzger D, Reggiani C, Schiaffino S, Sandri M: **Autophagy is required to maintain muscle mass**. *Cell Metab* 2009, **10**(6):507-515.

320. Hara T, Nakamura K, Matsui M, Yamamoto A, Nakahara Y, Suzuki-Migishima R, Yokoyama M, Mishima K, Saito I, Okano H *et al*: **Suppression of basal autophagy in neural cells causes neurodegenerative disease in mice**. *Nature* 2006, **441**(7095):885-889.

321. Chourasia AH, Tracy K, Frankenberger C, Boland ML, Sharifi MN, Drake LE, Sachleben JR, Asara JM, Locasale JW, Karczmar GS *et al*: **Mitophagy defects arising from BNip3 loss promote mammary tumor progression to metastasis**. *EMBO Rep* 2015, **16**(9):1145-1163.

322. Lee Y, Lee HY, Hanna RA, Gustafsson AB: **Mitochondrial autophagy by Bnip3 involves Drp1-mediated mitochondrial fission and recruitment of Parkin in cardiac myocytes**. *Am J Physiol Heart Circ Physiol* 2011, **301**(5):H1924-1931.

323. Kitada T, Asakawa S, Hattori N, Matsumine H, Yamamura Y, Minoshima S, Yokochi M, Mizuno Y, Shimizu N: **Mutations in the parkin gene cause autosomal recessive juvenile parkinsonism**. *Nature* 1998, **392**(6676):605-608.

324. Gomes LC, Di Benedetto G, Scorrano L: **During autophagy mitochondria elongate, are spared from degradation and sustain cell viability**. *Nat Cell Biol* 2011, **13**(5):589-598.

325. You L, Wang Z, Li H, Shou J, Jing Z, Xie J, Sui X, Pan H, Han W: **The role of STAT3 in autophagy**. *Autophagy* 2015, **11**(5):729-739.

326. Zielniok K, Motyl T, Gajewska M: **Functional interactions between 17 beta - estradiol and progesterone regulate autophagy during acini formation by bovine mammary epithelial cells in 3D cultures**. *Biomed Res Int* 2014, **2014**:382653.

327. Sobolewska A, Gajewska M, Zarzynska J, Gajkowska B, Motyl T: **IGF-I, EGF, and sex steroids regulate autophagy in bovine mammary epithelial cells via the mTOR pathway**. *Eur J Cell Biol* 2009, **88**(2):117-130.

328. Sobolewska A, Motyl T, Gajewska M: **Role and regulation of autophagy in the development of acinar structures formed by bovine BME-UV1 mammary epithelial cells**. *Eur J Cell Biol* 2011, **90**(10):854-864.

329. Zielniok K, Sobolewska A, Gajewska M: **Mechanisms of autophagy induction by sex steroids in bovine mammary epithelial cells**. *J Mol Endocrinol* 2017, **59**(1):29-48.

330. Humphreys RC, Bierie B, Zhao L, Raz R, Levy D, Hennighausen L: **Deletion of Stat3 blocks mammary gland involution and extends functional competence of the secretory epithelium in the absence of lactogenic stimuli**. *Endocrinology* 2002, **143**(9):3641-3650.

331. Pensa S, Lloyd-Lewis B, Sargeant TJ, Resemann HK, Kahn CR, Watson CJ: **Signal transducer and activator of transcription 3 and the**

phosphatidylinositol 3-kinase regulatory subunits p55alpha and p50alpha regulate autophagy in vivo. *FEBS J* 2014, **281**(20):4557-4567.